Fluorido complexes of Technetium

Department of Biology, Chemistry and Pharmacy

Institute of Inorganic chemistry

Freie Universität Berlin

Berlin

Samundeeswari Mariappan Balasekaran

July, 2013

1. Supervisor: Prof. Dr. Ulrich Abram

2. Supervisor: Prof. Dr. Dieter Lentz

Date of defense: 04-07-2013.

Acknowledgment

I would like to express my deep and sincere gratitude to my supervisor, Prof. Dr. Ulrich Abram for giving me the chance to work on an interesting and exciting research project. His patience, guidance, experience, enthusiasm, support and confidence in me were invaluable throughout my study.

I gratefully thank to Prof. Dr. Dieter Lentz for being my second supervisor.

I wish to express my warm and sincere thanks to Dr. Adelheid Hagenbach for her assistance throughout my work and for her patience, advice and investment of time into helping me in the areas of X-ray crystallography. Beyond the work, her intensive support and special care during my time in Germany is highly appreciable. It gives me immense pleasure to thank my best friend Juan Daniel Castillo Gomez for his tremendous help. I would like to thank Detlef Wille for the liquid scintilation measurements and Jacqueline Grewe for organizing the chemicals I needed and her constant support. Special thanks go to Dr. Johann Spandl and Rita Friese for the Raman measurements.

I warmely thank Jecob Jegathesh Jesudas for his brotherly relationship and kind support. I specially thank to Pham Chien Thang for his discussion about the general chemistry in the evenings and kindess towards me. I am also indebted to my friends Axel Rodenstein, Elisabeth Oehlke, Jennifer Schroer, Lars Kirsten, Janine Ackermann, Philip Schweighöfer, Christelle Noufele for their hearty support and encouragement throughout my research time. My special thanks to all the Brazillian friends, Andre, Pedro Ivo, Sailer, Rafaela, Barbara, Vania, Melina, Roberta, Murilo and I had a nice time together with them in Berlin. Special thanks to Dr. Matthias Molski for discussions, guidance and helpful suggestions. I would like to acknowledge the Institute of Chemistry and Biochemistry, Freie Universität Berlin, and the Graduate School "Fluorine as a Key Element", which provided such wonderful opportunity to pursue this work.

I owe my gratitude to Shanawaz Mohammed Ghouse for his constant support, help and encouragement for my doctoral degree in Germany. Meantime, I would like to express my deepest gratitude to my soulmate Reshma Banu Mustaq for her motherly care to me. I wish to thank my father Balasekaran Mariappan and my brother Arun Sankar Balasekaran and my sister Suba Nandhini Balasekaran for their love and support. Last, but not least I would like to dedicate this thesis to my late mother Mrs. Saraswathi Balasekaran, whose blessings boosting me always.

Summary of contents

Abbreviations

Å	Ångstrom
A	Hyperfinestructure tensor
aHF	absolute hydrofluoric acid
aq	aqueous
EPR	Electron paramagnetic resonance
g	g tensor
IR	Infrared
NMR	Nuclear magnetic resonance
NBu_4	Tetrabutylammonium
PFA	Perfluoroalkoxy
py	Pyridine
RT	Room temperature
R	Raman
TFA	Trifluoroacetic acid
UV/vis	Ultraviolet/visible
$\Delta\nu_{1/2}$	Line width

Abstract

Fluorine chemistry has received considerable interest during recent years due to its significant role in the life sciences, especially for drug development. Despite the great nuclear medicinal importance of the radioactive metal technetium in radiopharmaceuticals, its coordination chemistry with the fluorido ligand is by far less explored than that of other ligands. Up to now, only a few technetium fluorides are known.

This thesis contains the synthesis, spectroscopic and structural characterization of novel technetium fluorides in the oxidation states "+1", "+2", "+4" and "+6". In the oxidation state "+6", the fluoridotechnetates were synthesized either from nitridotechnetic(VI) acid or from pertechnetate by using reducing agent and have been isolated as cesium or tetraethylammonium salts. The compounds were characterized spectroscopically and structurally.

In the intermediate oxidation state "+4", hexafluoridotechnetate(IV) was known for long time and studied spectroscopically. This thesis reports novel and improved syntheses and solved the critical issues of early publications such as the color, some spectroscopic properties and the structure of this key compound. Single crystal analyses of alkali metal, ammonium and tetramethylammonium salts of hexafluoridotechnetate(IV) are presented. In aqueous alkaline solutions, the ammonium salt of hexafluoridotechnetate(IV) undergoes hydrolysis and forms an oxido-bridged dimeric complex. It is the first step hydrolysis product of hexafluoridotechnetate(IV) and was characterized by spectroscopic and crystallographic methods.

Low-valent technetium fluorides with the metal in the oxidation states of "+2" or "+1" are almost unknown. A detailed description of the synthesis and characterization of pentafluoridonitrosyltechnetate(II) is presented. The complex was isolated as alkali metal salts, and spectroscopic as well as structural features of the complexes are presented. Different salts of the *trans*-tetraamminefluoridonitrosyltechnetium(I) cation were prepared via a facile route and were characterized by spectroscopic and crystallographic methods. Ligand exchange reactions of the nitrosyltechnetium complexes are presented.

Chapter 1

1. Introduction

1. Introduction

1.1. Technetium

Technetium is an artificial radioactive element. It is a second-row transition metal and has the atomic number 43. The oxidation states of technetium range from +VII to -I. Although, technetium has no stable isotopes, two nuclides of this element play an important role. One is ^{99}Tc and the other one is ^{99m}Tc. Technetium-99 is a low-energy β-emitter (E_{max} = 293 keV; $t_{1/2} = 2.11 \times 10^5$ a). In nuclear fission reactors, the fission yield for ^{99}Tc is about 6 %. Thus, this isotope is available in macroscopic amounts for chemical studies. Almost all chemical and structural knowledge about technetium and its compounds has been gained with ^{99}Tc. The major driving force for the ^{99}Tc chemistry is linked with the practical applications of its γ-emitting isomer ^{99m}Tc. Technetium-99m is a pure γ-emitter (E = 140 keV; $t_{1/2}$ = 6 h). It is almost perfectly suitable as radiopharmaceutical isotope because of its appropriate energy and half-life. It is also readily available as a generator nuclide and is therefore the workhorse of diagnostic nuclear-medicine applications.[1]

1.2. Background considerations

It has long been known that electronegative ligands tend to stabilize metal centers in high oxidation states. As such, metals in their highest oxidation states are frequently surrounded by oxygen or fluorine atoms. A wide variety of transition metal fluorides and oxidofluorides have been synthesized and characterized in the solid state.[2,3] Technetium complexes with chlorido and bromido ligands are well explored. Their coordination chemistry with fluorido ligands is by far less explored.[4]

The nuclear fuel waste upon recycling by PUREX (Plutonium-Uranium Extraction) or UREX (Uranium Extraction) processes produces a waste solution containing considerable amounts of ^{99}Tc. The ^{99}Tc concentration from the PUREX process is about 5-100 mgL^{-1}. A 100 MW reactor produces about 2.5 g of ^{99}Tc per day. The estimated amount of ^{99}Tc produced from nuclear reactors from 1983 up to 1994 was about 78,000 kg.[5] The main motivation of basic research about technetium fluorides was commenced while analyzing the volatile technetium fluoride products obtained during the re-enrichment of ^{235}U. Reprocessing procedures involve fluorination of the used nuclear fuel in order to obtain UF_6 for isotope enrichment. This fluorination reactions also yield volatile TcO_3F, TcF_6 and other possible technetium oxidofluorides which enter the gaseous diffusion stream and remain as low-level contaminants in ^{235}U enriched UF_6. The importance of reprocessing of nuclear fuels and its consequence led to fundamental research about the fluoride and oxidofluoride chemistry of technetium. However, up to now, only a few compounds with Tc-F bonds, e.g. the neutral technetium hexafluoride and the four technetium oxidofluorides $TcOF_4$, TcO_3F, TcO_2F_3 and $TcOF_5$ have been unambiguously characterized. The structures and syntheses of the mixed oxido/fluoride complexes are summarized below.

Technetium hexafluoride is the only homoleptic Tc fluoride of technetium, which has been structurally characterized by single crystal X-ray diffraction. This volatile compound is obtained as a major product from the reaction of technetium metal with excess F_2 at 400 °C.[6] Crystal structure analysis showed that it has an almost octahedral geometry.[7]

Fluorination of technetium metal gave small amounts of yellow TcF_5 and blue $TcOF_4$[8] as by-products (Scheme 1.1). An X-ray crystal structure of this blue by-product revealed that it has a trinuclear structure with bridging fluorine atoms.

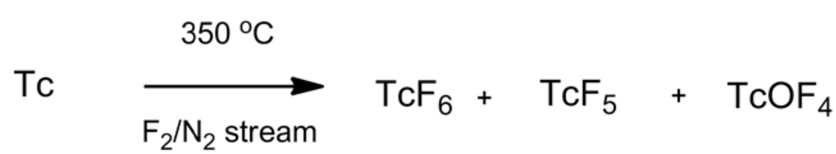

Scheme 1.1

A powder study was done on TcF_5 and the compound was found to be isostructural with chromium pentafluoride.[9] Reduction of TcF_6 with alkali metal chlorides and IF_5 resulted in the formation of alkali metal salts of hexafluoridotechnetate(V). Reflection studies, measurements of the magnetic susceptibility, and a powder X-ray study have been done on this compound.[10]

Pertechnetyl fluoride TcO_3F, was first prepared in quantitative amounts by the reaction of F_2 with TcO_2 at 150 °C (Scheme 1.2).[11] Later, it was prepared *in situ* by the dissolution of NH_4TcO_4 in aHF, but could not be isolated.[12] Recently, pure yellow crystals of TcO_3F were obtained from $KTcO_4$ in an aHF solution by using a HF/BiF_5 mixture.[13]

$$2\,TcO_2 + 2\,H_2O + 3\,F_{2(g)} \longrightarrow 2\,TcO_3F + 4\,HF$$

$$NH_4TcO_4 + 2\,HF \longrightarrow TcO_3F + H_2O + NH_4F$$

$$KTcO_4 + 2\,BiF_5 + 3\,HF \longrightarrow TcO_3F + KBiF_6 + (H_3O)BiF_6$$

Scheme 1.2

TcO_3F has a dimeric structure with bridging fluorine atoms. It reacts with HF in AsF_5 or SbF_5 and forms $[TcO_2F_2][AsF_6]\cdot 2HF$ and $[TcO_2F_2][SbF_6]\cdot 2HF$, respectively.[13]

The reaction of Tc_2O_7 in aHF leads to the formation of TcO_3F which upon further reaction with XeF_6 in aHF results in the formation of lemon yellow TcO_2F_3 (Scheme 1.3).[14]

$$Tc_2O_7 + 2\,HF \longrightarrow 2\,TcO_3F + H_2O$$

$$TcO_3F \xrightarrow{XeF_6} TcO_2F_3 + XeF_4 + {}^{1}/_{2}\,O_2$$

Scheme 1.3

The X-ray structure of TcO_2F_3 has been elucidated and shows the technetium atoms forming a "zigzag" chain linked by cis-bridging fluorine atoms. The remaining two fluorine and terminal oxygen atoms complete the distorted octahedral arrangement around the technetium atoms. Further studies about this compound such as Lewis acidity, coordination behavior with solvents[15] and reactions with fluoride ion acceptors[16] were done and the resultant products were analyzed by ^{19}F NMR, ^{99}Tc NMR and Raman spectroscopy. The spectroscopic evidences were confirmed by X-ray crystal structures.

It was expected that further fluorination of TcO_2F_3 would be possible by XeF_6, but this was not achieved. Fluorination of TcO_2F_3 was succeeded by using the strong fluorinating agent KrF_2 which resulted in the formation of volatile $TcOF_5$ (Scheme 1.4).

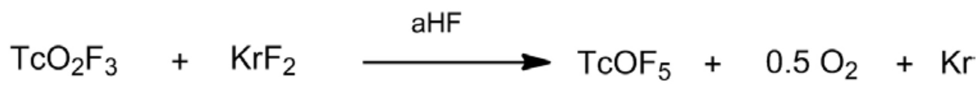

Scheme 1.4

The structure of this compound was established by ^{19}F NMR, IR and Raman spectroscopy. A subsequent X-ray crystal structure study confirmed the spectroscopic results.[17] The fluoride ion donor properties of $TcOF_5$ was also studied with AsF_5 or SbF_5 in HF solution, where the $Tc_2O_2F_9^+$ cation was formed and characterized both spectroscopically and crystallographically.

1.3. Goal of the present research

Synthesis of known technetium fluorides/oxidofluorides until up to date requires strong fluorinating agents like elemental fluorine, absolute hydrofluoric acid, noble gas fluorides etc. and the compounds are volatile. The main goal of this research is to shed light on the synthesis of aerobic stable unknown technetium fluoride compounds and to study their reactivity. For this purpose, aqueous hydrofluoric acid is employed as the main source of fluorinating agent.

This study is divided into three main chapters

(i) Fluoridonitridotechnetates(VI)

(ii) Hexafluoridotechnetates(IV)

(iii) Fluoridonitrosyltechnetates(II) and derived Tc(I) compounds

1.4. References

(1) Abram, U.; Alberto, R. *J. Braz. Chem. Soc.* **2006**, *17*, 1486.

(2) Clark, H. C. S.; Holloway, J. H. *Advanced Inorganic Fluorides* (Eds.: Nakajima, T., Žemva, B., Tressaud, A.); Elsevier: Switzerland, 2000, 51.

(3) Žemva, B. *Advanced Inorganic Fluorides* (Eds.: Nakajima, T., Žemva, B., Tressaud, A.); Elsevier: Switzerland, 2000, 79.

(4) Alberto, R. *Technetium*, in *Comprehensive Coordination Chemistry* (Eds.: McCleverty, J. A., Meyer, T. J.); Elsevier: 2005; Vol. 5, 127.

(5) Yoshihara, K. *Top. Curr. Chem.* **1996**, *176*, 17.

(6) Selig, H.; Chernick, C. L.; Malm, J. G. *J. Inorg. Nucl. Chem.* **1961**, *19*, 377.

(7) Drews, T.; Supel, J.; Hagenbach, A.; Seppelt, K. *Inorg. Chem.* **2006**, *45*, 3782.

(8) Edwards, A. J.; Jones, G. R.; Sills, R. J. C. *Chem.Comm.* **1968**, 1177.

(9) Edwards, A. J.; Hugill, D.; Peacock, R. D. *Nature* **1963**, *200*, 672.

(10) Hugill, D.; Peacock, R. D. *J. Chem. Soc. (A)* **1966**, 1339.

(11) Selig, H.; Malm, J. G. *J. Inorg. Nucl. Chem.* **1963**, *25*, 349.

(12) Binenboym.J; Elgad, U.; Selig, H. *Inorg. Chem.* **1974**, *13*, 319.

(13) Supel, J.; Abram, U.; Hagenbach, A.; Seppelt, K. *Inorg. Chem.* **2007**, *46*, 5591.

(14) Mercier, H. P. A.; Schrobilgen, G. J. *Inorg. Chem.* **1993**, *32*, 145.

(15) Casteel, W. J.; Dixon, D. A.; LeBlond, N.; Mercier, H. P. A.; Schrobilgen, G. J. *Inorg. Chem.* **1998**, *37*, 340.

(16) LeBlond, N.; Dixon, D. A.; Schrobilgen, G. J. *Inorg. Chem.* **2000**, *39*, 2473.

(17) LeBlond, N.; Mercier, H. P. A.; Dixon, D. A.; Schrobilgen, G. J. *Inorg. Chem.* **2000**, *39*, 4494.

Chapter 2

2. Fluoridonitridotechnetate(VI) complexes

2. Fluoridonitridotechnetate(VI) complexes

2.1. Introduction

The nitrido ligand (N^{3-}) is a potentially triple bonding ligand, which can establish one σ bond and two π bonds by the overlap of its p_x and p_y orbitals with the metal d_{xz} and d_{yz} orbitals.[1] It is a powerful π–electron donor because of its high negative charge. It is isoelectronic with the oxido ligand (O^{2-}). It can act as a terminal ligand but can also bridge two[2], three[3] or four[4] metal atoms in linear, triangular or tetrahedral arrangements. The first reported Tc≡N complexes are $[Tc^{V}N(S_2CNEt_2)_2]$, $[Tc^{V}NCl_2(PPh_3)_2]$ and $[Tc^{V}NCl_2(PR_2Ph)_3]$ (R = Me, Et).[5,6] In general, the length of the Tc≡N bond is in the range between 1.59 and 1.70 Å. The nitrido ligand stabilizes the technetium metal in the oxidation states +V to +VII. Notably, in the +VI oxidation state, the $[Tc^{VI}N]^{3+}$ core is resistant against hydrolysis. One peculiar behavior of the $[TcN]^{3+}$ core is the formation of dimeric $[NTcOTcN]^{4+}$ and $[NTc(\mu\text{–}O)_2TcN]^{2+}$ complexes. This unique feature of the $[TcN]^{3+}$ core is similar to the well–known isoelectronic $[OMo^{V}OMo^{V}O]^{4+}$ and $[OMo^{V}(\mu\text{–}O)_2Mo^{V}O]^{2+}$ complexes[7], while nitridomolybdenum complexes are sensitive against hydrolysis. In the case of monomeric $Tc^{VI}N$ compounds, the unpaired electron in the d^1 orbital is easily detected by electron paramagnetic resonance spectroscopy, whereas dimeric $Tc^{VI}N$ species are EPR silent due to spin pairing.

The key halide compounds, $R[TcNCl_4]$, $R[TcNBr_4]$ (R = $AsPh_4$, NBu_4)[8], $Cs_2[TcNCl_5]$[9] and $Cs_2[TcNBr_5]$[10] have been isolated and structurally well characterized. Until now, analogous fluorido compounds such as $[TcNF_4]^{-}$ or $[TcNF_5]^{2-}$ were synthesized and studied only *in situ* by electron paramagnetic resonance spectroscopy and all attempts to isolate crystalline materials failed.[11,12]

2.2. Attempted ligand exchange reactions

2.2.1. Reaction of $Cs_2[TcNCl_5]$ in $HF_{(aq)}$

Halogen exchange reactions of $Cs_2[TcNCl_5]$ by using aqueous hydrofluoric acid were attempted. A pale brown precipitate was formed by the addition of water to cesium pentachloridonitridotechnetate(VI). This precipitate was dissolved by the addition of methane sulfonic acid and formed a di(μ–oxido)aquanitrido cation (**2**). Formation of a cationic compound was confirmed on the basis of paper electrophoresis and the absence of EPR signals at 130 K.[13] Addition of $AsPh_4Cl$ resulted in no precipitation, and finally was concluded that the solution contains the cation (**2**) (Scheme 2.1). Dropwise addition of conc. HX (X= Cl, Br) to this solution resulted in the precipitation of $(AsPh_4)_2[\{TcNX_2\}_2(\mu\text{-}O)_2]$ (X = Cl, Br) complexes.[13] In order to prepare the analogue fluorido complex, $HF_{(aq)}$ (40%) was added to the solution containing the cation (**2**) and a small amount of a yellow complex was precipitated.

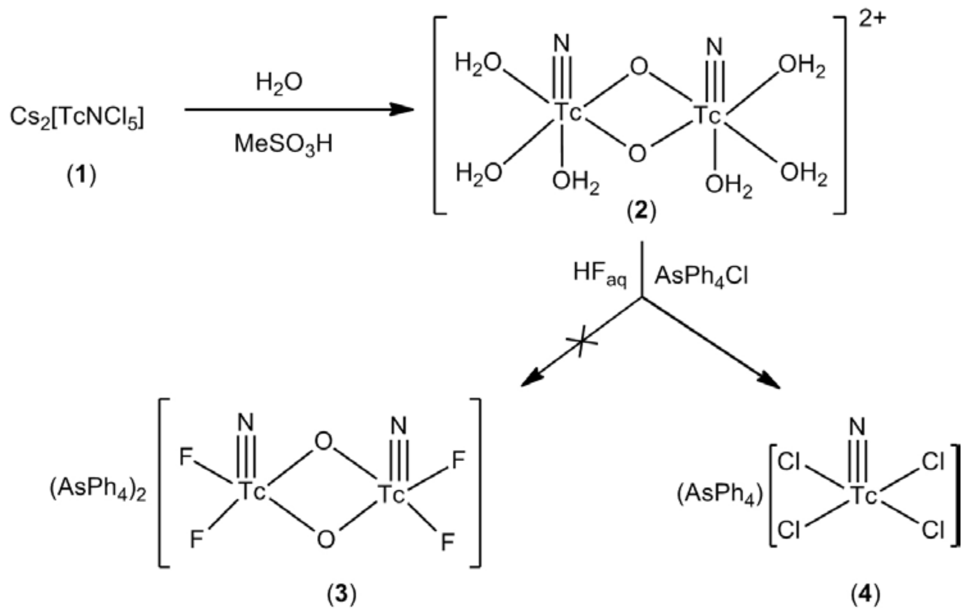

Scheme 2.1

The precipitate was recrystallized from CH_3CN solution and a single crystal measurement reveals that $AsPh_4[TcNCl_4]$ was re–formed. From this reaction it can be derived that chloride ions which are present in the solution by the addition of $AsPh_4Cl$ possess a much higher affinity to the TcN^{3+} core than F^- ions.

2.2.2. Reaction of $Cs_2[TcNCl_5]$ with aHF

The halogen exchange reaction of $Cs_2[TcNCl_5]$ in concentrated hydrobromic acid occurs immediately and gives a deep purple solution. The EPR spectrum of this solution confirms the formation of $[TcNBr_4]^-$. The chloride ligands in $[TcNCl_4]^-$ are labile enough to be substituted by bromide ions.[14] In contrast, dissolution of $Cs_2[TcNCl_5]$ in concentrated hydrofluoric acid results in the formation of mixed-ligand complexes of the type $[TcNF_{4-p}Cl_p]^-$ (p = 0 – 4) and the fluorido compounds could not be isolated in the solid state.[11] A possible reason for the formation of the mixture of species can be explained by the low concentration of fluoride ions in aqueous HF.

A reaction of $Cs_2[TcNCl_5]$ with absolute hydrofluoric acid did also not give salts of $[TcNF_4]^-$. Cesium pentachloridonitridotechnetate(VI) was added to aHF at –78 °C in a PFA tube and then the tube was sealed at the other end under vacumm. The mixture was allowed to warm up to room temperature. The red $Cs_2[TcNCl_5]$ was sparingly soluble in aHF and no further reaction was observed. Finally, the reaction mixture was kept at atmospheric conditions for the complete evaporation of the hydrofluoric acid and the color of the precipitate changed into bluish–black. The residue was insoluble in all solvents and was identified as polymeric nitridotechnetic(VI) acid $[\{TcN(OH)(OH_2)\}_2(\mu\text{-}O)_2]$ (**6**) (Scheme 2.2), which is also the hydrolysis product of $Cs_2[TcNCl_5]$ or $Cs_2[TcNBr_5]$.[13] This was proven by dissolution in HCl or HBr, which gave the corresponding halogenidonitridotechnetates(VI).

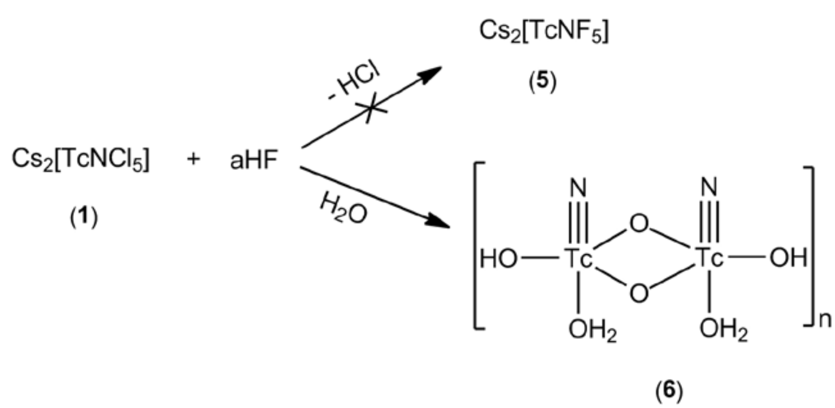

Scheme 2.2

The H_2O source for the hydrolysis is explained by the exposure of aHF to the atmosphere, which resulted in the condensation of water into the PFA tube. This experiment showed that even the higher concentration of HF did not result in a clear halogen exchange in $[TcNX_5]^{2-}$ (X= Cl, Br) complexes.

2.3. Synthesis from nitridotechnetic(VI) acid

It is understood from the previous experiments that the precursor should be halogen free in order to synthesize fluorido derivatives of nitridotechnetate(VI). Nitridotechnetic(VI) acid has proved to be a useful starting material, particularly in cases where competition by chloride has to be avoided. Nitridotechnetic(VI) acid can be prepared by the hydrolysis of $Cs_2[TcNCl_5]$. By repeated washings with water, it forms a chloride free brown precipitate. Absence of chloride ions was confirmed by the addition of silver nitrate. The infrared spectrum of this precipitate shows an absorption at 1053 cm^{-1}, which indicates that the Tc≡N core remains intact in the precipitate. It was reported that it has a polymeric structure with the empirical formula $[TcN(OH)_3]_n$.[11] Possible formulations include $[TcN(O)(OH)H_2O]_n$ or $[Tc_2N_2O_3 \cdot 3H_2O]_n$, with linear –TcN–O–TcN– bridges or a cross–linked structure **(A)**.

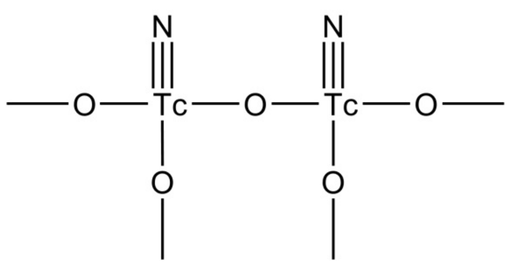

(A)

2.3.1. Reaction of $[TcN(OH)_3]_n$ with $HF_{(aq)}$

Reactions of nitridotechnetic(VI) acid with $HF_{(aq)}$ result in the formation of nitridofluorido compounds. The final product is a highly soluble complex, which could hitherto not be isolated in solid form. On the basis of its EPR spectrum (Figure 2.1), it has been attributed to a compound of the composition $[TcNF_4]^-$ in solution (Scheme 2.3).

Scheme 2.3

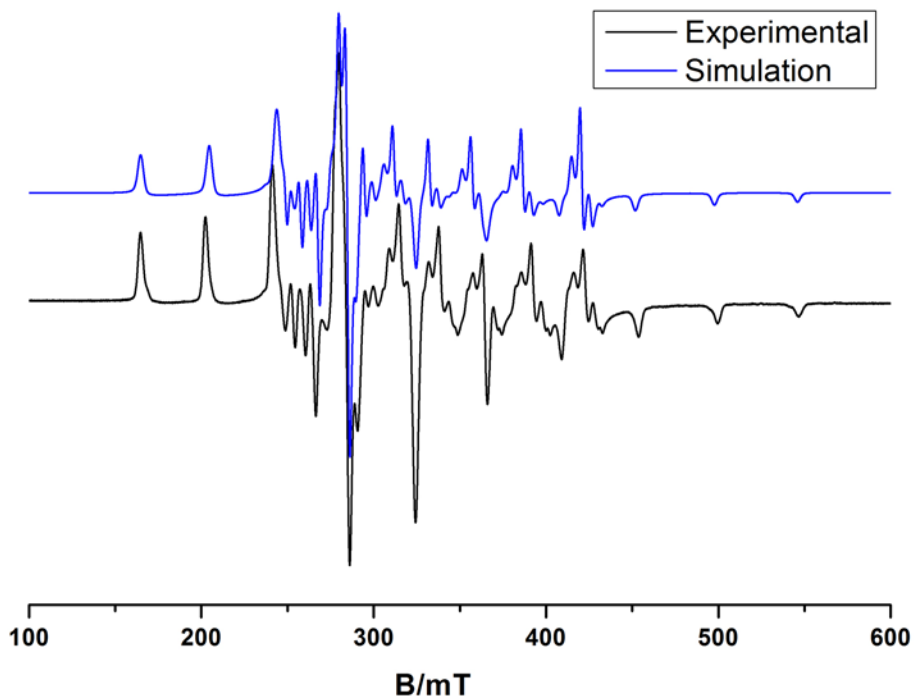

Figure 2.1: X–Band EPR spectrum of $[TcNF_4]^-$ in 27.5 M HF at 77K.

Spectral simulations were performed as described previously[10] by using an axially symmetric spin Hamiltonian (1).

$$\mathcal{H} = g_{\parallel}\beta B_z S_z + g_{\perp}(B_x S_x + B_y S_y) + A_{\parallel} S_z I_z + A_{\perp}(S_x I_x + S_y I_y) + Q[I_z^2 - I(I+1)/3] + \mathcal{H}_{shf} \quad (1)$$

where S = ½, I_{Tc} = 9/2. $\mathcal{H}_{shf}$ represents the ligand superhyperfine interaction and the other terms have their usual meaning. A comparison of the experimental and simulated spectra is shown in Figure 2.1. The EPR parameters obtained are given in Table 2.1. The spectrum shows no resolved ^{19}F hyperfine interactions in the parallel part, while in the perpendicular part lines are splitted by ^{19}F hyperfine interactions. As described by Baldas *et al*. the four fluoride ligands are physically and chemically equivalent. But they are magnetically equivalent only when the magnetic field is perpendicular to the XY plane, i.e., when the magnetic field is along the Tc≡N or z direction (**B**). From the spectrum it can be seen that two pairs of F^- ligands are magnetically equivalent. This gives rise to three equally spaced lines in the perpendicular part with an intensity ratio of 1:2:1 due to the nuclear spin of ^{19}F is ½.

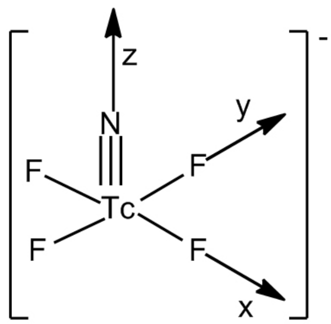

(**B**)

Linewidth considerations limit the component of the superhyperfine interaction parallel to the Tc≡N direction to less than 2×10^{-4} cm^{-1}. In contrast to this, the EPR spectrum of $[ReNF_4]^-$ showed resolved hyperfine couplings of ^{19}F in the parallel part (quintets with the intensity ratio of 1:4:6:4:1) as well as in the perpendicular part (distorted triplets).[15]

Table 2.1: EPR parameters for $[TcNF_4]^-$ anions in aqueous. HF (40%)

Anion	$g_\parallel$	$g_\perp$	$\mathbf{A}_{\parallel}^{\mathbf{Tc}}$	$\mathbf{A}_{\perp}^{\mathbf{Tc}}$	Q	a_x	a_y	a_z
$[TcNF_4]^-$ in $HF_{(aq)}$ [a]	1.895(2)	1.990(3)	376.5(5)	179.0(2.0)	5.2(3)	52	10	< 2
$[TcNF_4]^-$ in $HF_{(aq)}$ [b]	1.899(2)	1.987(2)	377.3(3)	178.2(2.0)	5.3(2)	53	12	< 2

[a] Ref.[11], [b]present work. All hyperfine and quadrupole interaction parameters are given in units of 10^{-4} cm^{-1}.

From the EPR spectrum, no evidence for the presence of a fluorido ligand *trans* to the nitrido ligand can be derived. The tendency is similar to that in the analogous oxido anion complexes, $[NbOF_5]^{3-}$, $[MoOF_5]^{2-}$ and $[ReOF_5]^{2-}$, where interactions with axial fluorido ligands were not observed.[16-18]

Addition of one equivalent of potassium fluoride to such solutions resulted in the disappearance of the signal in the EPR spectrum. The conclusion drawn from this fact by Baldas *et al*. was the formation of polymeric fluorido–bridged species and could not be confirmed. The detection of an intense ^{99}Tc NMR signal, which can be assigned to pertechnetate strongly suggests the oxidation and hydrolysis of tetrafluoridonitridotechnetate(VI) under such conditions. This is unexpected and a possible reaction pathway is given in Scheme 2.4.

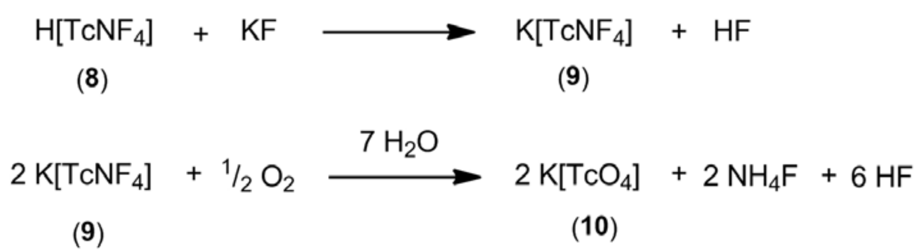

Scheme 2.4

The formation of pertechnetate was confirmed by an X–ray crystal measurement of the resulting potassium pertechnetate crystals obtained from the reaction mixture and does not only occur as a side path of the reaction.

2.3.2. Alkali metal salts of $[TcNF_4]^-$

From the solution obtained after the reaction of nitridotechnetic(VI) acid with $HF_{(aq)}$, solid precipitates could be isolated after the addition of alkali metal fluorides (RbF or CsF) in $HF_{(aq)}$. Slow evaporation of such mixtures at RT resulted in the formation of orange–yellow crystals containing an oxido-bridged, dimeric nitride fluoride compound (Scheme 2.5).

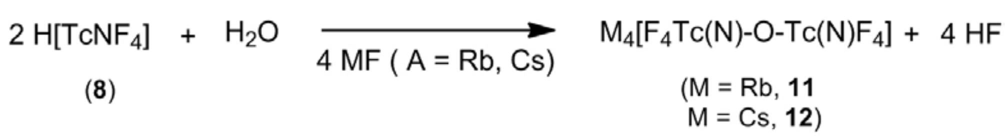

Scheme 2.5

In the solid state IR spectra, absorptions in the region 1000–1100 cm^{-1} are characteristic for terminal M≡N groups.[19] For the cesium salt of the compound, the presence of the Tc≡N group was confirmed by an intense absorption at 1053 cm^{-1} and the absorption at 700 cm^{-1} can be assigned to the ν_{asym}(Tc–O–Tc) stretch. These values are similar to the nitridotechnetic acid, which has a NTc–O–TcN units and shows an IR absorption at 1054 cm^{-1} (Tc≡N) and absorptions at 708 cm^{-1} (Tc–O–Tc).[11] The Tc–F stretchings are observed at 642 and 590 cm^{-1}.

EPR spectroscopy on $Cs_4[Tc_2N_2F_8O]$ in $HF_{(aq)}$

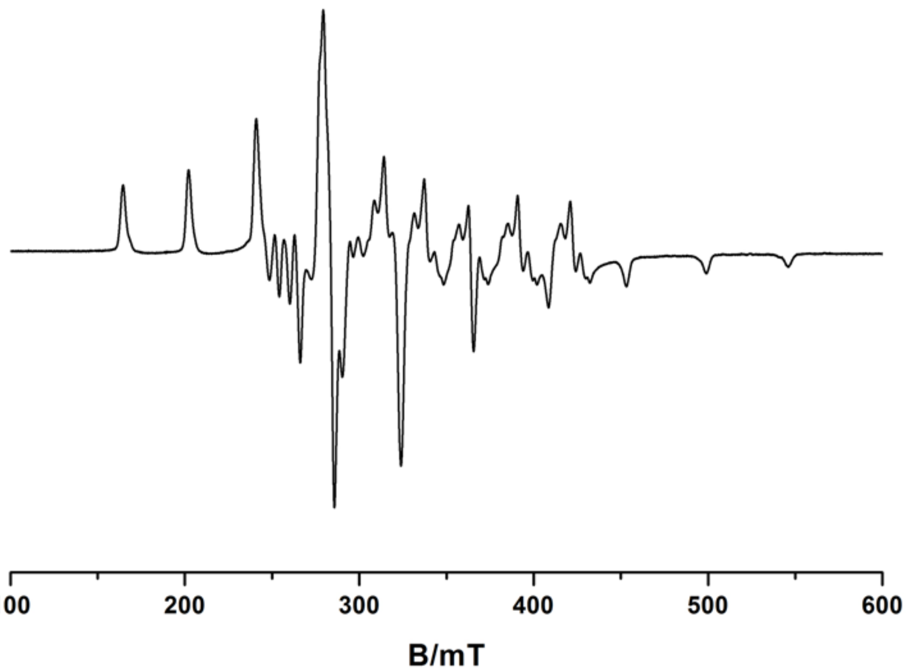

Figure 2.2: X–Band–EPR spectrum of $Cs_4[Tc_2N_2F_8O]$ in 27.5 M HF at 77K.

Dissolution of the dimeric compounds in conc. $HF_{(aq)}$ results in orange-yellow solutions, which show frozen solution EPR spectra, which are identical with that of $[TcNF_4]^-$ (Figure 2.2). The corresponding EPR parameters are given in Table 2.2. There is almost no deviation between the EPR parameters of the nitridofluorido compound formed in solution and the dissolved oxido–bridged dimeric compound. From this result, it can be concluded that there is equilibrium between the compound formed in solution and in the solid state (Scheme 2.6).

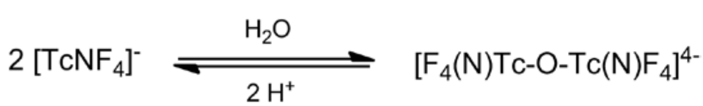

Scheme 2.6

Table 2.2: EPR parameters of Tc(VI) nitridofluorides (hyperfine interactions are given in 10^{-4} cm^{-1})

Anion	$g_{\parallel}$	$g_{\perp}$	$A_{\parallel}$	$A_{\perp}$	Q	a_x	a_y	a_z	Ref
$[TcNF_4]^-$ in $HF_{(aq)}$	1.895(2)	1.990(2)	376.5(1.0)	179.0(2.0)	5.2	52	10	< 2	11
$[TcNF_4]^-$ in CH_3CN	1.895(2)	1.987(2)	367.0(1.0)	175.0(2.0)	5.0	51	11	< 2	12
$[TcNF_5]^{2-}$ in CH_3CN	1.915(2)	2.000(2)	351.0(1.0)	165.0(2.0)	5.0	52	10	< 2	12
$[TcNF_4]^-$ in $HF_{(aq)}$	1.899(2)	1.987(2)	377.3(3)	178.2(2.0)	5.3(2)	53	12	< 2	this study
$Cs_4[Tc_2N_2F_8O]$ in $HF_{(aq)}$	1.897(3)	1.990(2)	377.3(3)	178.2(2.0)	5.3(2)	53	12	< 2	this study

This proposed equilibrium can be studied by measuring the EPR spectrum of the compound in H_2O. No EPR signals were observed in a frozen solution of $Cs_4[Tc_2N_2F_8O]$ in H_2O. Addition of $HF_{(aq)}$(48%) to this aqueous solution, restores the EPR signal. A similar behavior is observed for $Cs_2[TcNCl_5]$ in H_2O and in aqueous HCl solutions.[20] Baldas *et al*. also described that oxido–bridges in dimeric nitrido technetium(VI) complexes are sensitive to acidic conditions. The cleavage of the bridge occurs even after the addition of stoichiometric amounts of $AsPh_4X\cdot HX\cdot 2H_2O$ (X = Cl, Br) in CH_3CN and forms the monomer.[13] Thus, it is highly probable that the disappearance of the EPR signal after the addition of water to solutions of $Cs_4[Tc_2N_2F_8O]$ is the result of the formation of a EPR silent dimeric Tc(VI) compound. The cleavage of this sensitive bridge is observed by the addion of $HF_{(aq)}$(48%) and the resulting monomeric compound can be seen in the frozen EPR spectrum.

UV/visible Spectra

Monomeric $Tc^{VI}N$ complexes in solution are readily detected by EPR spectroscopy, while the Tc_2N_2O dimers are EPR silent in most cases. However, UV/vis spectroscopy offers a convenient method of distinguishing between the two forms. A 4 mM solution of $Cs_4[Tc_2N_2F_8O]$ in 5.7 M HF is orange–yellow, which upon dilution to 0.4 mM becomes pale yellow. The UV/vis spectrum of a

0.4 mM solution of $Cs_4[Tc_2N_2F_8O]$ is shown in Figure 2.3. The spectrum shows strong absorptions at 213 nm (ε = 1119 $M^{-1}cm^{-1}$) and 433 nm (ε = 278 $M^{-1}cm^{-1}$), which can be assigned to the monomeric $[TcNF_4]^-$.

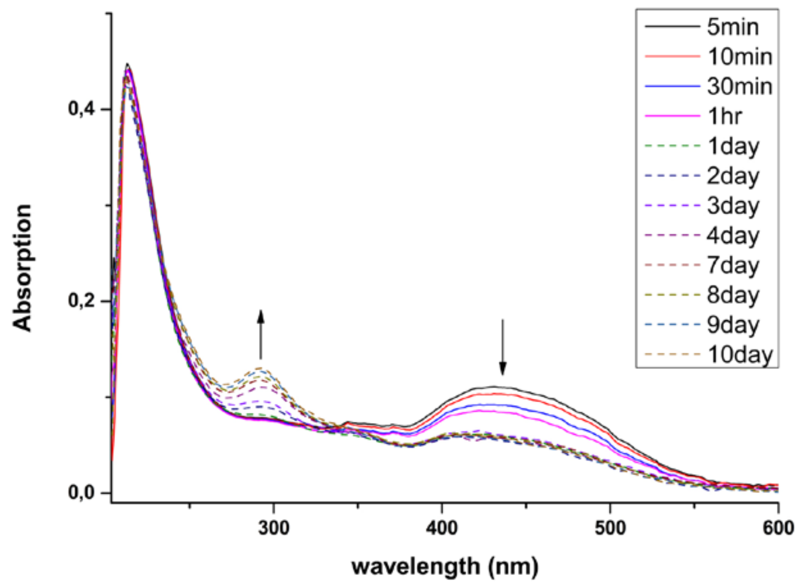

Figure 2.3: UV–Vis spectra of $Cs_4[Tc_2N_2F_8O]$ in 5.7M HF ([Tc] = $4x10^{-4}$M).

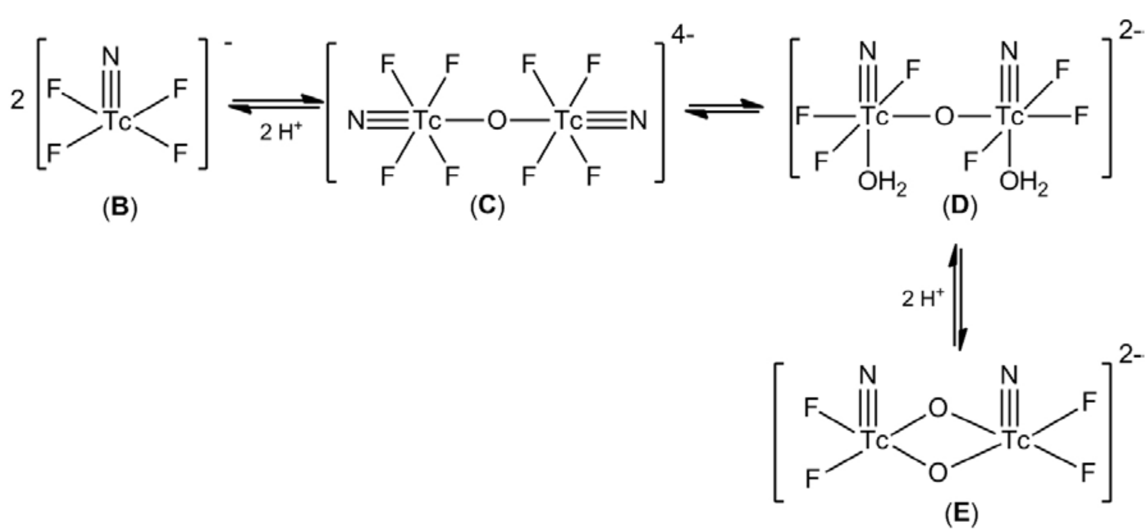

Scheme 2.7

As decribed by Baldas *et al*. various equilibria exist in highly diluted HF solutions. Some of them are given in Scheme 2.7. A decrease of the band at 433 nm was observed within a period of several days, while the intensity of the corresponding UV absorption remains almost unchanged. A new band appears within the course of the reaction at 293 nm. The observation of an isobestic point at 337 nm suggests the preferred formation of one hydrolysis product under these conditions. Ongoing reactions, which also include the species C, D, E of Scheme 2.7, however are not excluded with this study. The position of the equilibrium and the rates of interconversion of the species should depend on the acidity and coordinating ability of the medium.

2.3.3. Reaction of $[TcNF_4]^-$ solutions with NEt_4F

Addition of tetraethylammonium fluoride dihydrate to a solution of $[TcNF_4]^-$ results in the precipitation of a tetrameric compound. It crystallized as yellow–green crystals directly from an aqueous hydrofluoric acid solution. The reaction is described in Scheme 2.8:

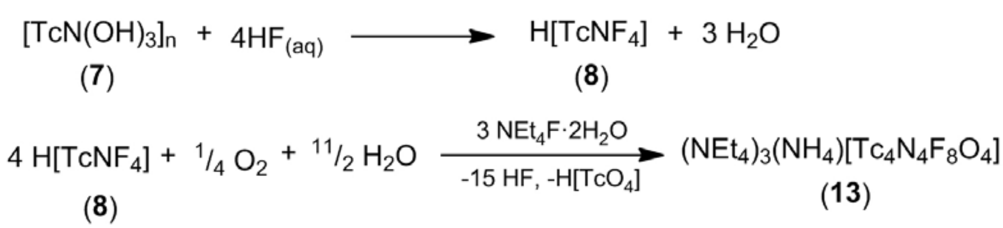

Scheme 2.8

2.3.3.1. Spectroscopic analysis

The infrared spectrum of this compound shows the ν(Tc≡N) stretch at 1050 (s) and ν(TcO_2) stretch at 999 (s) cm^{-1}. The TcO_2Tc ring system is readily detected in the IR spectrum by the presence of a strong asymmetric stretching mode at 707 cm^{-1}.[7,21] The bands at 631 and 598 cm^{-1} correspond to the Tc–F stretches.

EPR spectroscopy of $(NEt_4)_3(NH_4)[Tc_4N_4O_4F_8]$

The frozen solution EPR spectrum (Figure 2.4) of this compound was measured by dissolving the crystals in aqueous hydrofluoric acid. The spectrum is axially symmetric and the spectral parameters correspond to those of the $[TcNF_4]^-$ ion.This underlines the presence of an equilibrium between the oxido-bridged dimer and $[TcNF_4]^-$ in HF solution, which results in the formation of the latter compound in HF in an almost quantitative yield. Similar results have been described previously by Baldas *et al*. for corresponding chlorido compounds. $(AsPh_4)_2[\{TcNCl_2\}(\mu\text{–}O)_2]$ was readily cleaved by stoichiometric amounts of $AsPh_4X{\cdot}HX{\cdot}2H_2O$ (X = Cl, Br) in CH_3CN solution, forming the monomeric tetrahalogenido complex.[13]

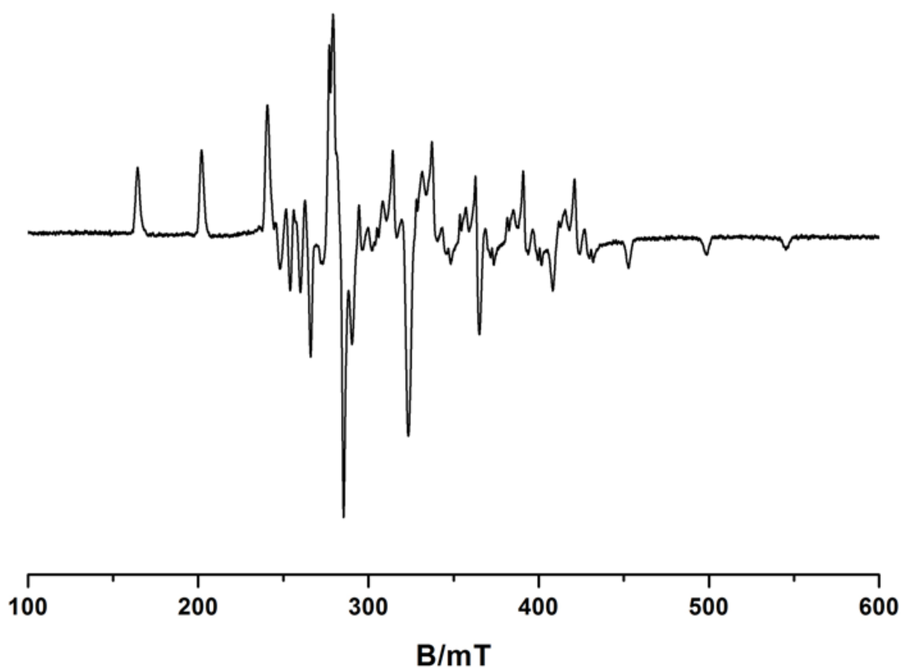

Figure 2.4: EPR spectrum of $(NEt_4)_3(NH_4)[Tc_4N_4O_4F_8]$ dissolved in $HF_{(aq)}$ at 77K.

2.3.3.2. Single crystal X–ray structural analysis

The compound crystallizes in the monoclinic space group $P2_1/c$. The crystal structure consists of three tetraethylammonium ions and an ammonium ion as cations and two $[\{TcNF_2\}(\mu\text{–}O)_2]^{2-}$ anions. The source for the ammonium ion might be the decomposition of the nitrido ligand from the precursor. The structure of the anion is tetrameric and consists of two $\{Tc_2N_2F_4O_2\}$ units. A perspective view of the anion including the numbering scheme is shown in Figure 2.5. A unit cell plot of the compound is shown in Figure 2.6. Selected bond lengths and angles are given in Table 2.3. The geometry of the $[Tc_2N_2O_2]^{2-}$ core is best described as two square pyramids sharing an edge with bridging oxygens to give a bent Tc_2O_2 ring. The di(μ–O) dimeric core of this complex is comparable to the isostructural $(AsPh_4)_2[\{TcNCl_2\}_2(\mu\text{–}O)_2]$[13], $(NBu_4)_2[\{TcNCl_2\}_2(\mu\text{–}O)_2]$[22] and $[\{TcN(S_2CNEt_2)\}_2(\mu\text{–}O)_2]$.[21]

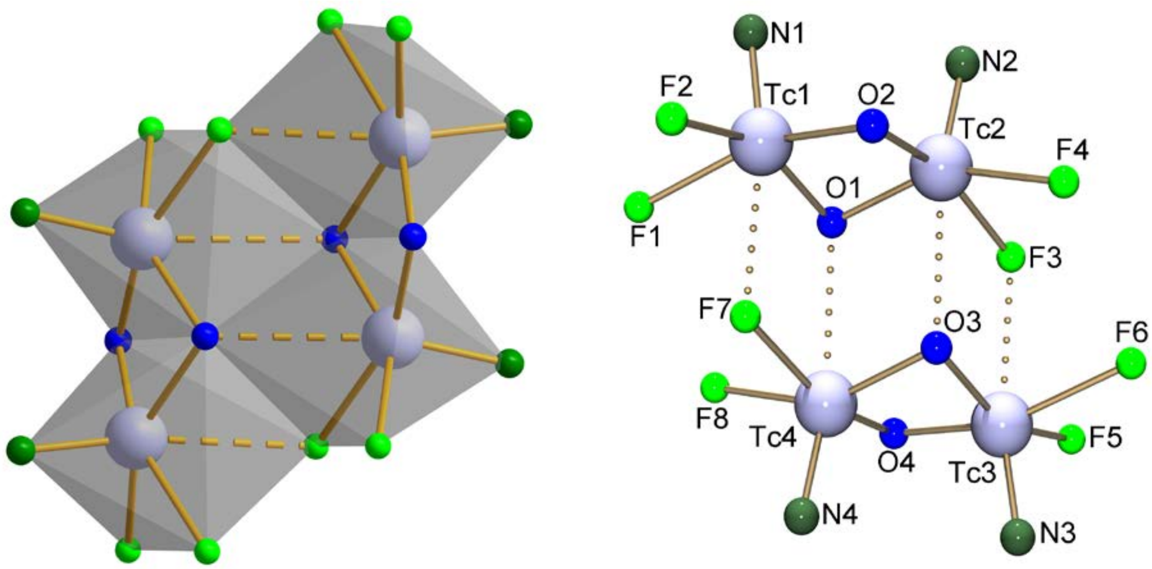

Figure 2.5: Molecular anion of $(NEt_4)_3(NH_4)[Tc_4N_4F_8O_4]$.

The Tc≡N bond lengths are in the typical range and are not identical. The Tc–F bond lengths are in the range between 1.944(4) to 2.141(5) Å. The very long Tc(1)–F(7), Tc(3)–F(3), Tc(2)–O(3) and Tc(4)–O(1) bond distances of 2.357(5), 2.372(4), 2.469(5) and 2.542(1) Å, respectively, are a manifestation of the strong *trans* influence of the nitrido ligand (one of the strongest π–electron donors known). Each Tc atom is displaced above the corresponding F_2O_2 basal planes by 0.3825(7) – 0.4132(7) Å.

The short Tc–Tc distances of 2.557(1) and 2.553(1) Å are comparable to the values in the isostructural complexes, $(AsPh_4)_2[TcNCl_2(\mu\text{-}O)_2]$ (2.579(1) Å), $(AsPh_4)_2[TcNBr_2(\mu\text{-}O)_2]$ (2.575(2) Å), $(AsPh_4)_2[TcN(CN)_2(\mu\text{-}O)_2]$ (2.560(1) Å).[7] The acute Tc–O–Tc angles of 81.6(2)°–

83.0(2)° indicates a direct metal–metal interaction, which corresponds to a d_{xy}^1–d_{xy}^1 single bond. The dihedral angles of O–Tc–O planes are 94.5(2)°–95.5(2)°. The two nitrogen atoms in $[Tc_2N_2O_2]^{2-}$ are bent back from each other to a N···N contact distance of 3.047(1) and 3.032(1) Å. This is longer than the sum of the nitrogen van der Waals radii of about 2.9 Å. In principle this should account for the absence of EPR spectrum. However, the solubility of the complex restricts the measurement only to highly acidic conditions, which results in the cleavage of the bridges.

Table 2.3: Selected bond lengths (Å) and angles (°) in $(NEt_4)_3(NH_4)[Tc_4N_4F_8O_4]$

Bond lengths (Å)					
Tc(1)–N(1)	1.635(7)	Tc(1)–O(2)	1.933(5)	Tc(3)–O(3)	1.958(5)
Tc(2)–N(2)	1.619(8)	Tc(2)–O(1)	1.943(5)	Tc(3)–O(4)	1.945(1)
Tc(3)–N(3)	1.626(7)	Tc(2)–O(2)	1.926(5)	Tc(4)–O(3)	1.946(6)
Tc(4)–N(4)	1.637(8)	Tc(2)–F(3)	2.044(4)	Tc(4)–O(4)	1.928(6)
Tc(1)–F(1)	2.141(5)	Tc(2)–F(4)	1.944(4)	Tc(4)–F(7)	2.030(4)
Tc(1)–F(2)	1.954(5)	Tc(3)–F(5)	1.952(4)	Tc(4)–F(8)	1.999(4)
Tc(1)–O(1)	1.971(5)	Tc(3)–F(6)	2.137(6)		
Bond angles (°)					
Tc(1)–O(1)–Tc(2)	81.6(2)	Tc(1)–O(2)–Tc(2)	83.0(2)		
Tc(3)–O(3)–Tc(4)	81.7(2)	Tc(3)–O(4)–Tc(4)	82.5(2)		

Crystallization of the $[Tc_4N_4F_8O_4]^{4-}$ as a mixed NEt_4^+/NH_4^+ salt could be understood by the formation of stable 1D chains, which are linked by the hydrogen bonded interactions between the nitrogen atoms of the ammonium cations and fluorido ligands of $[Tc_4N_4F_8O_4]^{4-}$ anions. (see Figure 2.6 b). The N···F distances between the ammonium nitrogen atom N(8) and F(1) as well F(6) of the next asymmetric unit are 2.41(1) Å and 2.43(1) Å respectively. These values are even shorter than the bond distance of N–H…F (2.66 Å) in solid ammonium fluoride. This informs that there is most probably a hydrogen bond between the ammonium nitrogen and the fluorine atoms.

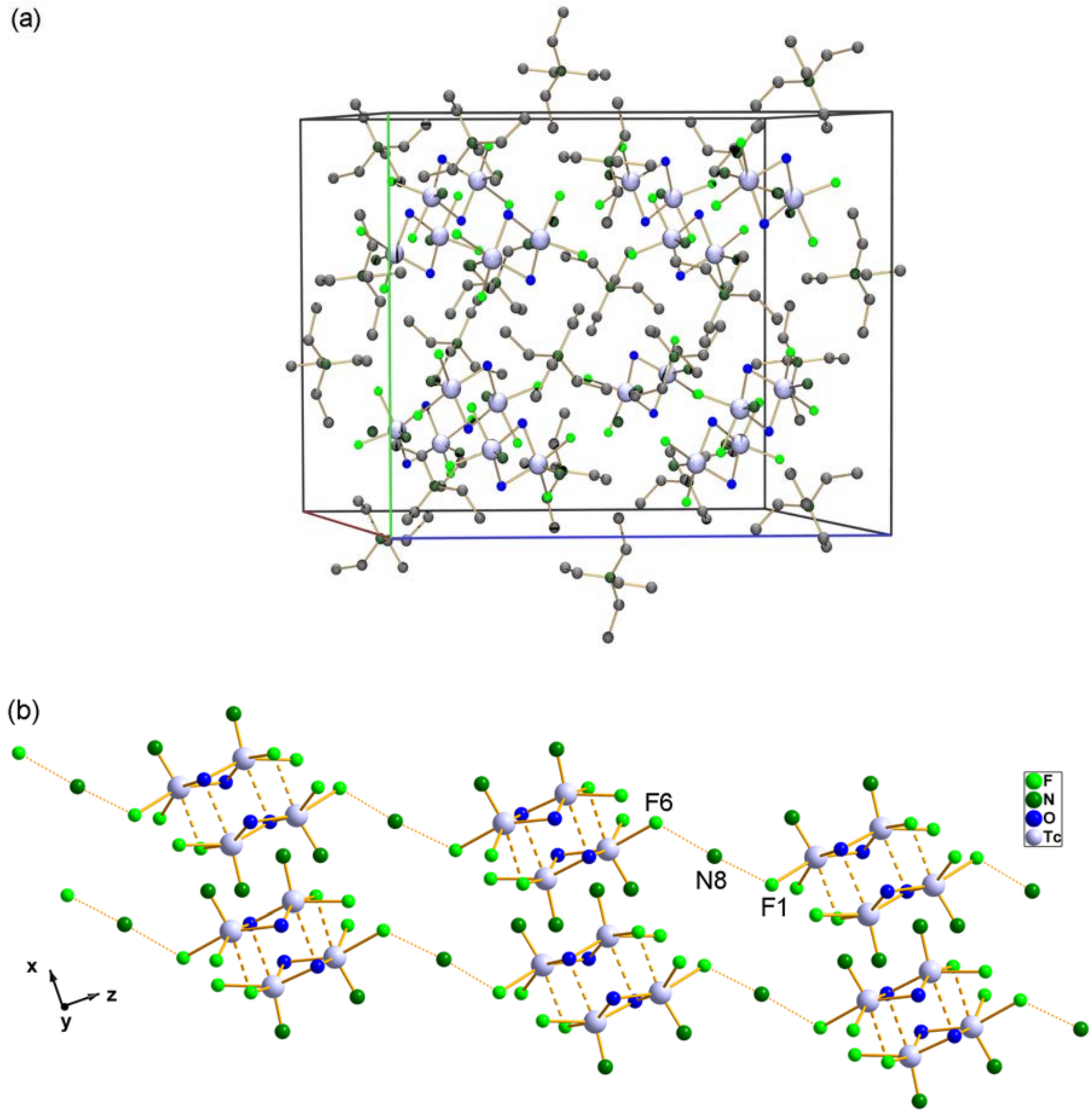

Figure 2.6: (a) Unit cell plot of $(NEt_4)_3(NH_4)[Tc_4N_4F_8O_4]$, (b) Packing motif (linear chain) in $(NEt_4)_3(NH_4)$ $[Tc_4N_4F_8O_4]$. The hydrogen atoms bonded to carbon atoms were omitted for clarity.

2.4. Synthesis from pertechnetate

2.4.1. Reaction without additional reducing agents

The key Tc(VI) nitrido complexes, the orange–red $[TcNCl_4]^-$ and the intensely blue $[TcNBr_4]^-$ are readily prepared in high yield by the reaction of $[TcO_4]^-$ in refluxing aqueous HX (X = Cl or Br) with excess of NaN_3. The products can be isolated in high yields by the precipitation with organic cations such as $AsPh_4^+$ or NBu_4^+.[8] In these reactions, HCl or HBr readily dissociate into H^+ and Cl^- or Br^- ions and the reducing potentials of the halogenido ions are sufficiently strong to reduce pertechnetate. A similar reaction was carried out under the same conditions with aqueous hydrofluoric acid (48%). The formation of $[TcNF_4]^-$ was confirmed by the EPR spectrum of the reaction mixture. However, the amount of $[TcNF_4]^-$ formed from this reaction was very small. The excess of sodium cations present in the reaction mixture led to the formation of only few crystals of $Na_4[Tc_2N_2F_8O]$. More than 90% of the starting material remained unchanged, which was confirmed with ^{99}Tc NMR spectroscopy. The intensity of the pertechnetate signal was not reduced over a period of 6h irrespective of the amount of azide used. Thus, it can be concluded, that expectedly F^- ions in aqueous HF cannot act as reductant for Tc(VII). The formation of small amounts of a Tc(VI) compound during the experiment may be attributed to reductive impurities in the agents used.

2.4.2. Reactions with $H_3PO_{2(aq)}$ as reducing agent

In 1977 it was first reported that the reduction of pertechnetate with H_3PO_2 in hydrochloric acid results in a dark green solution which upon addition of $(NBu_4)Cl$ gives an olive green crystalline solid of the composition $(NBu_4)_2[Tc_2Cl_8]$.[23] Later, $[TcOCl_4]^-$, was isolated from the same reaction.[24] In this reaction, H_3PO_2 serves as a reducing agent for the synthesis of chlorido compounds. An attempt was made to synthesize the nitridofluoridotechnetate(VI) directly from pertechnetate, NaN_3 and $HF_{(aq)}$ (48%) by using H_3PO_2 as reducing agent (Scheme 2.9). The reaction mixture was refluxed in order to destroy the residual azide. The progress of the reaction was followed by measuring the NMR and EPR spectra of the the reaction mixture.

$$2\,NH_4TcO_4 + 10\,HF + 4\,NaN_3 + H_3PO_2 \xrightarrow[-2\,NH_4F,\ -5\,N_2,\ -5\,H_2O]{} \underset{(\mathbf{14})}{Na_4[Tc_2N_2F_8O]} + H_3PO_4$$

Scheme 2.9

The absence of a $[TcO_4]^-$ signal in the ^{99}Tc NMR spectrum of the reaction mixture confirmed the complete reduction of the precursor. An EPR measurement of the same mixture indicated the formation of nitrido fluorido species in solution as a mixture of two compounds. The predominant species formed was attributed $[TcNF_4]^-$ (Figure 2.7). Comparison of EPR parameters are given in Table 2.4. However, a second paramagnetic species is contained in the reaction mixture (see arrows in Figure 2.7).

Baldas *et al*. studied the monomer, μ–oxido dimer and di(μ–oxido) dimer interconversion of nitridotechnetium(VI) complexes in solutions of sulfuric and phosphoric acids.[25] This study revealed that phosphoric acid undergoes a ligand exchange reaction in dilute aqueous solutions. The different coordinating species of phosphoric oxido acid show the differences only in the EPR coupling constants A_{Tc} values rather than g values. A comparison of ^{99}Tc coupling constants of the side product of the above discussed reaction with the values of the phosphoric acid species shows marked deviations. This suggests the presence of a TcN complex with mixed O/F coordinating sphere as a side product.

Attempts to isolate the paramagnetic species, e.g. by the addition of $(PPh_4)(BF_4)$ resulted in the precipitation of a bluish black solid, which was insoluble in all common solvents. Vibrational spectra strongly suggest the formation of a polymeric TcN acid as has also be observed in previous experiments. This has been proven by a reaction of the product with HCl. The precipitate dissolves immediately in conc. HCl and forms an orange-red solution. EPR measurement of this solution confirms the monomeric $[TcNCl_4]^-$. From the color and solubility of the compound in conc. HX (X = Cl or Br), the formula of the precipitate might as shown in (**6**)

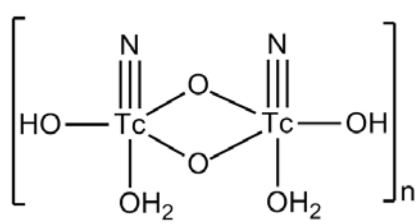

(**6**)

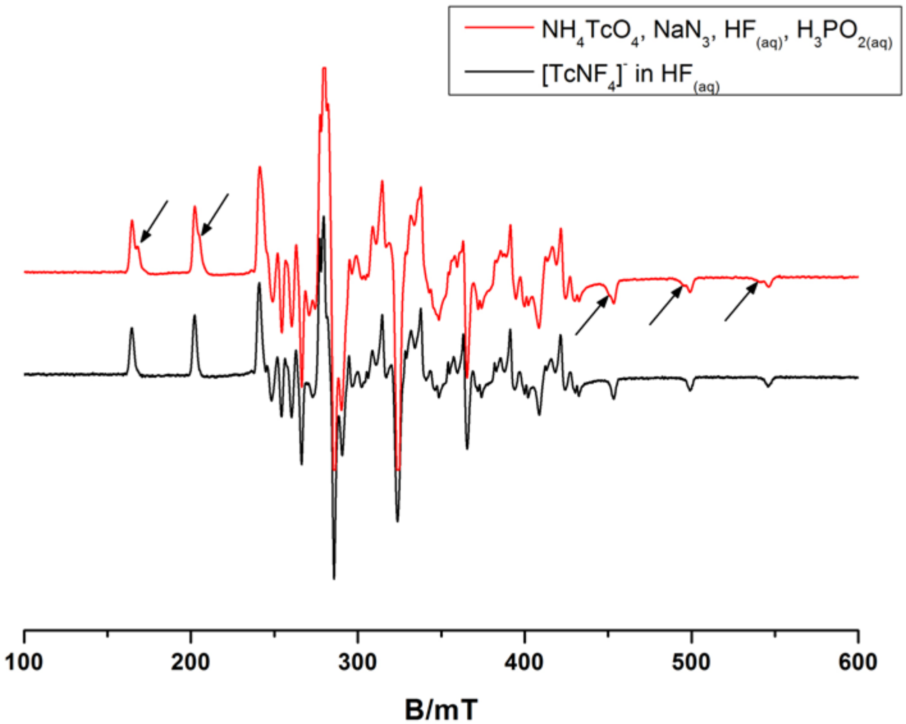

Figure 2.7: Comparison of EPR spectra of the reaction mixture of $NH_4[TcO_4]$, $HF_{(aq)}$, NaN_3 and H_3PO_2 with $[TcNF_4]^-$ in $HF_{(aq)}$.

Table 2.4: EPR spectral parameters of $[TcNX_4]^-$ species (X = F, Cl) in phosphoric acid and HF solutions

Anion	$g_\parallel$	$g_\perp$	$A_\parallel$ 10^{-4} cm^{-1}	$A_\perp$ 10^{-4} cm^{-1}	Reference
$Cs_2[TcNCl_5]$ in 2M H_3PO_3	1.909	1.986	347	164	[28]
$Cs_2[TcNCl_5]$in 2M $H_4P_2O_7$ (immediately)	1.912	1.985	347	162	[28]
$Cs_2[TcNCl_5]$in 2M $H_4P_2O_7$ (on standing)	1.905	1.985	348	165	[28]
$[TcNF_4]^-$ in $HF_{(aq)}$	1.897(3)	1.990(2)	377.3(3)	178.2(2.0)	present study
NH_4TcO_4, NaN_3, $HF_{(aq)}$, H_3PO_2	1.898(2)	1.991(2)	376.3(3)	179.2(2.0)	present study

2.4.3. Reactions with $Na_2S_2O_4$ as reducing agent

Neither the reaction from pertechnetate without any reducing agents nor with H_3PO_2 preparations appeared to be generally applicable. Thus, an alternative synthetic route was investigated. Sodium dithionite as a reducing agent for synthesis of technetium complexes under basic conditions is well known.[26-28] The reduction capacity of sodium dithionite depends on the pH value. Presumably, the reduction capacity of dithionite is much higher in acid medium than in alkaline medium. The reaction of pertechnetate with sodium azide and sodium dithionite in the presence of aqueous hydrofluoric acid under reflux forms the expected nitridofluorido compound in sufficient yields (Scheme 2.10).

The reaction was followed by both NMR and EPR spectroscopy. The absence of the pertechnetate signal in the NMR spectra indicated the reduction of the precursor. EPR measurement of the same reaction mixture confirms the formation of nitrido fluorido species in solution (Figure 2.8).

$$2\ NH_4TcO_4 + 8\ HF + 2\ NaN_3 + Na_2S_2O_4 \xrightarrow[\text{-2 } NH_4F,\text{ -2 NaF, -2 } NaHSO_4,\text{ -2 } N_2]{+\ 4\ CsF} \underset{(\mathbf{12})}{Cs_4[Tc_2N_2F_8O]} + 3\ H_2O$$

Scheme 2.10

The EPR spectrum of the reaction mixture is same as that of $[TcNF_4]^-$, which was also obtained from HF solutions of $Cs_4[Tc_2N_2F_8O]$. Addition of CsF to the solution results in the precipitation of the $Cs_4[Tc_2N_2F_8O]$ as orange–yellow crystals with 75% yield. The compound was purified by recrystallization from $HF_{(aq)}$ (48%). Solutions of the crystals of $Cs_4[Tc_2N_2F_8O]$ in $HF_{(aq)}$ give the same EPR spectrum as obtained earlier. The IR spectra of the crystals is the same as described earlier for the $Cs_4[Tc_2N_2F_8O]$.

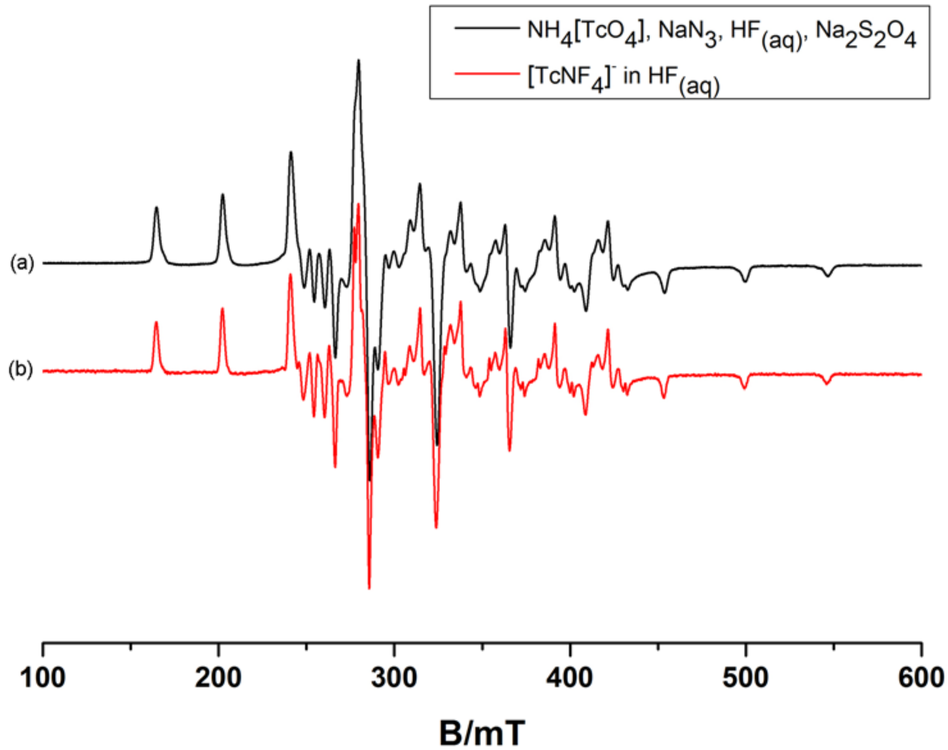

Figure 2.8: X–band EPR spectrum of $[TcNF_4]^-$ (a) formed from a reaction mixture containing $[TcO_4]^-$, NaN_3 and $Na_2S_2O_4$ in $HF_{(aq)}$ and (b) from nitridotechnetic(VI) acid in $HF_{(aq)}$ at 77K.

All attempts to isolate tetralkylammonium salts of the nitridofluoridotechnetate(VI) from this reaction failed.

2.5. Reactions of $[TcNF_4]^-$

2.5.1. Reaction with potassium cyanide

The reaction of $Cs_2[TcNCl_5]$ with aqueous KCN resulted in the formation of the $[TcN(CN)_4(OH_2)]^{2-}$ ion. The product was isolated by the addition of $AsPh_4Cl \cdot xH_2O$.[29] The same reaction was carried out by dissolution of $Rb_4[Tc_2N_2F_8O]$ in aqueous KCN. $(AsPh_4)_2[TcN(CN)_4(OH_2)] \cdot 5H_2O$ was isolated by the addition of $AsPh_4Cl \cdot xH_2O$ and was recrystallized from hot water. The crystal structure of the compound is already known.

2.5.2. Reaction with hydrogen peroxide

The reaction of $Cs_2[TcNCl_5]$ in 10% H_2O_2 results in the formation of a peroxido complex of the formula $Cs[TcN(O_2)_2Cl]$.[30] A similar reaction was attempted to prepare the analogous fluorido complex. Dissolution of $Rb_4[Tc_2N_2F_8O]$ in 10% H_2O_2 resulted in the formation of a yellow colored solution similar to the chlorido compound. However, slow evaporation of the solvent at room temperature resulted in the formation of pertechnetate and was confirmed by the ^{99}Tc NMR spectrum of the product.

2.6. Summary and Conclusions

The synthesis of tetrafluoridonitridotechnetate(VI) was attempted following different routes. The use of H_3PO_2 as reducing agent forms the nitridofluorido compound in solution. An attempt to isolate this compound in the solid state forms a polymeric aqua coordinated nitridotechnetate(VI) compound. Alkali metal salts of the dimeric μ–oxido nitrido fluoridotechnetate(VI) were successfully synthesized from pertechnetate in a one–pot reaction by using $Na_2S_2O_4$ as reducing agent with good yields. On the other hand, nitridotechnetic(VI) acid is a good starting material for the synthesis of nitridofluorido compounds, especially when the competition of other halogen had to be avoided. The products, which can be isolated from solutions of nitridotechnetic(VI) acid with $HF_{(aq)}$ are dependent on the nature of the added cation. Addition of alkali metal cations such as Rb^+ or Cs^+ gave dimeric μ–oxido bridged complexes of the formula $M_4[Tc_2N_2F_8O]$ (M = Rb, Cs), while NEt_4^+ allows the isolation of the di (μ–O) tetrameric compound of the formula $(NEt_4)_3(NH_4)[Tc_4N_4F_8O_4]$.

2.7. References

(1) Lin, Z. Y.; Hall, M. B. *Coord. Chem. Rev.* **1993**, *123*, 149.

(2) Ciechanowicz, M.; Skapski, A. C. *J. Chem. Soc. (A)* **1971**, 1792.

(3) Ciechanowicz, M.; Griffith, W. P.; Pawson, D.; Skapski, A. C.; Cleare, M. J. *J. Chem. Soc. D, Chem. Comm.,* **1971**, 876.

(4) Dao, N. Q.; Breiting, D. *Spectrochim. Acta, Part A.* **1971**, *A 27*, 905.

(5) Baldas, J.; Bonnyman, J.; Pojer, P. M.; Williams, G. A.; Mackay, M. F. *J. Chem. Soc., Dalton Trans.* **1981**, 1798.

(6) Kaden, L.; Lorenz, B.; Schmidt, K.; Sprinz, H.; Wahren, M. *Isotopenpraxis* **1981**, *17*, 174.

(7) Baldas, J. *Top. Curr. Chem.* **1996**, *176*, 37.

(8) Baldas, J.; Boas, J. F.; Bonnyman, J.; Williams, G. A. *J. Chem. Soc., Dalton Trans.* **1984**, 2395.

(9) Baldas, J.; Bonnyman, J.; Williams, G. A. *Inorg. Chem.* **1986**, *25*, 150.

(10) Baldas, J.; Boas, J. F.; Bonnyman, J. *J. Chem. Soc., Dalton Trans.* **1987**, 1721.

(11) Baldas, J.; Boas, J. F.; Bonnyman, J. *Aust. J. Chem.* **1989**, *42*, 639.

(12) Baldas, J.; Boas, J. F.; Ivanov, Z.; James, B. D. *Transition Met. Chem.* **1997**, *22*, 74.

(13) Baldas, J.; Boas, J. F.; Colmanet, S. F.; Ivanov, Z.; Williams, G. A. *Radiochim. Acta* **1993**, *63*, 111.

(14) Kirmse, R.; Stach, J.; Abram, U. *Inorg. Chim. Acta* **1986**, *117*, 117.

(15) Voigt, A.; Abram, U.; Kirmse, R. *Inorg. Chem. Commun.* **1998**, *1*, 141.

(16) Shock, J. R.; Rogers, M. T. *J. Chem. Phys.* **1973**, *58*, 3356.

(17) Manoharan, P. T.; Rogers, M. T. *J. Chem. Phys.* **1968**, *49*, 5510.

(18) Holloway, J. H.; Raynor, J. B. *J. Chem. Soc., Dalton Trans.* **1975**, 737.

(19) Dehnicke, K.; Strähle, J. *Angew. Chem., Int. Ed. Engl.* **1981**, *20*, 413.

(20) Baldas, J.; Boas, J. F. *J. Chem. Soc., Dalton Trans.* **1988**, 2585.

(21) Baldas, J.; Boas, J. F.; Bonnyman, J.; Colmanet, S. F.; Williams, G. A. *J. Chem. Soc., Chem. Commun.* **1990**, 1163.

(22) Nicholson, T.; Kramer, D. J.; Davison, A.; Jones, A. G. *Inorg. Chim. Acta* **2001**, *316*, 110.

(23) Schwochau, K.; Hedwig, K.; Schenk, H. J.; Greis, O. *Inorg. Nucl. Chem. Lett.*, **1977**, *13*, 77.

(24) Cotton, F. A.; Davison, A.; Day, V. W.; Gage, L. D.; Trop, H. S. *Inorg. Chem.* **1979**, *18*, 3024.

(25) Baldas, J.; Boas, J. F.; Ivanov, Z.; James, B. D. *Inorg. Chim. Acta* **1993**, *204*, 199.

(26) Davison, A.; Orvig, C.; Trop, H. S.; Sohn, M.; Depamphilis, B. V.; Jones, A. G. *Inorg. Chem.* **1980**, *19*, 1988.

(27) Schwochau, K.; Linse, K. H.; Pleger, P.; Pleger, U.; Kremer, C.; de Graaf, A. A. *J. Labelled Compd. Radiopharm.* **1996**, *38*, 1031.

(28) Lu, J.; Clarke, M. J. *Inorg. Chem.* **1990**, *29*, 4123.

(29) Baldas, J.; Boas, J. F.; Colmanet, S. F.; Mackay, M. F. *Inorg. Chim. Acta* **1990**, *170*, 233.

(30) Baldas, J.; Colmanet, S. F.; Mackay, M. F. *J. Chem. Soc., Chem. Commun.* **1989**, 1890.

Chapter 3

3. Hexafluoridotechnetate(IV)

3. Hexafluoridotechnetate(IV)

3.1. Introduction

One of the most stable oxidation states of technetium is '+4'. Nevertheless, complexes of Tc^{IV} are relatively limited in number when compared to the neighboring oxidation states. Technetium(IV) complexes often tend to hydrolyze or form polymeric compounds. $TcO_2 \cdot nH_2O$ is the most stable Tc^{IV} compound.

Only two neutral Tc(IV) halides are structurally characterized: $TcCl_4$ and $TcBr_4$. Chlorination of technetium metal with Cl_2 produces dark red $TcCl_4$[1,2] and the structure of this compound was characterized by a single–crystal measurement. The structure consists of polymeric chains, in which the Tc centers are bridged by chlorine atoms, resulting in an edge–sharing, distorted octahedral environment around Tc. It is a suitable starting material for the synthesis of further Tc(IV) compounds, but because of the difficulty of its preparation it is rarely used. The reaction of $TcCl_4$ with Me_3SiBr results in the exchange of the chloride for bromide and gives $TcBr_4$.[3] An improved synthesis of $TcBr_4$ was reported recently by the bromination of Tc metal.[4] The single crystal analysis showed that the structure of $TcBr_4$ consists of infinite ordered chains of edge–sharing $\{TcBr_6\}$ octahedra. Up to date, the neutral TcF_4 is unknown. But its structure was predicted on the basis of the density functional theory.[5] The structure might consist of distorted edge–sharing octahedral groups of TcF_6 linked into endless *cis* chains.

The most common and convenient Tc(IV) starting materials are the binary halide complexes $[TcX_6]^{2-}$ (X = Cl, Br, I). The hexahalogenidotechnetate(IV) anions have been known for a long time and can be prepared by several routes. The most convenient method starts from $[TcO_4]^-$ and conc. HX (X = Cl/Br). Heating is required to ensure that the kinetic intermediate $[TcOX_4]^-$ is completely converted into $[TcX_6]^{2-}$. An alternative procedure is the reduction of $[TcO_4]^-$ in conc. HCl with KI.[6] Recrystallization yields yellow crystals of $K_2[TcCl_6]$. The corresponding bromido/iodido complexes can be prepared by ligand exchange reactions in conc. HX (X = Br/I).[7-9] The K^+, Rb^+, Cs^+ and NH_4^+ salts of $[TcX_6]^{2-}$ (X = Cl, Br, I) have been reported.[10] The above mentioned convenient procedures are not applicable for the preparation of the fluorido analogue.

The hexahalogenidotechnetate(IV) (X= Cl, Br, I) complexes undergo easily hydrolysis with the final formation of the polymeric '$TcO_2 \cdot nH_2O$'. On the other hand, hexafluoridotechnetate is described to be stable towards hydrolysis. $K_2[TcF_6]$ was prepared by analogy with the synthesis of $K_2[ReF_6]$,[11] i.e. from $K_2[TcBr_6]$ in a melt of KHF_2 (T = 220 °C) followed by an aqueous work up.[12] However, this method of synthesis is lengthy and the yield is relatively low. In 1985, R.Alberto *et al*. used an alternative method to prepare the same compound in a higher yield by treating $K_2[TcBr_6]$ with $HF_{(aq)}$ and AgF.[13] The hitherto used method to prepare $[TcF_6]^{2-}$ salts are lengthy and the syntheses of the compounds directly from pertechnetate are unknown.

3.2. Syntheses by metathesis reactions

3.2.1. Reactions of $M_2[TcBr_6]$ (M = K or NH_4) with aHF

An initial attempt was made to do the halogen exchange using aHF. Potassium hexabromidotechnetate(IV) was taken as starting material. The red salt of this compound was then added to aHF under an inert gas atmosphere at –78 °C. This did not result in any reaction even after 5h.

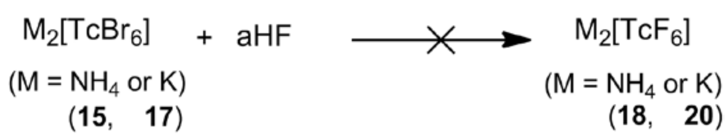

Scheme 3.1

After the complete evaporation of hydrofluoric acid, the hexabromidotechnetate remains as such. This was confirmed by the isolation of single crystals from the reaction mixture. From this reaction it was suspected that the potassium salt has low solubility in aHF. In order to increase the solubility of the starting material, the ammonium salt of hexabromidotechnetate was taken as the technetium precursor. Addition of ammonium hexabromidotechnetate to aHF also resulted in no reaction (Scheme 3.1). The reaction mixture was allowed to warm up to room temperature. The hexabromidotechnetate was completely insoluble in HF even upon heating up to 50 °C and could be recovered quantitatively.

3.2.2. Synthesis by aqueous metathesis reactions using AgF

The metathesis reaction of hexabromidotechnetate with aqueous HF (48%) and AgF resulted in a high yield of hexafluoridotechnetate.[13]

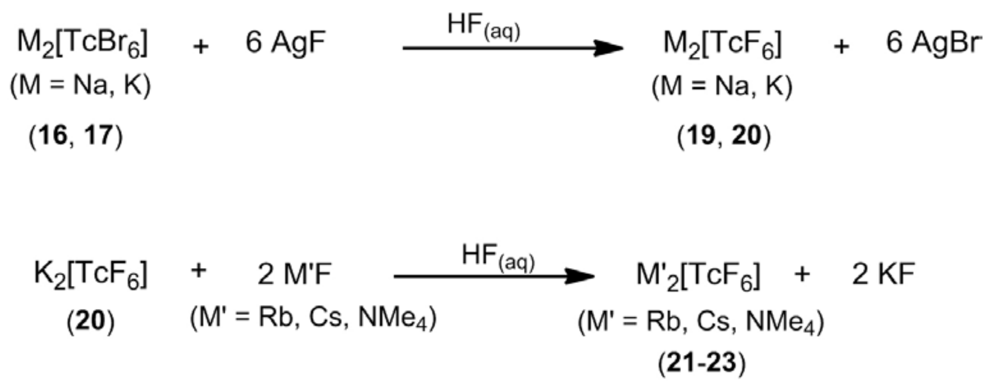

Scheme 3.2

A representative selection of hexafluoridotechnetate salts of $Rb_2[TcF_6]$, $Cs_2[TcF_6]$ and $(NMe_4)_2[TcF_6]$ have been prepared by cation exchange reactions (Scheme 3.2). The driving force of the reaction is the relatively good solubility of $K_2[TcF_6]$ in HF, which allows the precipitation of salts with heavier alkali metal ions and tetramethylammonium cations. Since potassium hexafluoridotechnetate(IV) has a low solubility compared to the corresponding sodium salt, the sodium salt could not be prepared in this way. Thus, sodium hexafluoridotechnetate(IV) was prepared directly from $Na_2[TcBr_6]$ (Scheme 3.2).

3.3. Synthesis from pertechnetate

3.3.1 Reduction by zinc dust

During the reaction of pertechnetate with solutions of HX (X = Cl, Br or I), the X^- ions are readily avaible for coordination, which is not the case with aqueous HF, since the thermodynamic activity coefficient of the fluoride anion is low. Moreover, such solutions contain the mixture of HF_2^- and related species and have strong hydrogen bonded ion pairs such as H_3O^+/F^- and H_3O^+/HF_2^-. Additionally, a reducing agent must be supplied.

Zinc is a common reducing agent for the preparation of low-valent rhenium and technetium complexes.[14,15] The choice of using zinc metal was preferred for the reduction of $[TcO_4]^-$ in acid media.

The synthesis of ammonium hexafluoridotechnetate(VI) was carried out by this reduction/coordination route. Pertechnetate is reduced first with zinc metal and then, the reduced metal center is coordinated with fluorido ligands in the presence of $HF_{(aq)}$ (Scheme 3.3). This reaction led to the reduction of technetium (VII) to technetium (IV).

$$NH_4[TcO_4] + 8\,HF + {}^{3}/_{2}\,Zn \xrightarrow[-\,4\,H_2O]{+\,NH_4F} \underset{(\mathbf{18})}{(NH_4)_2[TcF_6]} + {}^{3}/_{2}\,ZnF_2$$

Scheme 3.3

Upon evaporation of the acid, colorless crystals of $(NH_4)_2[TcF_6]$ were formed, which were mixed with crystals of $ZnF_2{\cdot}4H_2O$. The separation of $(NH_4)_2[TcF_6]$ from this side-product is the main difficulty in the reported procedure, since both compounds possess similar solubilities in HF and water.

3.3.2. Reduction by sodium dithionite

Several hexafluoridotechnetate(IV) salts were successfully synthesized in high yields in one–pot reactions with sodium dithionite as a reducing agent. Reduction of pertechnetate is carried out by the dithionite ion and then, the reduced metal center is coordinated with fluorido ligands in the presence of $HF_{(aq)}$ under reflux (Scheme 3.4). The reaction can readily be tracked by the ^{99}Tc NMR.

$$NH_4[TcO_4] + 5\,HF + {}^{1}/_{2}\,Na_2S_2O_4 \xrightarrow[-\,2\,H_2O,\ -\,NH_4F]{+\,2\,MF} M_2[TcF_6] + NaHSO_4$$

(M = Na, K, Rb, Cs, NMe_4)

(**19-23**)

Scheme 3.4

Sodium bisulfate, which is formed as a side product in this reaction can be removed from the reaction by dissolving the crude product in cold water. Recrystallization of the product from $HF_{(aq)}$ yields pure crystals of the hexafluoridotechnetates(IV). Using this method, alkali metal salts or tetramethylammonium salts of the hexafluoridotechnetate(IV) can be prepared in almost quantitative yields.

3.3.3. Spectroscopic analysis of $M_2[TcF_6]$ salts

Ammonium, alkali metal and tetramethylammonium salts of hexafluoridotechnetate(IV) were characterized by spectroscopic methods. The Tc–F vibrations are observed at about 560 cm^{-1} in the IR spectrum of a series of hexafluoridotechnetate(IV) salts. These values are close to the already reported potassium salt of hexafluoridorhenate(IV) which shows the ν(Re–F) at 550 cm^{-1}.[12]

Krasser and Schwochau reported that the octahedral $[MF_6]^{2-}$ (M = Tc, Re) may show a D_{4h} distortion according to their vibrational spectra.[16] A careful remeasurement of the Raman spectra of $K_2[TcF_6]$, $Rb_2[TcF_6]$ and $Cs_2[TcF_6]$, however, showed another result. The octahedra formed by the $[TcF_6]^{2-}$ anions are compressed along the crystallographic z axis, which lowers the local symmetry of the ion from O_h to D_{3d}. This is reflected by the vibrational spectra of the compounds and can be demonstrated by the Raman spectra of $M_2[TcF_6]$ (M = K, Rb, Cs).

The following irreducible representations apply to the point symmetry D_3d: $\Gamma = 2A_{1g} + A_{1u} + 2A_{2u} + 2E_g + 3E_u$. The A_{1g} and E_g vibrations are Raman active. In case of O_h symmetry, the Raman spectrum exhibits three bands of the symmetry species A_{1g}, E_g and F_{2g}. When the symmetry is lowered to D_{3d}, the F_{2g} band is split into two Raman active bands of the symmetry species A_{1g} and E_g. Depending on the degree of symmetry lowering this splitting of the F_{2g} bending mode can be observed in the Raman spectra.

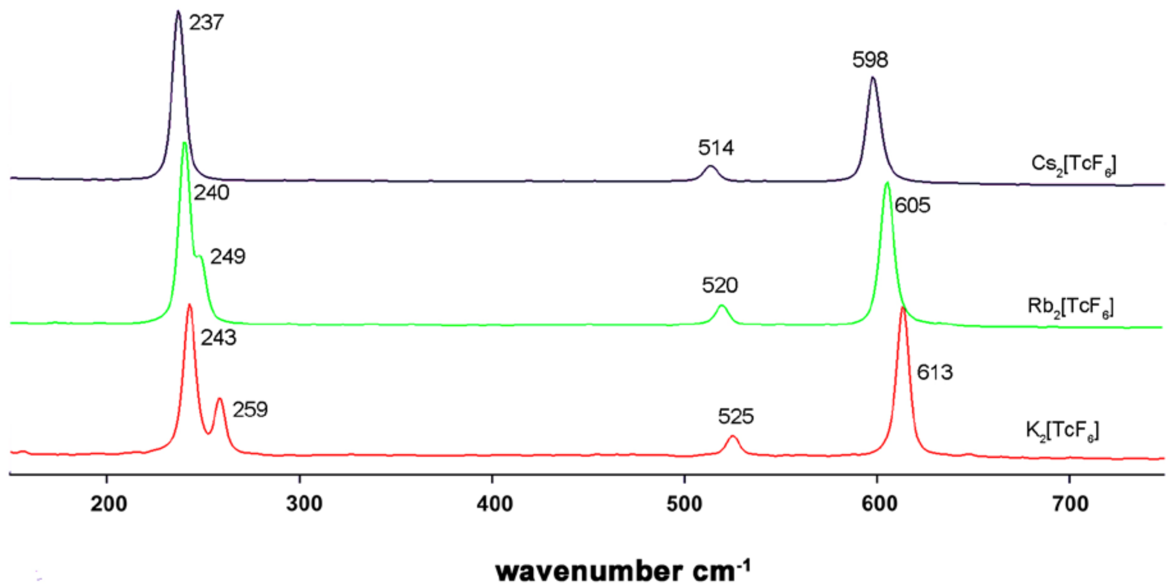

Figure 3.1: Raman spectra of $M_2[TcF_6]$ (M= K, Rb,Cs).

The Raman spectrum of $K_2[TcF_6]$ clearly shows two bands of the Tc–F stretching vibrations (613 and 525 cm^{-1}, A_{1g}, E_g) and two bands in the region of the bending modes (259 and 243 cm^{-1} $F_{2g} \rightarrow A_{1g}$, E_g). Due to the different degree of symmetry lowering, the splitting of the F_{2g} band decreases continuously from $K_2[TcF_6]$ to $Cs_2[TcF_6]$ (Figure 3.1), where it is finally no more resolved. This is completely consistent with single crystal data, which show a variation of F–Tc–F angles (Table 3.2). The Tc–F bond lengths slightly increase from $K_2[TcF_6]$ to $Cs_2[TcF_6]$, which leads to the expected shifts of the Raman bands to lower frequencies. The Raman spectra are completely consistent with single crystal analysis data. Thus, a D_4h symmetry of alkaline metal hexafluoridotechnetate(IV) as was suggested by Krasser can be excluded.[16]

3.3.4. X–ray crystal structures of $M_2[TcF_6]$

Early literature reports that $K_2[TcF_6]$ is pale pink in color.[12] However, no single crystal analysis was done for this compound. Only potassium hexafluoridotechnetate(IV) was studied by the powder X–ray diffraction method.[12] In this work, alkali metal and tetramethylammonium salts of $[TcF_6]^{2-}$ were isolated as colorless crystals and characterized by single crystal X–ray diffraction. The principal crystallographic informations for all the compounds are given in Table 3.1. The compounds

$M_2[TcF_6]$ (M = Na, K, Rb, Cs, NH_4) crystallize in the trigonal system and belong to the space group $P\bar{3}m$. A representative molecular anion and a unit cell plot are given in Figure 3.2.

Table 3.1: Crystal structure data for M_2TcF_6 (M = Na, K, Cs, NH_4, NMe_4)

	$Na_2[TcF_6]$	$K_2[TcF_6]$	$Rb_2[TcF_6]$	$Cs_2[TcF_6]$	$(NH_4)_2[TcF_6]$	$(NMe_4)_2[TcF_6]$
Crystal system	Trigonal	Trigonal	Trigonal	Trigonal	Trigonal	Trigonal
a/Å	5.958(1)	5.796(1)	5.949(1)	6.240(1)	5.943(1)	7.992(1)
b/Å	5.958(1)	5.796(1)	5.949(1)	6.240(1)	5.943(1)	7.992(1)
c/Å	4.757(1)	4.613(1)	4.759(1)	4.980(1)	4.738(1)	20.039(1)
V/Å^3	146.24(5)	134.22(4)	145.86(5)	167.93(5)	144.92(5)	1108.5(2)
Space group	$P\bar{3}m$	$P\bar{3}m$	$P\bar{3}m$	$P\bar{3}m$	$P\bar{3}m$	$R\bar{3}$

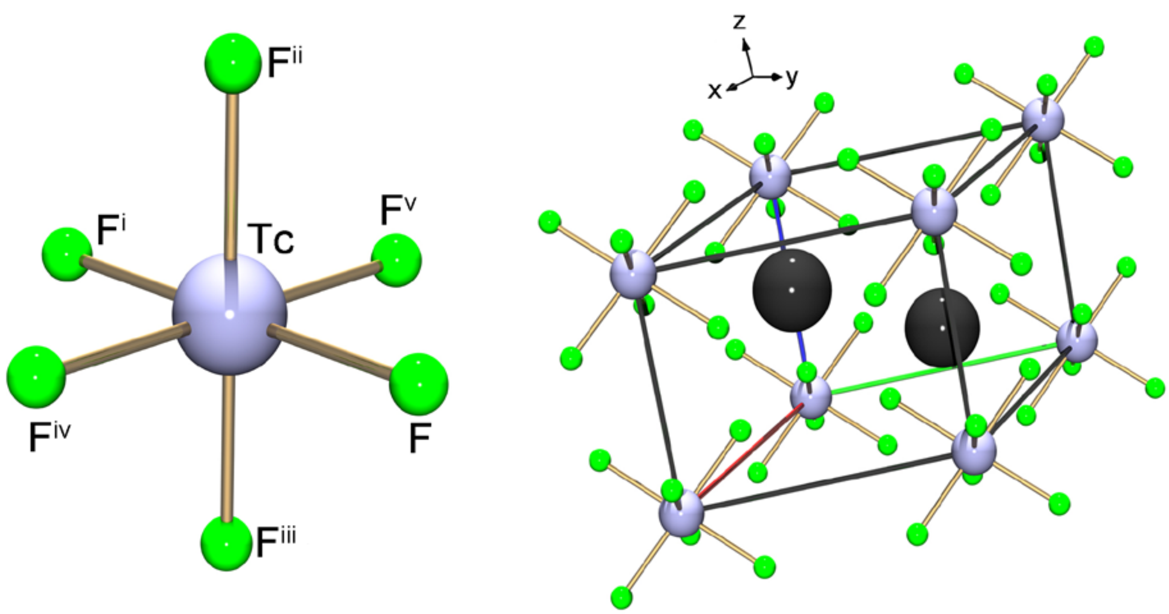

Figure 3.2: Molecular anion of $K_2[TcF_6]$ (left) and unit cell plot of $K_2[TcF_6]$ as representative for $M_2[TcF_6]$ salts (M = Na, K, Rb, Cs, NH_4) (right). Symmetry operations: ^{i} -x-y,-z; ^{ii} y, x-y, -z; ^{iii} -y,x-y,z; ^{iv} -y,-x,z; ^{v} y,x,-z

The unit cell sizes of the alkali metal salts (except potassium) increase in the same order as the ionic radii of the alkali metals increase. Ammonium hexafluoridotechnetate resembles most other ammonium hexafluoridometallates in having a unit cell size comparable to that of the corresponding rubidium salts.

Alkali and ammonium salts of hexafluoridotechnetate are isomorphous and belong to the $K_2[GeF_6]$ structure type.[17] Compounds belonging to the $K_2[GeF_6]$ structure type include $M_2[M'F_6]$ (M = Rb, Cs; M' = Zr, Hf)[18], $M_2[ReF_6]$ (M= Rb, Cs, NH_4)[11,19], $K_2[ReF_6]$[20], $K_2[TcF_6]$ and $Rb_2[TcF_6]$.[21] Bond lengths and selected bond angles of the series of these hexafluoridotechnetate(IV) compounds are given in Table 3.2. The Tc–F bond lengths are in the characteristic range. The octahedral $[TcF_6]^{2-}$ ions are not perfectly regular. For example, in $K_2[TcF_6]$ the Tc–F lengths, 1.928(1) Å, are required to be equal, but the F–Tc–F angles are 180.0(1), 93.0, 86.9(4)°, which shows that the octahedron is slightly compressed along the z axis. A similar compressions were observed for the analogues rhenium compound, $K_2[ReF_6]$[20] and the isoelectronic $[OsF_6]^{-}$ anion in $K[OsF_6]$[22]. The same trend is observed for all other salts of $[TcF_6]^{2-}$ (Table 3.2).

Table 3.2: Bond lengths (Å) and selected bond angles (°) of $M_2[TcF_6]$

Compounds	Bond lengths (Å)	Bond angles (°)		
	Tc–F	F^{i}–Tc–F	F^{i}–Tc–F^{ii}	F–Tc–F^{ii}
$(NH_4)_2[TcF_6]$	1.922(6)	180	92.3(2)	87.7(2)
$Na_2[TcF_6]$	1.895(6)	180	92.4(3)	87.6(3)
$K_2[TcF_6]$	1.928(1)	180	93.07(5)	86.93(5)
$Rb_2[TcF_6]$	1.933(3)	180	92.8(2)	87.2(2)
$Cs_2[TcF_6]$	1.935(5)	180	92.2(2)	87.8(2)

Symmetry operations: ^{i} -x-y,-z; ^{ii} y, x-y, -z

In compounds of the type $M_2[TcF_6]$ (M = Na, K, Rb, Cs and NH_4), the cations are not coplanar with the hexagonal closed packing layer of the F atoms. For example, in $K_2[TcF_6]$, each K^{+} ion has 12 neighboring fluorine atoms in a 3+6+3 arrangement at a distance of 2.784(1) Å, 2.917(1) Å and 2.985(1) Å respectively (Figure 3.3). A similar arrangement was observed in $K_2[ReF_6]$ (2.789(4), 2.957(4), 2.998(4))[20] and $K_2[TiF_6]$ (2.75, 2.87, 3.08).[23] The observed arrangements for the other salts of $[TcF_6]^{2-}$ are given in Table 3.3. In $K_2[GeF_6]$ a 9+3 situation is found.[17]

Table 3.3: 3+6+3 Arrangement with M – F distances in $M_2[TcF_6]$ (M = NH_4, Na, K, Rb, Cs)

Compound	3+6+3 Arrangement with M–F distances (Å)		
$(NH_4)_2[TcF_6]$	2.895(1)	2.996(1)	3.096(1)
$Na_2[TcF_6]$	2.931(1)	3.009(1)	3.112(1)
$K_2[TcF_6]$	2.784(1)	2.917(1)	2.985(1)
$Rb_2[TcF_6]$	2.908(4)	2.999(1)	3.083(4)
$Cs_2[TcF_6]$	3.119(6)	3.156(1)	3.260(5)

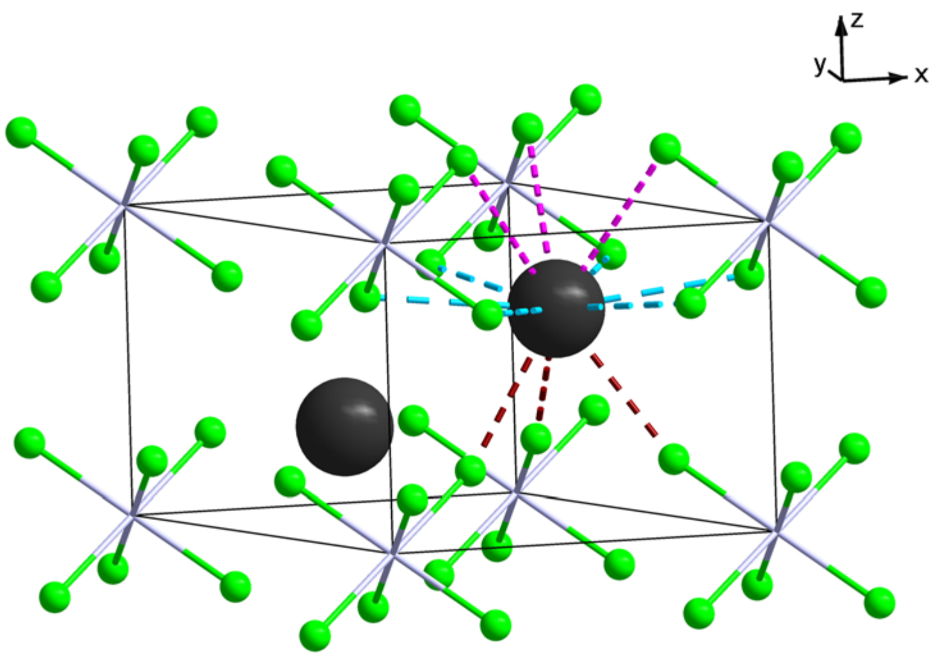

Figure 3.3: 3+6+3 Arrangement in the unit cell plot of $M_2[TcF_6]$ (M = Na, K, Rb, Cs and NH_4).

3.3.5. X–ray crystal structure of $(NMe_4)_2[TcF_6]$

$(NMe_4)_2[TcF_6]$ was prepared by a cation exchange reaction from the potassium salt in aqueous hydrofluoric acid. Upon slow evaporation of the acid, single crystals of the compound were obtained. $(NMe_4)_2[TcF_6]$ crystallizes in the rhombohedral space group $R\bar{3}$. The infrared spectrum of $(NMe_4)_2[TcF_6]$ reveals the Tc–F vibrations at 565 cm^{-1}. The C–H vibrations are observed around

3000 and 1396 cm^{-1}. Vibrations attributable to the C–N bonds are observed at 948 cm^{-1}. The assignments are consistent with $(NMe_4)_2[TiF_6]$ (Table 3.4).

Table 3.4: Infrared vibrations (cm^{-1}) for $(NMe_4)_2[MF_6]$ (M = Tc, Ti)

Compound	M–F	C–N	C–H	Reference
$(NMe_4)_2[TcF_6]$	565	948	3012, 1487	present
$(NMe_4)_2[TiF_6]$	556	950	3033, 1488	[24]

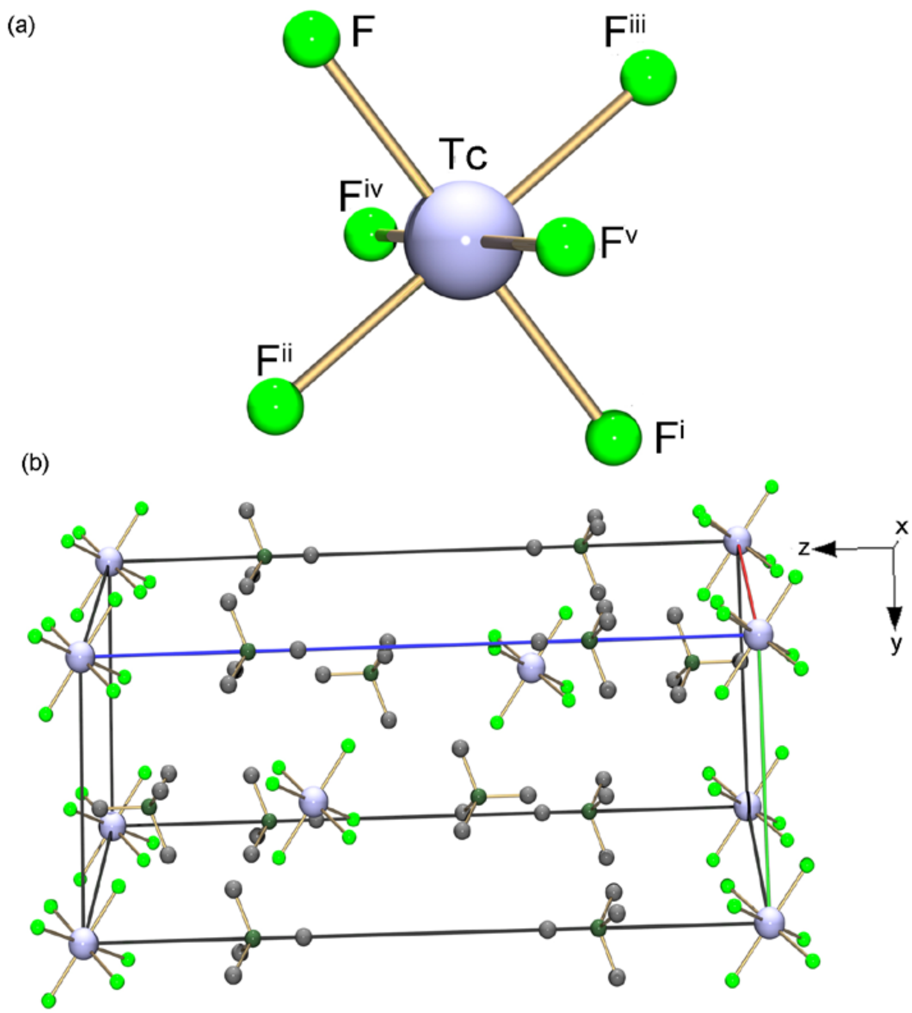

Figure 3.4: (a) Molecular structure of the complex anion and (b) unit cell plot of $(NMe_4)_2[TcF_6]$. Hydrogen atoms bonded to carbon atoms were omitted for clarity. Symmetry operations: ^{i} –x+4/3,-y+2/3,-z+2/3; ^{ii} –y+1,x-y,z; ^{iii} –x+y+1,-x+1,z; ^{iv} x-y+1/3,x-1/3,-z+2/3; ^{v} y+1/3,-x+y+2/3,-z+2/3

Figure 3.4 shows the molecular structure of the complex anion and a unit cell plot of $(NMe_4)_2[TcF_6]$. The crystal structure is composed of regular $[TcF_6]^{2-}$ octahedra and well separated counter ions, which results in a zero–dimensional molecular compound such as the isostructural $(NMe_4)_2[TiF_6]$.[24] Selected bond lengths and angles are given in Table 3.5. The bond length Tc–F is 1.922(2) Å. The F–Tc–F bond angles cis and *trans* to each other are 89.81(8)°, 90.19(8)° and 180.0° respectively.

Table 3.5: Selected bond lengths (Å) and angles(°)for $(NMe_4)_2[MF_6]$ (M = Tc, Ti)

Bondlengths (Å)	$(NMe_4)_2[TcF_6]$	$(NMe_4)_2[TiF_6]$[24]
Tc–F	1.929(2)	1.849(2)
Bond angles (°)		
$F–Tc–F^{i}$	180.0	180.0(2)
$F^{i}–Tc–F^{ii}$	90.2(1)	90.2(1)
$F–Tc–F^{ii}$	89.8(1)	89.8(1)

3.4. Hydrolysis of $[TcF_6]^{2–}$

Technetium(IV) complexes frequently tend to hydrolyse and finally form the polymeric ‘$TcO_2 \cdot n\ H_2O$’. Thus, the aqueous chemistry of $[TcX_6]^{2–}$ (X = Cl, Br, I) is very limited. The reaction of $[TcX_6]^{2–}$ (X = Cl, Br) with aqueous ammonia results in a brown–black precipitate of ‘$TcO_2 \cdot n\ H_2O$’(Scheme 3.5).[25]

$$(NH_4)_2[TcX_6] \ + \ 4\ NH_3 \ + \ 4\ H_2O \longrightarrow TcO_2 \cdot 2H_2O \ + \ 6\ NH_4X$$

(X = Cl, Br)

Scheme 3.5

$[TcF_6]^{2–}$ is known to be stable against hydrolysis. The compound can be recrystallized from water. The color of the compound was described as pale pink in early reports.[12] This is surprising, since the isolated single crystals of the $[TcF_6]^{2–}$ salts are colorless. The reason for the pale pink color can now be attributed to the hydrolysis product of $[TcF_6]^{2-}$. A hydrolysis of pure $(NH_4)_2[TcF_6]$ in aqueous ammonia was observed and the product of the first hydrolysis step of $[TcF_6]^{2–}$, the dimeric oxido–bridged complex $[Tc_2OF_{10}]^{4-}$ could be isolated as pale pink colored crystals (Scheme 3.6).The color of the crystals cleared up the early uncertainties about the color of the $[TcF_6]^{2-}$. The triammonium sodium salt of the dimeric complex crystallizes from a solution of $(NH_4)_2[TcF_6]$ in aqueous ammonia after the addition of NaF as pale pink crystals. This compound was characterized by both spectroscopic and single crystal X–ray analyses.

$$\underset{(\mathbf{18})}{2\,(NH_4)_2[TcF_6]} + 2\,NH_3 + H_2O \xrightarrow{NaF} \underset{(\mathbf{24})}{Na(NH_4)_3[Tc_2OF_{10}]\cdot 2NH_4F} + NH_4F$$

Scheme 3.6

3.4.1. Spectroscopic analysis of $(NH_4)_3Na[Tc_2OF_{10}]$

In the IR spectrum, an absorption at 913 cm^{-1} is assigned to the Tc–O stretching vibration. The absorption at 731 cm^{-1} is assigned to the Tc–O–Tc vibration. The band at 555 cm^{-1} is assigned to the Tc–F vibration. In the Raman spectrum, the band at 1086 cm^{-1} was assigned to the Tc–O vibration. The bands between 606 and 235 cm^{-1} are assigned to the Tc–F vibrations.

UV/visible Spectra

UV/vis spectroscopy offers a convenient method for studying the ongoing hydrolysis of the compound in solution. Freshly prepared samples of the $K_2[TcF_6]$ salt are completely colorless. The previously described pale pink color could not be detected visually or in the UV/Vis spectra of the compound. They show the previously detected intense absorptions at 291 nm ($\varepsilon = 22.5\ M^{-1}cm^{-1}$) and 352 nm ($\varepsilon = 16.2\ M^{-1}cm^{-1}$), but no band in the range between 300 and 600 nm. Aqueous solutions of $K_2[TcF_6]$, however, slowly turn their color and appear pale pink after a period of 5 weeks. This goes along the increase of the absorption around 290 nm and a decrease of that at 350 nm. Additionally, a very weak absorption appears around 550 nm (Figure 3.5). This band is consistent with an absorption, which is observed in the spectrum of a hydrolysis product of $[TcF_6]^{2-}$.

Thus, the pink color is not directly related with hexafluoridotechnetate, but with ongoing hydrolysis in (alkaline) aqueous media. This conclusion is supported by the discussion in an early report about the rhenium analogue $[ReF_6]^{2-}$, where a pink color was only observed in samples which came from the fusion of KHF_2 and $K_2[ReBr_6]$ with subsequent aqueous work-up, but not for $K_2[ReF_6]$, which resulted from gas phase reactions between the same precursor and absolute HF.[11]

Figure 3.5 shows the UV/Vis spectrum of the hydrolysis product with absorptions at 290 nm (ε = 2096 $M^{-1}cm^{-1}$), 547 nm (38.9 $M^{-1}cm^{-1}$). It is highly probably that the spectral changes in aqueous solutions of $[TcF_6]^{2-}$ in the long-term experiment discussed above can be explained by the slow formation of a decomposition product, with the formula $(NH_4)_3Na[F_5Tc–O–TcF_5]\cdot 2(NH_4F)$, as could be seen in the X-ray structure analysis.

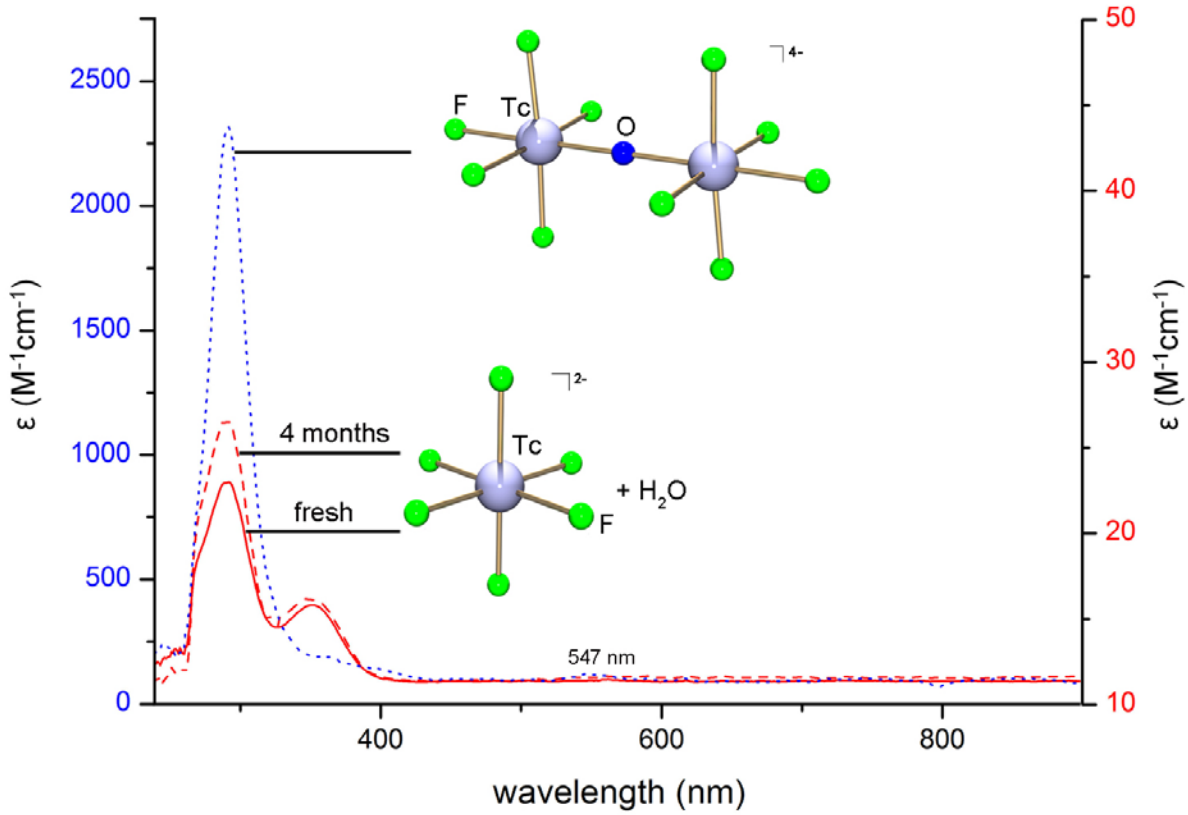

Figure 3.5: UV/vis spectra of (a) K_2TcF_6 immediately after dissolution in H_2O (red solid line) and after 4 months (red dotted line) and of $(NH_4)_3Na[F_5Tc–O–TcF_5]\cdot 2(NH_4F)$ (blue line).

3.4.2. X–ray crystal analysis of $(NH_4)_3Na[Tc_2OF_{10}]\cdot 2(NH_4F)$

The compound crystallizes in the centrosymmetric orthorhombic space group Pbam. The solid state structure contains 5 ammonium, 1 sodium, 2 fluoride and the complex $[Tc_2OF_{10}]^{4-}$ ions. The molecular structure of the anion and the unit cell plot of the compound are shown in Figure 3.6. The structure confirms the composition of the pink crystal as an oxido–bridged dimeric complex. Selected bond lengths and angles are given in Table 3.6. The Tc–F bond lengths fall into two groups: (a) 1.928 Å-1.947 Å for Tc–F1 and Tc–F3 bonds; and (b) 1.977 Å for the Tc–F2 bond. The Tc–O bond length of 1.8519(6) in the central Tc–O–Tc unit is relatively short and suggests considerable π-bonding involving the donation of electrons from the p_x and p_y orbitals of oxygen to d_π orbitals of the metal ion. A similar bonding situation is observed for $[\{TcCl_3(H_2O)\}_2O]$ with a Tc–O bond length of 1.8124(8) in the central Tc–O–Tc unit.[26] The $[F_5Tc–O–TcF_5]^{4-}$ crystallizes after the addition of NaF. The co-crystallized NaF stabilizes the solid state structure: they connect the complex anions by the formation of stable $\{NaF_6\}$ octahedra (see (b) in Figure 3.6)

Table 3.6: Selected bond lengths (Å) and angles (°) in $Na(NH_4)_3[Tc_2OF_{10}]\cdot 2NH_4F$

Bond lengths (Å)					
Tc–O1	1.852(1)	N(1)–F1	3.101(3)	Na–F3	2.350(3)
Tc–F1	1.928(3)	N(1)–F2	2.759(3)	Na–F4	2.228(6)
Tc–F2	1.977(5)	N(1)–F3	3.087(3)	N(3)–F1	2.900(1)
Tc–F3	1.947(3)	N(1)–F4	3.075(5)	N(3)–F3	2.917(1)
N(2)–F1	2.923(2)	N(2)–F2	3.100(5)	N(2)–F3	2.917(3)
N(2)–F4	2.740(3)				
Bond angles (°)					
O1–Tc–F3	92.8(1)	F3–Tc–F3^{i}	90.4(2)	O1–Tc–F2	179.5(2)
Tc–O1–Tc^{ii}	180	F1–Tc–F3	174.2(2)	F1–Tc–F1^{i}	92.0(2)
O1–Tc–F1	92.9(1)	F1^{i}–Tc–F3	88.5(2)	F3–Tc–F2	87.6(1)
F1–Tc–F2	86.8(2)				

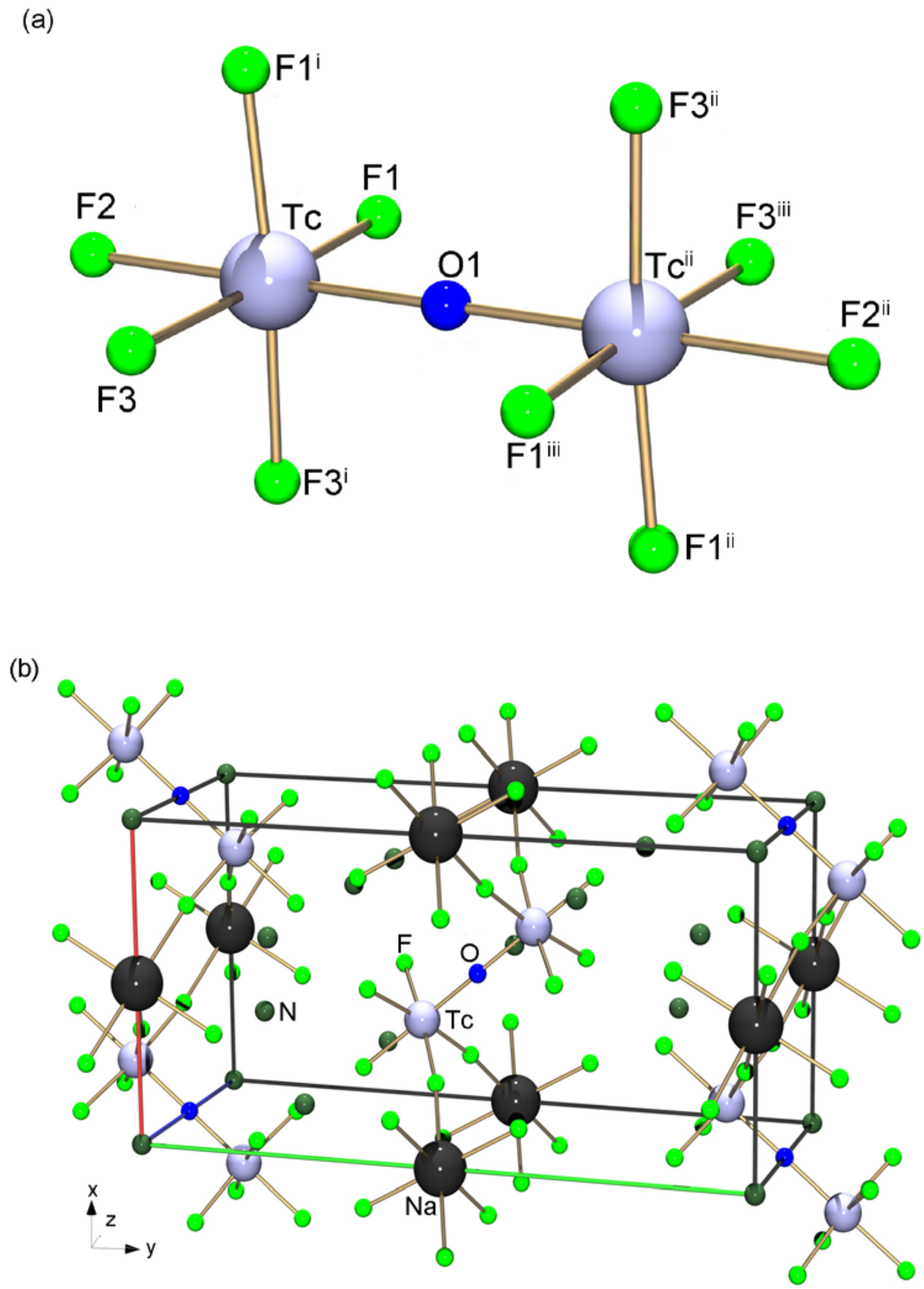

Figure 3.6: (a) Molecular anion of $[Tc_2F_{10}O]^{4-}$ and (b) unit cell plot of $(NH_4)_3Na[Tc_2F_{10}O]\cdot 2NH_4F$. Symmetry operators: ^{i} x,y,-z+1; ^{ii} –x,-y+2,-z+1; ^{iii} -x,-y+2,z

A slightly distorted octahedral arrangement around technetium is observed. The technetium atom is situated about 0.096(1) Å above the basal plane, towards the oxido ligand. The N···F distances between the ammonium nitrogen and fluorine atoms are in the range of 2.740 – 3.101 Å, which is comparable to the distance found in $(NH_4)_2[TcF_6]$ (2.930 – 3.114 Å) and in $(NH_4)_2NaMF_6$ (M = Fe, Ga, Cr) (2.996 – 3.109).[27] This indicates the presence of hydrogen bonds in this structure. The Na–F distances are 2.228 and 2.350 Å respectively. The distances of ammonium and sodium cations to the fluoride anions are comparable with the distances found for the $M_2[TcF_6]$ (M = NH_4, Na) salts.

3.5. Reactions of $M_2[TcF_6]$ salts

Attempts to prepare $M_2[TcF_6]$ (M = K, Rb or Cs) with bulky organic cations such as NBu_4^+ or $AsPh_4^+$ by cation exchange reactions, with crown ethers and with ionic liquids by cation capturing failed. A possible reason may be strong ionic interactions between the cations and the hexafluoridotechnetate(IV) anions, which prevents the precipitation of the anion with the organic cations. Alkali metal salts of hexafluoridotechnetate are soluble in both $HF_{(aq)}$ and water. However, attempted reactions with water soluble ligands such as sodium maleonitriledithiolate, potassium trispyrazolylborate also failed even under aqueous conditions and reflux. In these cases, the precursors were recovered.

The reaction of $K_2[TcF_6]$ with KCN under aqueous conditions leads to the formation of $K_3[TcO_2(CN)_4]$. In this case a oxidation of Tc(IV) to Tc(V) occurs. However, this compound is already known.[28]

3.6. Reactions of $[TcF_6]^{2-}$ with Lewis acids

Fluoride-ion capture from their anionic derivatives by strong fluoride ion acceptors such as AsF_5 or SbF_5 in aHF solutions provides a general approach for the synthesis of binary fluorides.[29] K_2TcF_6 has been known for a long time but the parent binary fluoride, TcF_4, has not yet been isolated. The only information known up to now about TcF_4 is a calculation by density functional theory (DFT), which predicts stability for this compound.[5] Recently, it was reported that the polymeric tetrafluorides, MF_4 (M = Mo, Ru, Pd, Re and Os) were precipitated from their $[MF_6]^{2-}$ salts in absolute HF in the presence of Lewis acids at 20 °C and studied by powder X–ray diffraction.[30] AsF_5 was used to displace the fluorido ligands for M = Ru, Os and Pd, and SbF_5 was used for M = Re and Mo, since ReF_4 and MoF_4 are more easily oxidized during the reaction with AsF_5 and rapidly give M^V products. Due to these results, a reaction with SbF_5 was chosen for technetium. The proposed synthesis of TcF_4 can therefore be given by the following equations:

$$K_2[TcF_6] + 2\ SbF_5 \longrightarrow TcF_4 + 2\ KSbF_6$$

Scheme 3.7

The reaction was carried out in an S shaped PFA tube sealed at one end. $K_2[TcF_6]$ was added to a mixture of aHF and SbF_5 at –196° C. The reaction mixture was brought to –20° C and a pale tan–yellow compound was precipitated. The compound redissolved in excess of aHF at 25° C leaving behind a trace amount of precipitate. The precipitate formed was carefully separated and transferred into the Schlenk tube under inert conditions. More precipitate of the compound, dissolved in the excess of aHF was observed when the temperature was kept below –20° C. The precipitate was carefully dried under vacuum at –20° C after decanting the aHF, by which $KSbF_6$ was removed from the reaction mixture. It was also noted that the precipitate in the PFA tube remains pale yellow–tan in color when the temperature is kept below –20° C. At RT, the color of the compound changed from yellow to orange–red and finally to dark violet. The Raman measurement of the tan–yellow precipitate was measured in the PFA tube (Figure 3.7).

The color of the precipitate in the Schlenk glass tube changed from pale yellow to dark violet and the Raman measurement of this precipitate showed only fluorescence. The product formed is extremely air sensitive and moisture sensitive and is only stable below –20° C. The extreme sensitivity of the tetrafluoride is also observed for niobium.[31] Notably, NbF_4 reacts with glass container in the presence of traces of water. Similar tendency was observed for the yellow precipitate of the technetium fluoride compound formed.

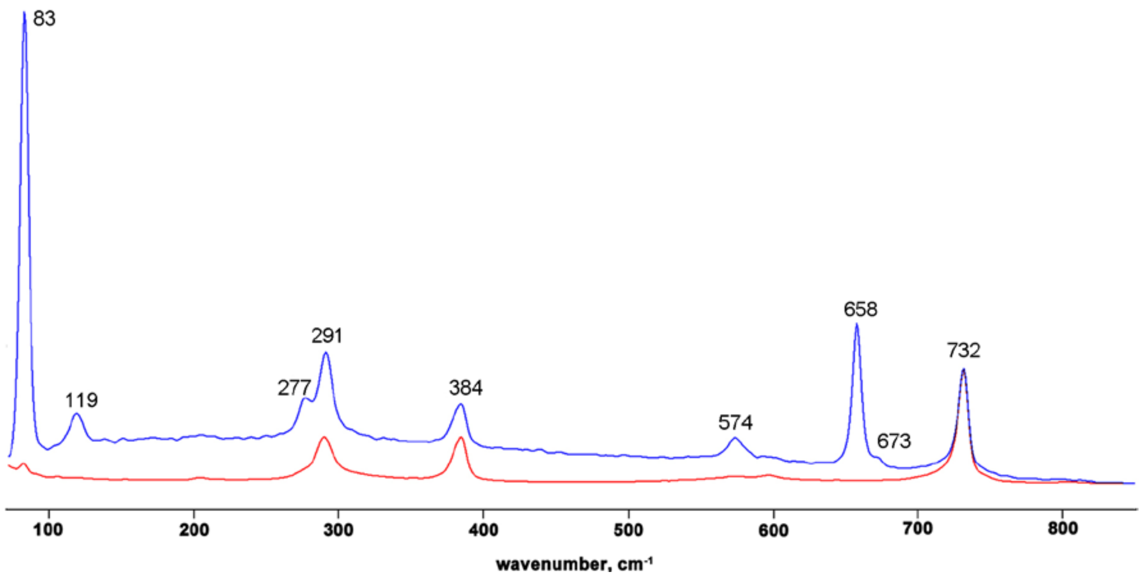

Figure 3.7: Raman spectrum of the precipitate from the $K_2[TcF_6]$, SbF_5, aHF reaction. Red color: PFA tube; Blue color: Yellow-tanTcF_4 solid in PFA tube

Table 3.7: Comparison of bands due to Tc-F stretching modes

TcF_4 (a)	TcF_5 (b)	TcF_6 (b)	MoF_4 (c)
673(sh)	749(s)	713(s)	746
658(s)	693(s)	639	710
574(w)	669(w)	239	690
277(sh)	282(w)	145	280
119(w)	225(w)		251
	139(w)		211
			176
			142

(a) present work, (b) Ref [32] (c)[33]

DFT calculations predicted that TcF_4 is isomorphous with $TcCl_4$ and $TcBr_4$ structures. In this case, the structure of TcF_4 also consists of distorted cis edge-sharing bioctahedra linked to endless chains.[5] The structure of this yellow tan TcF_4 is not reported here, but it also is expected to be dominated by Tc-F-Tc bridging. The frequencies from the Raman spectrum of TcF_4 are compared with the Raman spectra of TcF_5, TcF_6 and MoF_4 are given in Table 3.7. The structure of TcF_5 consists of two crystallographically different octahedra, which are linked through cis-bridging fluorine atoms to form endless chain. Apparently TcF_6 is octahedral in the solid state. The bands at 713 cm^{-1} in TcF_6 and at 749 and 693 cm^{-1} in TcF_5 arise from the symmetric Tc-F stretching modes. The strong band at 658 cm^{-1} and a shoulder at 673 cm^{-1} in TcF_4 is likely due to a symmetric stretching mode. The frequency at 673 and 658 cm^{-1} of this mode is lower than the corresponding mode of TcF_5 (749 and 693 cm^{-1}). This observation is consistent with the trend observed for MoF_4 (722 cm^{-1}) and MoF_5 (759 and 738 cm^{-1}).[33]

A broad absorption at 574 cm^{-1} is assigned to Tc-F-Tc bridging mode and is consistent with the infrared bands of ReF_4 (528 cm^{-1}, br), OsF_4 (532 cm^{-1}, br) and IrF_4 (545 cm^{-1}, br).[34] This band is further evidence for the highly bridged polymeric structure of the yellow tan solid.

An initial attempt of the same reaction with an excess of SbF_5 in aHF in a PFA tube was carried out. In this way, decantation and back distillation of aHF could not be done. However, a blue colored precipitate was isolated from the reaction mixture after evaporation of aHF. The by-product, $KSbF_6$ could not be excluded from the reaction mixture. It was proposed that, the product might be TcF_4. Thus, a reaction with CH_3CN was carried out. This attempt was made by an analogy to a reaction of $TcCl_4$ with CH_3CN, which resulted in the formation of a $[TcCl_4(CH_3CN)_2]$ complex.[26] It was expected that the reaction of dry acetonitrile with the blue precipitate might result in the formation of $[TcF_4(CH_3CN)_2)]$. The product mixture, TcF_4 and $KSbF_6$ was transferred into a Schlenk tube. Addition of acetonitrile to the reaction mixture resulted in a dark green solution. While reducing the volume, it gave green crystals of an oxido–bridged dimeric technetium acetonitrile complex.

The green crystals obtained were characterized both spectroscopically and crystallographically. The infrared spectrum of this compound exhibits characteristic ν(C≡N) stretching vibrations at 2324 and 2299 cm^{-1}, which correspond to coordinated acetonitrile ligands. The Tc–O–Tc stretch is observed at 852 cm^{-1}. The presence of $[SbF_6]^-$ is readily discernible by the appearance of a strong Sb–F near 657 cm^{-1}. The Raman spectrum of the crystals shows vibrations at 2327 and 2295 cm^{-1}, which were assigned to coordinated CH_3CN ligands. The vibration at 955 cm^{-1} was assigned to the Tc–O–Tc stretching. The vibration at 644 cm^{-1} was assigned to the Sb–F stretching of $[SbF_6]^-$.

An X–ray crystal analysis of the green crystals revealed that the compound crystallizes in the monoclinic space group C2/c. The structure of this compound is shown in Figure 3.8. Selected bond lengths and angles are given in Table 3.8. The product is a dimeric oxido-bridged acetonitrile complex. From the crystal structure, it was critical to define the anion present in the compound was either $[TcF_6]^{2-}$ or $[SbF_6]^{-}$. In this case, the oxidation state of technetium present in the cation would be decided by the anion of the complex. Technetium analysis of the crystalline samples by liquid scintillation method provided the solution of this problem. The experimentally obtained technetium value is 11.9% and is close to the calculated technetium value for the formula of $[Tc_2O(CH_3CN)_{10}][SbF_6]_4{\cdot}CH_3CN$, which is 12.3%. Thus, the anion of the complex was refined as $[SbF_6]^{-}$ ion which define the oxidation state of technetium as +3 in this complex.

Table 3.8: Selected bond lengths (Å) and angles (°) in $[Tc_2O(CH_3CN)_{10}][SbF_6]_4{\cdot}CH_3CN$

Bond lengths (Å)		Bond angles (°)	
Tc(1)–N(1)	2.085(5)	Tc(1)–O(1)–Tc(1)’	180.0
Tc(1)–N(2)	2.069(5)	O(1)–Tc(1)–N(4)	178.9(2)
Tc(1)–N(3)	2.077(5)	N(1)–Tc(1)–N(5)	175.0(2)
Tc(1)–N(5)	2.069(5)	N(1)–Tc(1)–N(2)	90.6(2)
Tc(1)–N(4)	2.132(5)	N(2)–Tc(1)–N(4)	87.2(2)
Tc(1)–O(1)	1.792(1)	N(5)–Tc(1)–N(4)	88.9(2)

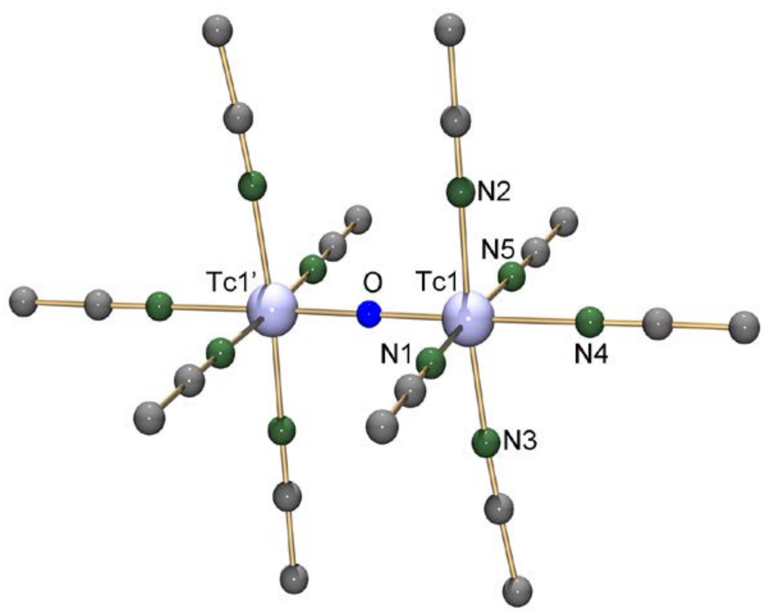

Figure 3.8: Molecular anion of $[Tc_2O(CH_3CN)_{10}][SbF_6]_4{\cdot}CH_3CN$. Symmetry operators (’) -x+1,-y+1,-z+1. Hydrogen atoms were omitted for clarity.

The technetium atom in the $[Tc_2O(CH_3CN)_{10}]^{4+}$ cation is coordinated in a distorted octahedral environment. It is situated about 0.0858(4) Å above the basal plane, toward the oxido ligand. The Tc–O bond length of the central Tc–O–Tc unit is 1.792(1) Å. The axial Tc–N bond lengths of 2.069 – 2.085 Å are comparable to that of the Tc–N bond lengths of 2.062 Å in $[Tc_2(CH_3CN)_{10}](BF_4)_4$.[35] The Tc–N bonds, which are *trans* to the oxido ligand are slightly longer than the Tc–N bonds in equatorial position. This can be understood by the *trans* influence of the oxido ligand in the bridging position.

3.7. Summary and conclusions

Straightforward syntheses of $[TcF_6]^{2-}$ from pertechnetate in one-pot reactions by using Zn dust or $Na_2S_2O_4$ as reducing agents were presented. For the first time, single crystal analyses of hexafluoridotechnetates(IV) for the series of alkali metal, ammonium and tetramethylammonium salts were performed. The isolation of first step hydrolysis product of hexafluoridotechnetate(IV) allowed the characterization of an oxido-bridged fluoridotechnetium(IV) compound. Synthesis of TcF_4 was attempted by using SbF_5 and aHF and the compound was characterized by Raman spectroscopy.

3.8. References

(1) Colton, R. *Nature* **1962**, *193*, 872.

(2) Guest, A.; Lock, C. J. L. *Can. J. Chem.* **1972**, *50*, 1807.

(3) Abram, U.; Wollert, R.; Hiller, W. *Radiochim. Acta* **1993**, *63*, 145.

(4) Poineau, F.; Rodriguez, E. E.; Forster, P. M.; Sattelberger, A. P.; Cheetham, A. K.; Czerwinski, K. R. *J. Am. Chem. Soc.* **2009**, *131*, 910.

(5) Weck, P. F.; Kim, E.; Poineau, F.; Rodriguez, E. E.; Sattelberger, A. P.; Czerwinski, K. R. *Inorg. Chem.* **2009**, *48*, 6555.

(6) Elder, M.; Fergusson, J. E.; Gainsford, G. J.; Hickford, J. H.; Penfold, B. R. *J. Chem. Soc. (A)* **1967**, 1423.

(7) Colton, R. *The Chemistry of Rhenium and Technetium*; Interscience Publishers: London, **1965**,

(8) Peacock, R. D. *The Chemistry of Technetium and Rhenium*; Elsevier: Amsterdam, **1966**,

(9) Dalziel, J.; Gill, N. S.; Nyholm, R. S.; Peacock, R. D. *J. Chem. Soc.* **1958**, 4012.

(10) Bandoli, G.; Mazzi, U.; Roncari, E. *Coord. Chem. Rev.* **1982**, *44*, 191.

(11) Weise, E. *Z. Anorg. Allg. Chem.* **1956**, *283*, 377.

(12) Schwochau, K.; Herr, W. *Angew. Chem., Int. Ed.* **1963**, *75*, 95.

(13) Alberto, R.; Anderegg, G. *Polyhedron* **1985**, *4*, 1067.

(14) Young, R. C.; Irvine, J. W. *J. Am. Chem. Soc.* **1937**, *59*, 2648.

(15) Eakins, J. D.; Humphreys, D. G.; Mellish, C. E. *J. Chem. Soc.* **1963**, 6012.

(16) Krasser, W.; Schwochau, K. *Z. Naturforsch. A.* **1970**, *A 25*, 206.

(17) Hoard, J. L.; Vincent, W. B. *J. Am. Chem. Soc.* **1939**, *61*, 2849.

(18) Bode, H.; Teufer, G. *Z. Anorg. Allg. Chem.* **1956**, *283*, 18.

(19) Peacock, R. D. *J. Chem. Soc.* **1956**, 1291.

(20) Clark, G. R.; Russell, D. R. *Acta Crystallogr., Sect. B: Struct. Sci.* **1978**, *34*, 894.

(21) Schwochau, K. *Z. Naturforsch. A.* **1964**, *A 19*, 1237.

(22) Hepworth, M. A.; Jack, K. H.; Westland, G. J. *J. Inorg. Nucl. Chem.* **1956**, *2*, 79.

(23) Siegel, S. *Acta Cryst.* **1952**, *5*, 683.

(24) Kim, E.; Lee, D. W.; Ok, K. M. *J. Solid State Chem.* **2012**, *195*, 149.

(25) Jones, A. G.; Davison, A. *Int. J. Appl. Radiat. Isot.* **1982**, *33*, 867.

(26) Yegen, E.; Hagenbach, A.; Abram, U. *Chem.Comm.* **2005**, 5575.

(27) Mi, J.-X.; Luo, S.-M.; Sun, H.-Y.; Liu, X.-X.; Wei, Z.-b. *J. Solid State Chem.* **2008**, *181*, 1723.

(28) Trop, H. S.; Jones, A. G.; Davison, A. *Inorg. Chem.* **1980**, *19*, 1993.

(29) Žemva, B.; Lutar, K.; Chacon, L.; Felebeuermann, M.; Allman, J.; Shen, C.; Bartlett, N. *J. Am. Chem. Soc.* **1995**, *117*, 10025.

(30) Casteel, W. J.; Lohmann, D. H.; Bartlett, N. *J. Fluorine Chem.* **2001**, *112*, 165.

(31) Gortsema, F. P.; Didchenko, R. *Inorg. Chem.* **1965**, *4*, 182.

(32) Schwochau, K.;*Technetium chemistry and Radiopharmaceutical applications*. Wiley-VCH: New York, 2000.

(33) Bates, J. B. *Inorg. Nucl. Chem. Lett.*, **1971**, *7*, 957.

(34) Paine, R. T.; Asprey, L. B. *Inorg. Chem.* **1975**, *14*, 1111.

(35) Cotton, F. A.; Haefner, S. C.; Sattelberger, A. P. *J. Am. Chem. Soc.* **1996**, *118*, 5486.

Chapter 4

4. Fluoridonitrosyltechnetium complexes

4. Fluoridonitrosyltechnetium complexes

4.1. Introduction

Transition metal nitrosyl complexes have been known for many years and they have attracted as much as attention as metal carbonyls. The NO molecule can bind to a metal ion either with the N or O atoms to give nitrosyl (M–NO) or isonitrosyl (M–ON) ligands. In most cases, the nitrogen atom of the NO group is bonded to the metal ion. The M–N–O angles can be linear or bent, up to ca. 120°. The NO ligand in the metal complexes may exist as NO^+ (nitrosonium cation), $NO^{\cdot}$ and NO^- (nitroxide anion). In a molecular orbital approach, the bonding of NO to a metal is considered to be made up of two components. The first involves donation of electron density from a σ–type orbital of NO onto the metal, and the second back–donation from the metal d orbitals to π* orbitals of NO.[1]

The first low valent nitrosyl complex of technetium was prepared by Eakins *et al*. from the reaction of $[TcCl_6]^{2-}$ with hydroxylamine.[2] The complex formed was originally formulated as $[Tc(NH_2OH)_2(NH_3)_3(H_2O)]Cl_2$. This compound was reformulated as $[Tc(NO)(NH_3)_4(H_2O)]Cl_2$ by Armstrong and Taube,[3] which was later confirmed by a crystal structure analysis. The compound is diamagnetic with Tc in the formal oxidation state of "1".[4] The corresponding Tc(II) compound was prepared by a one electron oxidation of the compound by potassium dichromate or ceric sulfate in perchloric acid and was studied by EPR spectroscopy. [5] In an earlier study, Armstrong and Taube showed that it is possible to exchange the ammine ligands by chloride ligands in 2M hydrochloric acid. Isolation of this compound opens the new branch for low-valent nitrosyl complexes of technetium.

Nitrosyl complexes of technetium are frequently prepared by the reactions of common Tc starting materials such as phosphine complexes of Tc(III), TcO_2, hexahalogenidotechnetate(IV), tetrahalogenidooxidotechnetate(V) or pertechnetate with NO gas or with hydroxylamine hydrochloride.[6-12] Only in some exceptional cases, the nitrosyl ligand was introduced by other sources such as NO^+ salts, HNO_3, $NaNO_2$ or NO_2.[13-15] Most of the products contain the metal in its formal oxidation states "1" or "2" with almost linear coordinated nitrosyl ligands, which are consequently considered as "NO^+" species. Only, a limited number of compounds is known with the metal in the oxidation state "+3".[16] Hitherto, nitrosyltechnetium complexes with fluorido ligands are unknown.

Hydroxamic acid undergoes hydrolysis to hydroxylamine and carboxylic acid.[17] Especially, acetohydroxamic acid (AHA) has drawn some attention due to its reducing and complexing capability. Recently Gong *et al*. reported that the reductive nitrosylation of pertechnetate in aqueous nitric acid and perchloric acid solutions forms a hydrophilic technetium complex of the formula $[Tc(NO)(AHA)_2(H_2O)]^+$,[18] which was proposed for its impact for the recovery of technetium in the nuclear fuel cycle. However, the complex could not be isolated in the solid state and was only analyzed by spectroscopic methods. This alternate synthetic approach for the nitrosyl ligand was considered to be interesting to prepare nitrosyl fluorido complexes of technetium.

4.2. Synthesis of $[Tc(NO)(NH_3)_4F]_4[TcF_6][HF_2]_2$

The reaction of $[TcF_6]^{2-}$ with acetohydroxamic acid (AHA) in aqueous hydrofluoric acid results in a reductive nitrosylation and the formation of $[Tc(NO)(NH_3)_4F]_4[TcF_6][HF_2]_2$. This compound was characterized by IR and Raman spectroscopy and the structure was determined by single crystal X–ray analysis. Reductive nitrosylation of ammonium pertechnetate by $CH_3CONHOH$ (AHA) in HNO_3 results in the Tc(II) complex $[Tc^{II}(NO)(AHA)_2H_2O]^+$.[18] This compound was studied in detail by spectroscopic methods. The reaction requires an aqueous medium and acidic condition. The nitrosyl source for the product was explained by the stepwise decomposition of AHA under acidic conditions, since hydroxamic acids are known to decompose into hydroxylamine and the corresponding carboxylic acids.[17] Thus, hydroxyl amine most probably is involved in the nitrosyl formation, eventhough the final product most probably contains AHA^- ligands. Gong *et al*. also reported that $(n–Bu_4N)_2[TcCl_6]$ and AHA in dry ethanol did not undergo any reaction. In contrast, the reaction of $[TcF_6]^{2-}$ with acetohydroxamic acid in aqueous solution in the presence of hydrofluoric acid results in the formation of orange–red crystals of $[Tc(NO)(NH_3)_4F]_4[TcF_6][HF_2]_2$ after a few days (Scheme 4.1).

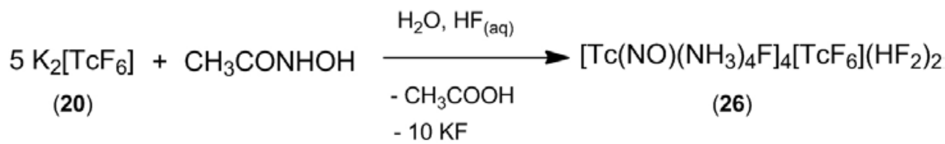

Scheme 4.1

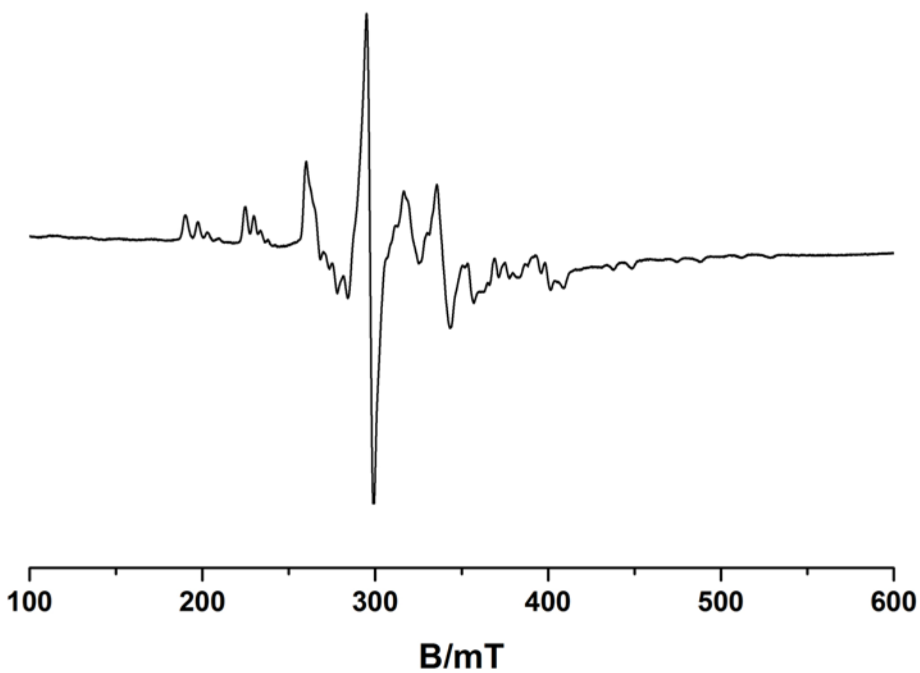

Figure 4.1: Frozen solution X-Band EPR spectrum of a reaction mixture between $K_2[TcF_6]$ and AHA in $HF_{(aq)}$.

The reaction occurs very slowly at room temperature, but the transformation is almost quantititative after a period of several days. The corresponding reaction in warm (60°C) or boiling HF does not form the technetium(I) ammine complex immediately, but forms Tc(II) compounds of various compositions as could be confirmed by EPR spectroscopy (Figure 4.1). Pure samples or single crystals of these Tc(II) compounds could not been obtained from this reaction mixture. However, after a few days, the technetium (I) ammine complex, $[Tc(NO)(NH_3)_4F]^+$ was isolated. This explains the Tc(II) complexes were formed as intermediate products in the reactions, which undergo further reduction and forms the final Tc(I) complex as a single product .

4.2.1. Spectroscopic analysis

The IR and Raman spectra of crystals of the compound were measured at room temperature and the normal modes of vibrations were assigned based on C_{4v} symmetry. The complete assignments are given in Table 4.1 and compared with $[M(NO)(NH_3)_4F]SiF_6$ (M = Os, Ru)[19] and $[Ru(NO)(NH_3)_5]Br_3$.[20]

Table 4.1: Experimental IR and Raman vibrational frequencies, assignments and mode

Mode	$[Tc(NO)(NH_3)_4F]_4X$	$[M(NO)(NH_3)_4F]SiF_6$ M = Os	M = Ru	$[Ru(NO)(NH_3)_5]Br_3$
ν(N–O)	1676(IR)	1840(IR)	1894(IR)	1927(IR)
ν_{as}(N–H)	3341, 3262(IR), 3351, 3273(R)	3320, 3220(IR)	3327, 3225(IR)	3240(IR)
ν_s(N–H)	3187(IR), 3203(R)	–	–	3150(IR), 3180(R)
δ_s(H–N–H)	1377, 1278(IR) 1257, 1290, 1312(R)	1370, 1350, 1340(IR)	1347, 1325, 1300(IR)	1358(IR)
δ_{as}(H–N–H)	1650(IR), 1608, 1626, 1659(R)	–	–	1606(IR)
δ(M–N–H)	836(IR), 778(R)	895–800	847	844(IR)
δ(M–N–O)	635(IR), 628(R)	630(IR), 629(R)	620(R)	602(IR)
ν(M–NO)	602(R)	650(IR), 650(R)	648(IR), 648(R)	594(R)
ν(Tc–F)	559(IR), 504, 521, 619(R)	560(IR), 560(R) 524(IR), 524(R)	547(IR), 543(R) 508(IR), 510(R)	–

X = $[TcF_6][HF_2]_2$; IR: infrared; R: Raman

The N–O stretching vibration of $[Tc(NO)(NH_3)_4(F)]^+$ is observed at 1679 cm^{-1}, which is similar to the value of $[Tc(NO)(NH_3)_4(H_2O)]Cl_2$, in which the N–O stretch is observed at 1680 cm^{-1}.[3] The bending vibrations of H–N–H and Tc–N–H are observed at 1376 cm^{-1}, 836 and 809 cm^{-1} respectively. The Raman active Tc–NO stretch is observed at 602 cm^{-1} and is comparable with that of the ruthenium complex. The strong band at 559 cm^{-1} in IR and 619 cm^{-1} in Raman spectra are assigned to Tc–F.

The bands at 1278, 1215 cm^{-1} are assigned to the ν_2(E) mode and the band at 635 cm^{-1} is assigned to the $\nu_1(A_1g)$ mode of HF_2^- by comparision with $NaHF_2$.[21] The vibrations at 744 and 765 cm^{-1} are assigned to the F···H–N type hydrogen bonds between the ammonia molecules and $[TcF_6]^{2-}$. These assignments are made by comparison with $[M(NO)(NH_3)_4F][SiF_6]$ (M = Os, Ru).[19] The ^{99}Tc NMR signal of the diamagnetic $[Tc(NO)(NH_3)_4F]^+$ cation can be detected at 1928 ppm ($\Delta\nu_{1/2}$ = 2600 Hz) (Figure 4.2). This value is outside the range of Tc(I) complexes, the signals of which normally appear between -400 to -3350 ppm.[22-24] The reason for this unusal chemical shift cannot be explained unambiguously, since there are no other ^{99}Tc NMR data of nitrosyl compounds for comparison.[14] The relatively large linewidth is not unusual and due to distortions of the octahedral symmetry of the complex by the presence of three different ligands. This increases the electric field gradient at the metal nucleus and strengthens the quadrupole relaxation of the system.[24] The ^{19}F NMR spectrum shows a resonance at -143.5 ppm, which is in accordance with values, which have been found earlier for fluorido ligands in the axial positions of transition metal nitrosyl complexes of $[Ru(NO)F_5]^{2-}$ or $[Os(NO)F_5]^{2-}$.[25] Protons of the NH_3 ligands rapidly exchange with D_2O.

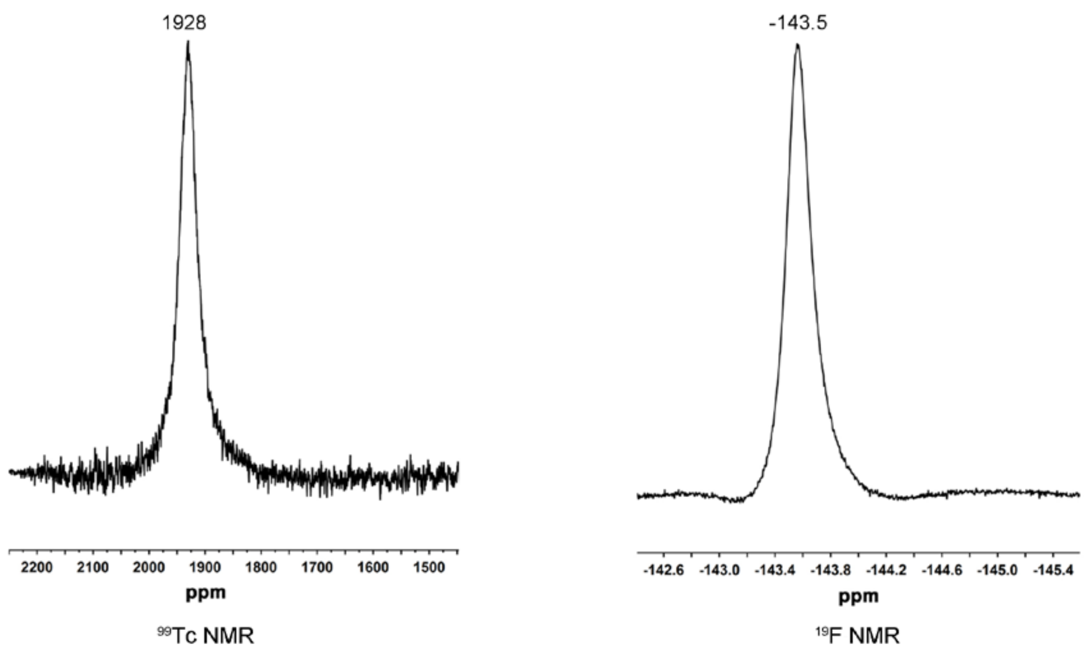

Figure 4.2: ^{99}Tc and ^{19}F NMR spectra of the $[Tc(NO)(NH_3)_4F]^+$ cation.

4.2.2. Single crystal X–ray analysis

The compound $[Tc(NO)(NH_3)_4F]_4[TcF_6][F_2H]_2$ crystallizes in the monoclinic space group C2/m with 2 formula units in the unit cell. The *trans* configuration of the $[Tc(NO)(NH_3)_4F]^+$ cation in this complex was confirmed by crystal structure determination and the same motif is observed in $[Tc(NO)(NH_3)_4(OH_2)]Cl_2$[4] and $[M(NO)(NH_3)_4F]^{2+}$ (M = Os, Ru).[19] The molecular structure of $[Tc(NO)(NH_3)_4F]_4[TcF_6][F_2H]_2$ is shown in Figure 4.3. Selected bond lengths and angles are given in Table 4.2. The bonding situation in the Tc–NO linkage shows Tc–NO bond lengths of 1.718(4) Å and 1.716(5) Å with relatively long N–O bond lengths of 1.227(6) Å and 1.207(6) Å. These N–O bond lengths are expectedly ~ 0.07 and 0.05 Å longer than the length of the free NO molecule (N–O: 1.1507 Å). The average length of the $Tc–NH_3$ bonds is 2.162 Å. This is in the characteristic range for Tc–N single bonds. The Tc–F bond length in the $[[Tc(NO)(NH_3)_4F]^+$cation, in which the fluorine atom is coordinated *trans* to a nitrosyl group is considerably longer than the Tc–F bond lengths in the $[TcF_6]^{2-}$ ions. This longer bond length reflects the *trans* influence of the nitrosyl ligand.

Table 4.2: Selected bond lengths (Å) and angles (°) for $[Tc(NO)(NH_3)_4(F)]_4[TcF_6][F_2H]_2$

Bond lengths (Å)			
Tc(1)–N(1)	1.718(4)	Tc(2)–N(5)	1.716(5)
N(1)–O(1)	1.227(6)	N(5)–O(2)	1.207(6)
Tc(1)–N(2)	2.172(5)	Tc(2)–N(5)	2.171(3)
Tc(1)–N(3)	2.163(3)	Tc(2)–N(6)	2.161(3)
Tc(1)–N(4)	2.142(5)	Tc(2)–F(2)	2.036(3)
Tc(1)–F(1)	1.988(3)	Tc(3)–F(3)	1.922(3)
H(10)–F(5)	1.16(1)	Tc(3)–F(4)	1.915(2)
Bond angles (°)			
Tc(1)–N(1)–O(1)	178.0(4)	Tc(2)–N(5)–O(2)	179.5(4)
N(1)–Tc(1)–F(1)	179.0(2)	N(5)–Tc(2)–F(2)	178.8(1)
N(1)–Tc(1)–N(4)	97.3(2)	N(5)–Tc(2)–N(7)	95.4(1)
N(1)–Tc(1)–N(3)	96.7(2)	N(5)–Tc(2)–N(6)	95.4(1)

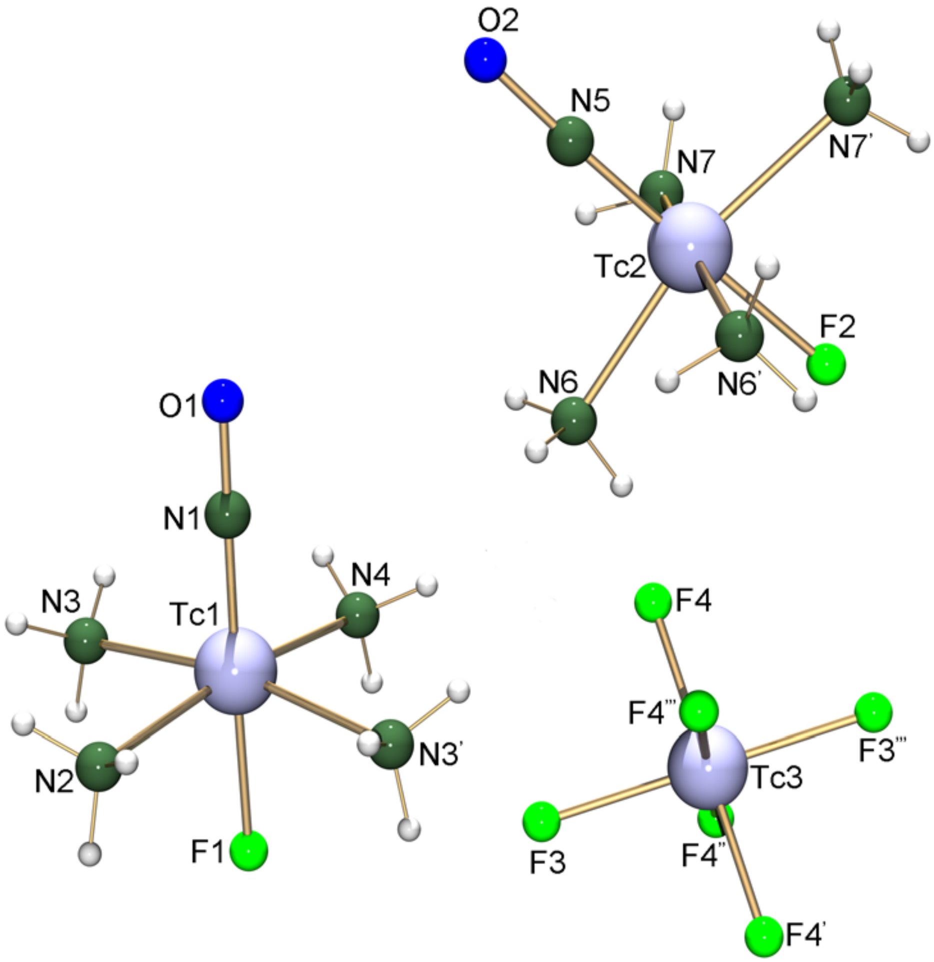

Figure 4.3: Molecular representation of the technetium containing species in $[Tc(NO)(NH_3)_4F]_4[TcF_6][F_2H]_2$.Symmetry operators: ’ x,-y+1,z; ’’ -x,y,-z; ’’’i -x,-y+1,-z.

The average Tc–N–O angle of 178.75° confirms the linearity of the Tc–NO linkage. The steric bulk of the nitrosyl ligand causes some ‘roof effect’, which results in N1/N5–Tc–NH_3 angles all being larger than 90°. The technetium atoms of the two $[Tc(NO)(NH_3)_4F]^+$ cations are displaced from the mean least-square planes of the four NH_3 ligands by 0.1942(2) Å and 0.2020(2) Å, respectively. A series of hydrogen bonds formed between the ammine ligands in the cation and fluorine atoms of the hydrogendifluoride and hexafluoridotechnetate(IV) ions are shown in the unit cell plot of the compound (Figure 4.4). They are listed in Table 4.3.

Table 4.3: Hydrogen bonds in $[Tc(NO)(NH_3)_4F]_4[TcF_6][F_2H]_2$

D–H···A	d(D–H)	d(H···A)	d(D···A)	<(DHA)
N(3)-H(3B)...F(5)	0.89	2.24	3.061(4)	153.1
N(4)-H(4A)...F(4)	0.89	2.43	3.182(5)	142.2
N(4)-H(4C)...F(5)	0.89	2.06	2.916(3)	161.1
N(6)-H(6C)...F(4)	0.89	2.59	3.321(4)	139.6
N(2)-H(2B)...F(4)^{iv}	0.89	2.59	3.031(4)	111.6
N(2)-H(2C)...F(4)^{v}	0.89	2.59	3.031(4)	111.6
N(3)-H(3A)...F(1)^{iv}	0.89	2.09	2.902(4)	151.5
N(3)-H(3C)...F(3)^{iv}	0.89	2.15	3.000(5)	158.9
N(4)-H(4A)...F(4)^{i}	0.89	2.43	3.182(5)	142.2
N(4)-H(4B)...F(5)^{vi}	0.89	2.06	2.916(3)	161.1
N(7)-H(7A)...N(7)^{vii}	0.89	2.55	3.423(6)	165.5
N(7)-H(7B)...F(5)^{vii}	0.89	2.17	2.893(4)	138.2
N(7)-H(7C)...O(2)^{vii}	0.89	2.18	3.056(4)	167.6
N(6)-H(6A)...F(3)^{iii}	0.89	2.57	2.998(4)	110.2
F(5)-H(10)...F(5)^{viii}	1.16(1)	1.16(1)	2.259(5)	153(4)

symmetry operators: ^{i} x,-y+1,z; ^{iii} -x,-y+1,-z; ^{iv} -x+1/2,-y+1/2,-z; ^{v} -x+1/2,y+1/2,-z; ^{vi} -x,y,-z+1; ^{vii} -x+1/2,-y+1/2,-z+1; ^{viii} x,-y,z

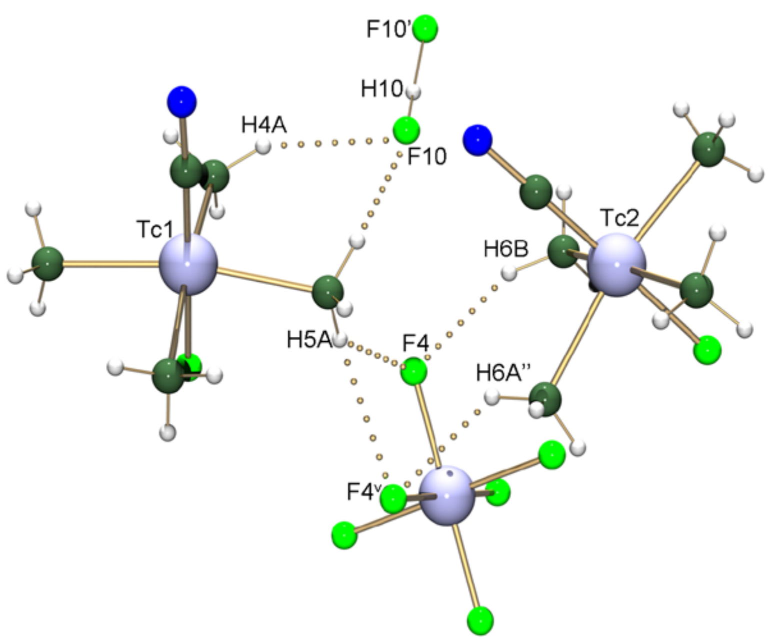

Figure 4.4: Hydrogen bonds within the asymmetric unit in $[Tc(NO)(NH_3)_4F]_4[TcF_6][F_2H]_2$

4.3. Synthesis of $M_2[Tc(NO)F_5]$ (M = K, Rb, Cs)

Aqueous acetohydroxamic acid reacts with $NH_4[TcO_4]$ in aqueous hydrofluoric acid (48%) under formation of an orange-red solution, which turned into bluish–green under reflux. The reductive nitrosylation was followed by both ^{99}Tc NMR and EPR spectroscopy. The absence of a pertechnetate signal in the ^{99}Tc NMR spectrum of this reaction mixture confirms the complete reduction of the precursor. EPR measurement of the reaction mixture show that a mixture containing at least two paramagnetic complexes is formed (Figure 4.5). The same reaction with conc. HCl forms exclusively the monomeric $[Tc(NO)Cl_5]^{2-}$ in solution.

Further treatment with alkali metal fluoride salts MF (M = Rb, Cs) or KPF_6 gave blue crystals of $M_2[Tc(NO)F_5]\cdot H_2O$ (M = K, Rb, Cs) as a first product. The second Tc(II) compound (see arrow in Figure 4.5) could not be isolated. Nevertheless, the remaining solution upon slow evaporation at room temperature after a few days yielded orange-red crystals of a Tc(I) ammine complex of the composition $[Tc(NO)(NH_3)_4F](HF_2)\cdot 1/2$ MF (M = Rb, Cs) or $[Tc(NO)(NH_3)_4F](PF_6)\cdot 1/2\ KPF_6$ as a second product from the reaction mixture (Scheme 4.2). The sources for the nitrosyl and ammine ligands can be explained by the decomposition of acetohydroxamic acid.

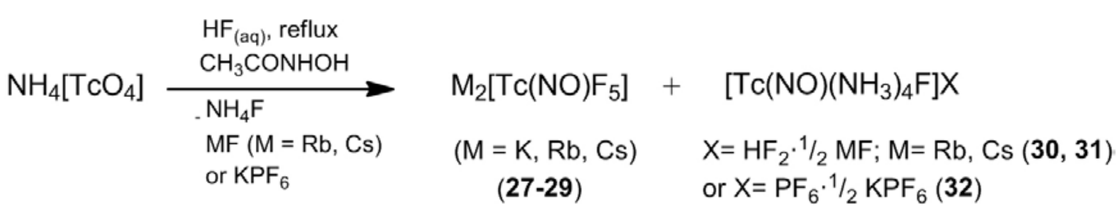

Scheme 4.2

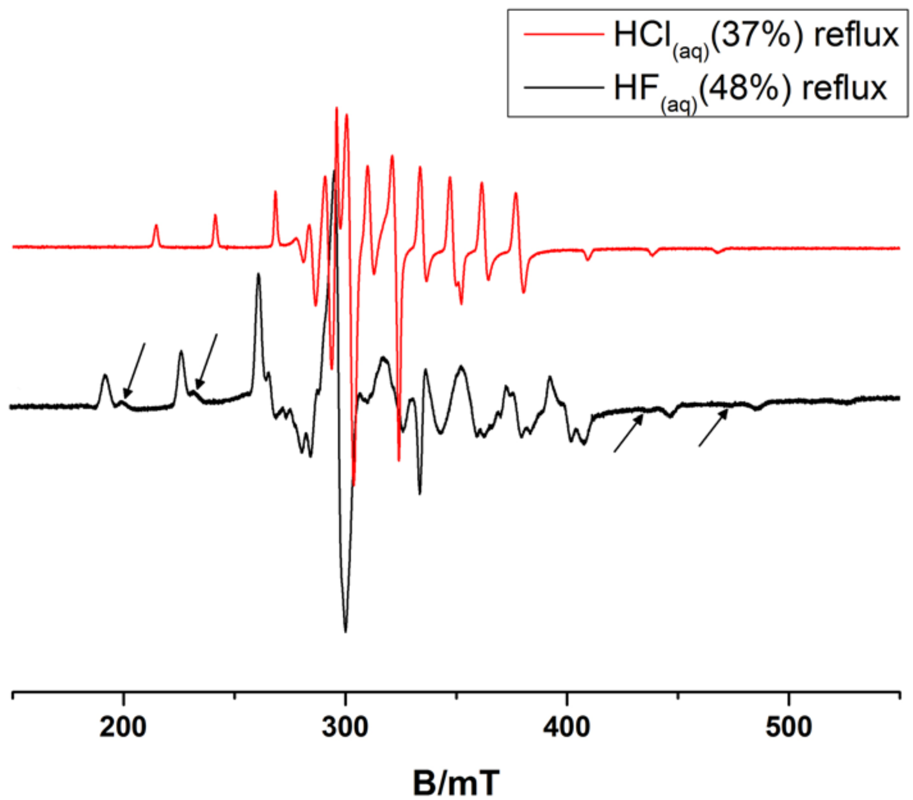

Figure 4.5: Frozen solution X-Band EPR spectra of the reaction mixtures of $NH_4[TcO_4]$ and AHA in $HX_{(aq)}$ (X = F/Cl).

4.3.1. Spectroscopic analysis

IR and Raman spectra of $M_2[Tc(NO)F_5]\cdot H_2O$ (M = K, Rb, Cs) were recorded at room temperature. The frequencies and assignments for $K_2[Tc(NO)F_5]\cdot H_2O$ are listed in Table 4.4 and the spectrum is shown in Figure 4.6. For C_{4v} symmetry, thirteen vibrational modes ($\Gamma = 5A_1+2B_1+B_2+5E$) are expected, all of which are Raman active. Only A1 and the E modes are IR active.

$M_2[Tc(NO)F_5]\cdot H_2O$ salts (where M = K, Rb, Cs) crystallize in the space group Cmcm, which belongs to the crystal class mmm (D_{2h}). While isolated ions $[Tc(NO)F_5]^{2-}$ are C_{4v} symmetric, in the aforementioned salts, their local symmetry is lowered to C_{2v}. The atoms Tc1, F4, N1 and O1 lie on the special position m2m. Depending on the degree of symmetry lowering this can lead to an observable splitting of the E modes. Additionally, in the crystal class D_{2h}, a weak splitting of the normal modes may occur due to the coupling of the normal modes of the four anions of the unit cell.

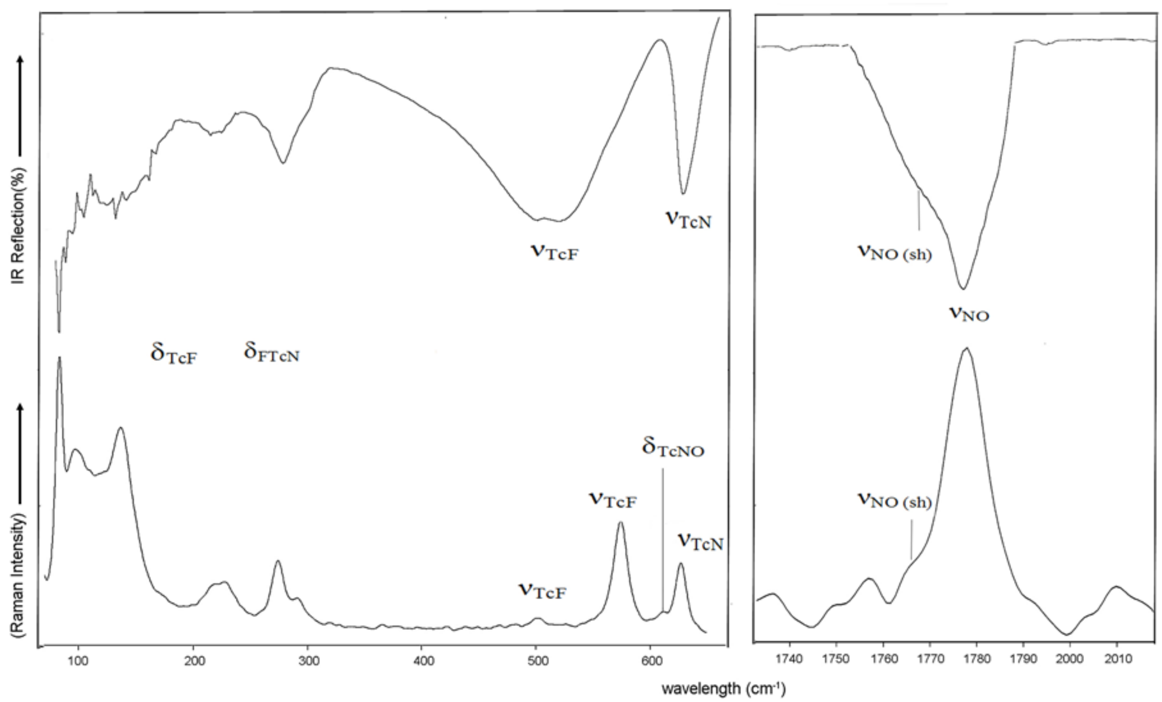

Figure 4.6: IR and Raman spectra of $K_2[Tc(NO)F_5]\cdot H_2O$.

The intense double band at ca. 1780 cm^{-1} and 1768 cm^{-1} in the IR and Raman spectra is attributed to the N-O stretching vibration. The splitting can be explained by the interaction of the four anions in the unit cell. The two bands at 627 cm^{-1} and 610 cm^{-1} are assigned to the ν(TcN) stretching vibration and δ(TcNO) bending vibration by comparison with $Na_2[Ru(NO)F_5]\cdot H_2O$[26] and $(CH_2py_2)[Ru(NO)FCl_4]$.[27] The band at ca. 520 cm^{-1} is assigned to the $\nu_3(A_1)$ mode of ν(TcF) vibrations.

The vibrational modes between 574 and 482 cm^{-1} correspond to $\nu(Tc\text{-}F_{ax})$ and $\nu(Tc\text{-}F_{eq})$ bonds. The observed vibrational modes between 265 and 97 cm^{-1} correspond to bending modes. Further assignments cannot be made because of the complexity of the possible band splittings. This would require either the recording of the spectra of the pentafluoridonitrosyltechnetate(II) salts in solution, which is not possible due to its low solubility or data of computed spectra, which are not available. It cannot be ruled out that the very weak bands in the region of the ν(TcF) vibrations may arise from trace impurities in the sample.

Table 4.4: Vibrational spectra of crystalline $K_2[Tc(NO)F_5]\cdot H_2O$

IR	Raman	Expected modes for C_{4V}	Assignements
1780	1778	A_1	ν_{NO}
1768(sh)	1766(sh)		
627	627	A_1	ν_{TcN}
610	610	E	δ_{TcNO}
567	574	$2\times A_1$	ν_{TcF}
529	527(vw)	B_1	
	534(vvw)	E	
501	501		
482	482(vw)		
287	291	A_1	δ_{TcF}, δ_{FTcN}
265	274	B_1	
	227	B_2	
~212	218	$3\times E$	
	137		
	97		

UV/visible spectra

The UV/visible spectrum of $Cs_2[Tc(NO)F_5]\cdot H_2O$ in HF (13.8 M) exhibits three different maxima between 200 and 700 nm and is shown in Figure 4.7. The assignment of the bands of $[Tc(NO)F_5]^{2-}$ is done by comparison with $[Re(NO)Cl_5]^{2-}$, which was studied on the basis of a simplified molecular orbital diagram.[28] In $Cs_2[Tc(NO)F_5]$, absorptions at 586 nm (ε = 13.9 $M^{-1}cm^{-1}$) and 397 nm (ε = 23.1 $M^{-1}cm^{-1}$) and the shoulder at 237 nm (ε = 334.2 $M^{-1}cm^{-1}$) are assigned to d→d transitions. The absorptions at 216 nm (ε=541.3 $M^{-1}cm^{-1}$) and at 315 nm (ε = 28.8 $M^{-1}cm^{-1}$) are assigned to the d→π^*_{NO} transitions.

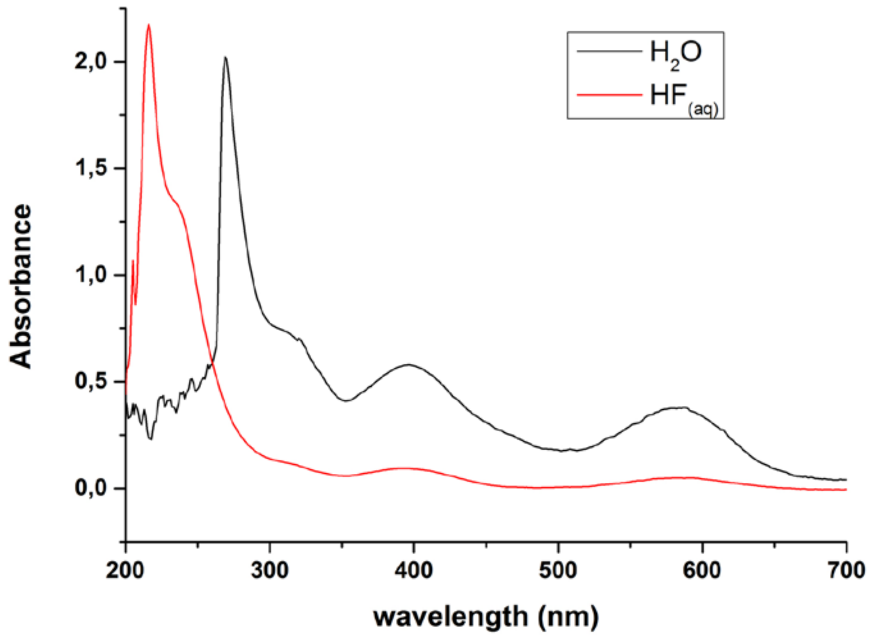

Figure 4.7: UV/visible spectrum of $Cs_2[Tc(NO)F_5]\cdot H_2O$ in H_2O (black line) and $HF_{(aq)}$ (red line).

Hydrolysis of $Cs_2[Tc(NO)F_5]\cdot H_2O$ is accelerated in aqueous solution. This can be seen by the red shift in the UV/visible spectrum of an aqueous solution of $Cs_2[Tc(NO)F_5]\cdot H_2O$. This hydrolysis process is further supported by the absence of EPR signal of $Cs_2[Tc(NO)F_5]\cdot H_2O$ in water.

EPR spectroscopy

The d^5 low-spin configuration (S = ½) of $M_2[Tc(NO)F_5]\cdot H_2O$ (M= K, Rb, Cs) is readily detected by EPR spectroscopy. A frozen solution EPR spectrum of $Rb_2[Tc(NO)F_5]\cdot H_2O$ in $HF_{(aq)}$ is given in Figure 4.8 and is characteristic for an axially symmetric spectrum.

Line width considerations limit the component of the superhyperfine interactions parallel to the Tc–NO direction to less than $2\times10^{-4}cm^{-1}$. The EPR parameters are given in Table 4.5.

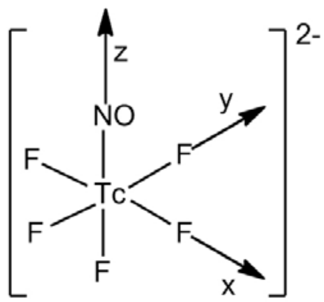

(**C**)

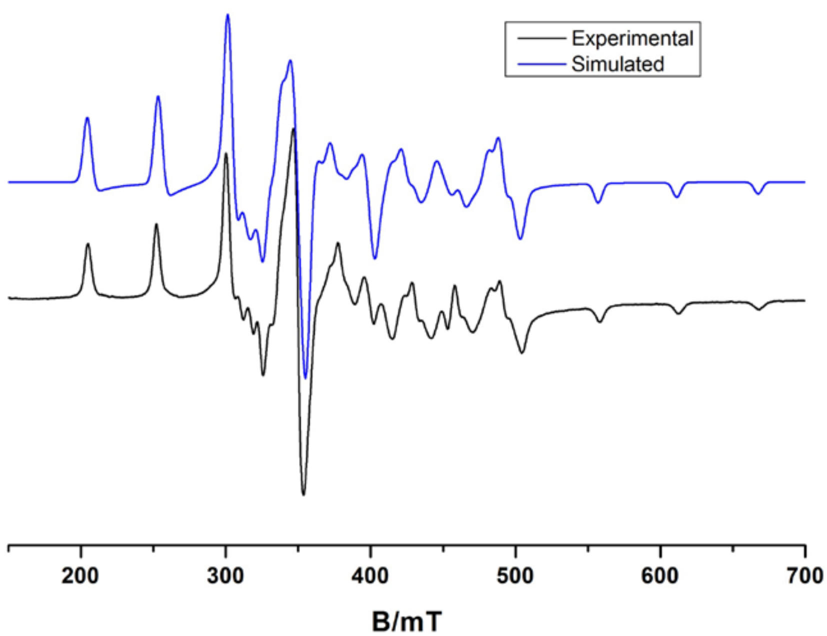

Figure 4.8: Frozen solution X- band-EPR spectrum of $[Tc(NO)F_5]^{2-}$ at 77 K.

There is no experimental evidence for the presence of the fifth fluorido ligand coordinated *trans* to the nitrosyl group. It should be noted that the absence of superhyperfine splitting due to the *trans* fluoride is not unusual. The same is observed in the cases of $[MoOF_5]^{2-}$, $[NbOF_5]^{2-}$ and $[ReOF_5]^{2-}$, where the coordination of *trans* fluoride is well established.[29-31] A frozen solution EPR spectrum of $[Tc(NO)F_5]^{2-}$ in H_2O is EPR silent. Addition of $HF_{(aq)}$(48%) to this aqueous solution brought back the signal. This implies that in aqueous solution a species with Tc–Tc interactions is formed. The so formed bridged compound is sensitive against acid and forms the monomer again in HF solution.

Table 4.5: EPR parameters of Tc(II) nitrosyl complexes. Coupling constants in 10^{-4} cm^{-1}

Compound	Solvents	$g_{\parallel}$	$g_{\perp}$	$A_{\parallel}$	$A_{\perp}$	g_0	a_0^{Tc}	Reference
$[Tc(NO)F_5]^{2-}$	HF/CH_2Cl_2	1.883	2.019	332	144	1.9736	203.5	This study
$[Tc(NO)Cl_5]^{2-}$	CH_2Cl_2	1.985	2.037	259.8	111.0	2.029	157.6	[5]
$[Tc(NO)Br_4]^{-}$	CH_2Cl_2	2.105	2.081	216.5	89.3	2.089	132.0	[32]
$[Tc(NO)I_4]^{-}$	CH_3COCH_3	2.262	2.144	155.0	73	2.171	103.0	[33]

$a_x^F = a_y^F = 50\times10^{-4}$ cm^{-1}; $a_z^F = 2\times10^{-4}$ cm^{-1}

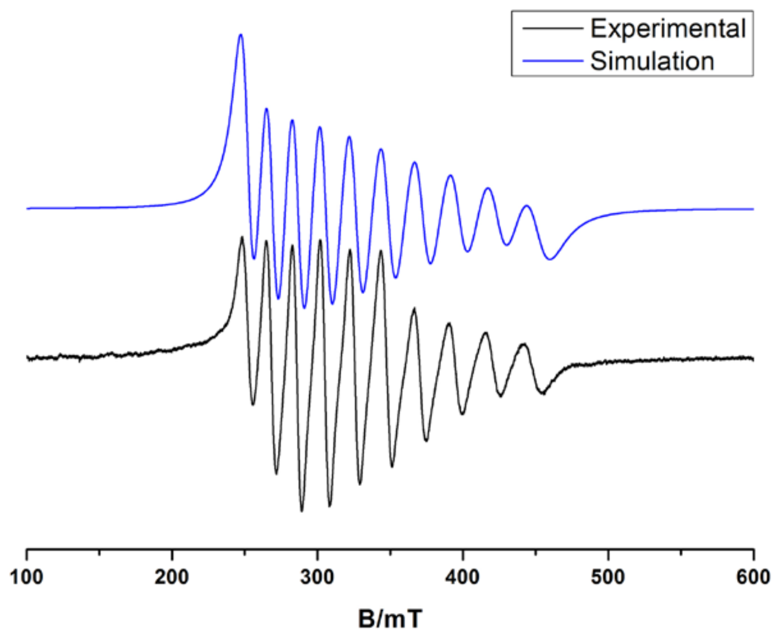

Figure 4.9: X-band EPR solution spectrum of $[Tc(NO)F_5]^{2-}$ in CH_2Cl_2 at 298 K.

$[Tc(NO)F_5]^{2-}$ can be extracted from aqueous HF solutions of $Cs_2[Tc(NO)F_5]$ into CH_2Cl_2 after addition of $(NBu_4)F\cdot xH_2O$. This allows the measurement of a room temperature EPR spectrum (Figure 4.9). EPR parameters are given in Table 4.5. There is expectedly no superhyperfine splitting due to the fluorido ligands resolved.

4.3.2. Single crystal X–ray analysis

The structure of pentafluoridotechnetate(II) was determined by the single–crystal diffraction method for a series of alkali metal salts. The main crystallographic data for $M_2[Tc(NO)F_5]\cdot H_2O$ (M = K, Rb, Cs) are given in Table 4.6. The compounds crystallize in the orthorhombic space group Cmcm. The compounds are crystallized from concentrated aqueous hydrofluoric acid (48%) as monohydrates and are isostructural with $M_2^I[M(NO)F_5]\cdot H_2O$ (M^I = K, Rb, M= Ru; M^I = K, Rb, Cs, M = Os). [34]

Table 4.6: Crystallographic data for $M_2[Tc(NO)F_5]\cdot H_2O$

	$K_2[Tc(NO)F_5]\cdot H_2O$	$Rb_2[Tc(NO)F_5]\cdot H_2O$	$Cs_2[Tc(NO)F_5]\cdot H_2O$
a/Å	6.203(1)	6.469(1)	6.688(1)
b/Å	18.654(4)	18.960(3)	19.479(2)
c/Å	6.301(2)	6.492(1)	6.765(1)
V/Å^3	729.1(3)	796.3(2)	881.3(2)
Space group	Cmcm	Cmcm	Cmcm

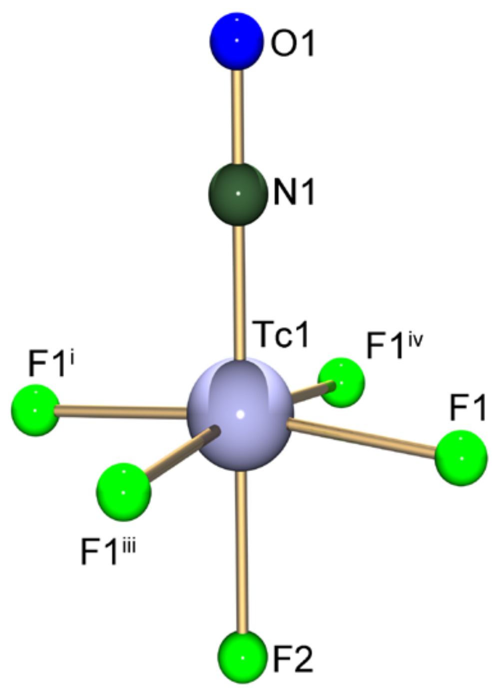

Figure 4.10: Molecular anion of $Cs_2[Tc(NO)F_5]\cdot H_2O$. Symmetry operators: ^{i} –x+1,y,-z-1/2; ^{ii} x,y,-z-1/2; ^{iii} –x+1,y,z.

The unit cell sizes increase as the ionic radii of alkali metals increase in the group. A similar trend is observed for the analogous osmium and ruthenium compounds. The anion of $Cs_2[Tc(NO)F_5]\cdot H_2O$ is shown in Figure 4.10. Selected bond lengths and angles are given in Table 4.7.

Table 4.7: Bond lengths (Å) and angles (°) for $M_2[Tc(NO)F_5]\cdot H_2O$ complexes

Bond lengths (Å)				
	Tc1–N1	N1–O1	Tc1–F1	Tc1–F2
$K_2[Tc(NO)F_5]\cdot H_2O$	1.74(2)	1.15(3)	1.937(8)	1.96(1)
$Rb_2[Tc(NO)F_5]\cdot H_2O$	1.78(1)	1.10(2)	1.961(4)	2.00(1)
$Cs_2[Tc(NO)F_5]\cdot H_2O$	1.73(2)	1.17(2)	1.960(5)	1.976(9)
Bond angles (°)				
	Tc1–N1–O1	N1–Tc1–F1	N1–Tc1–F2	F1–Tc1–F2
$K_2[Tc(NO)F_5]\cdot H_2O$	180.0	95.4(2)	180.0	84.6(2)
$Rb_2[Tc(NO)F_5]\cdot H_2O$	180.0	94.8(1)	180.0	85.2(1)
$Cs_2[Tc(NO)F_5]\cdot H_2O$	180.0	94.5(2)	180.0	85.5(2)

The technetium atoms in these complexes are in a slightly distorted octahedral environment. The technetium atoms are displaced from the mean least-square planes of the four fluorido ligands by 0.182(1) Å, 0.164(1) Å and 0.153(1) Å in the potassium, rubidium and cesium complexes, respectively. The F1–Tc1–F2 angles are smaller than 90° and N1–Tc1–F1 angles are larger than 90°. These deviations of the angles from 90° can be explained by the steric bulk of the nitrosyl ligand which causes some ‘roof effect’.

Table 4.8: 4+2+2+1 Arrangement in $M_2[Tc(NO)F_5]\cdot H_2O$

Compound	4	4	2	2
	M1–F1	M1–F1	M1–F2	M1–F2
$K_2[Tc(NO)F_5]\cdot H_2O$	2.902(9)	2.904(8)	3.104(1)	3.151(1)
$Rb_2[Tc(NO)F_5]\cdot H_2O$	2.984(5)	3.020(5)	3.237(1)	3.246(1)
$Cs_2[Tc(NO)F_5]\cdot H_2O$	3.129(5)	3.166(5)	3.355(1)	3.384(1)

The two alkali metal cations M1 and M2 have different types of coordination by the F atoms of the $[Tc(NO)F_5]^{2-}$ octahedra and the O2 atom of the co-crystallized water molecule.The interactions between the cation and fluorido ligands of $Cs_2[Tc(NO)F_5]\cdot H_2O$ are shown in Figure 4.11. The Cs1 cation is located in such a way that it has a 4+4+2+2 environment and therefore a coordination number of 12 (Table 4.8). The Cs2 cation has a distorted octahedral environment formed by the

$4F_{(eq)}$+$1F_{(ax)}$+$O_{(water)}$ and therefore a coordination number of 6 (Table 4.9). The distances from the cations to the axial fluorine atoms are larger than to the equatorial ones. This tendency increases in the order K<Rb<Cs.

Table 4.9: 4+1+1 Arrangement in $M_2[Tc(NO)F_5]\cdot H_2O$

Compound	4	1	1
	M2–F1	M2–F2	M2–O2
$K_2[Tc(NO)F_5]\cdot H_2O$	2.597(8)	2.67(1)	2.67(3)
$Rb_2[Tc(NO)F_5]\cdot H_2O$	2.763(4)	2.830(1)	2.82(2)
$Cs_2[Tc(NO)F_5]\cdot H_2O$	2.944(5)	3.108(9)	2.97(2)

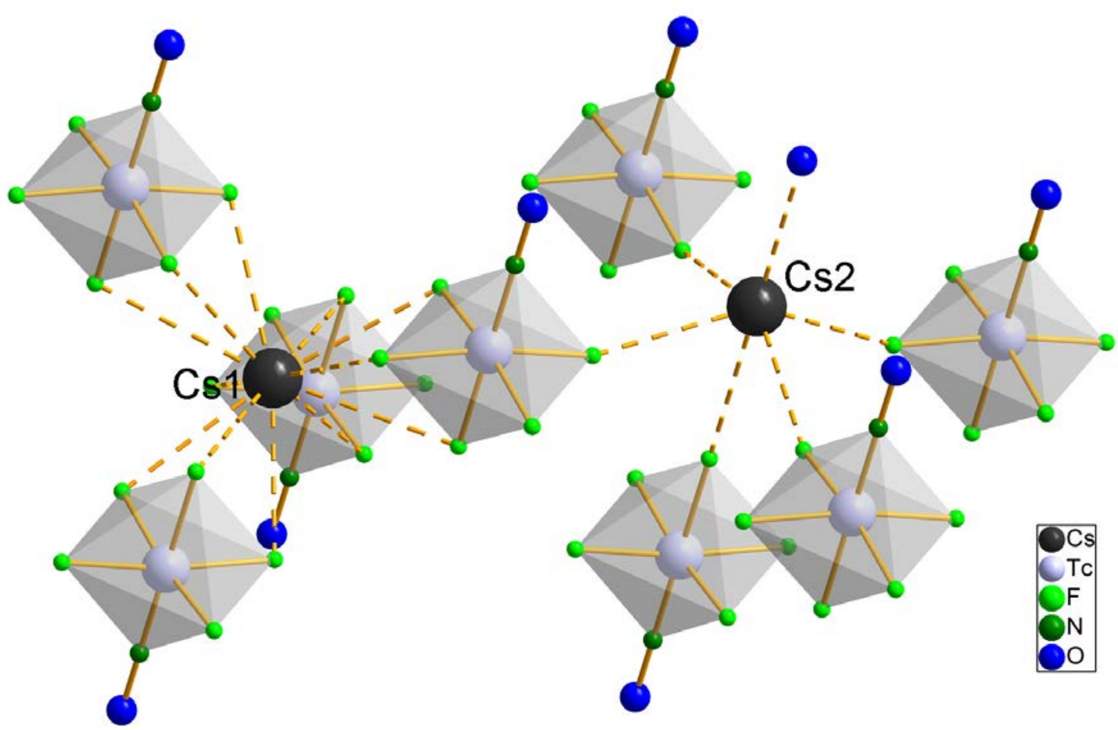

Figure 4.11: Interactions between the cations and fluorido ligands in $Cs_2[Tc(NO)F_5]\cdot H_2O$.

The distances between the oxygen atom (O2) of the co-crystallized water and the equatorial fluorine atoms are 3.12(2) Å, 3.04(1) Å and 3.02(1) Å in the potassium, rubidium and cesium complexes, respectively. These distances indicate that there are most probably hydrogen bonds between these atoms.

4.4. Synthesis of $[Tc(NO)(NH_3)_4F]X\cdot 1/2$ MF (X = HF_2 or PF_6; MF = Rb, Cs or KPF_6)

After isolation of the pentafluoridonitrosyltechnetate(II) from the AHA/$HF_{(aq)}$/TcO_4^- reaction mixture, the cationic complex $[Tc(NO)(NH_3)_4F]^+$ was isolated as a second product in crystalline form as $[Tc(NO)(NH_3)_4F](HF_2)\cdot 1/2$ RbF (**30**), $[Tc(NO)(NH_3)_4F](HF_2)\cdot 1/2$ CsF (**31**) directly from the reaction mixture or as $[Tc(NO)(NH_3)_4F](PF_6)\cdot 1/2$ KPF_6 (**32**) after the addition of KPF_6 to the mother solution.

4.4.1. Spectroscopic analysis

Compound **30**, **31** and **32** are readily soluble in water or aqueous HF, but almost insoluble in organic solvents.

Table 4.10: Vibrational frequencies (IR: infrared, R: Raman) in compounds **30**, **31** and **32**

Mode	$[Tc(NO)(NH_3)_4F](HF_2)\cdot 1/2$ MF		$[Tc(NO)(NH_3)_4F](PF_6)_2\cdot 1/2$ KPF_6
	M = Rb	M = Cs	
ν_{as}(N-O)	1620 (IR)	1622 (IR)	1677 (IR)
ν_{as}(N-H)	3322 (IR)	3328 (IR)	3367, 3303 (IR)
		3360, 3262 (R)	
ν_s(N-H)	3194 (IR)	3194 (IR), 3203 (R)	3202 (IR)
δ_s(H-N-H)	1417 (IR)	1428 (IR), 1251 (R)	1317, 1291, 1268 (IR)
δ_{as}(H-N-H)	1647 (IR)	1653 (IR)	1626 (IR)
		1631, 1686 (R)	
δ(Tc-N-H)	757, 734 (IR)	742, 723 (IR)	740 (IR)
		783 (R)	
δ(Tc-N-O)	635 (IR)	635 (IR), 635 (R)	629 (IR)
ν(Tc-NO)		559 (R)	
ν(Tc-NH_3)		469, 441,422 (R)	
δ(N-Tc-N)		229, 187 (R)	
ν(P-F)			868, 824, 553 (IR)
ν(Tc-F)	525	528	

The infrared spectra of the compounds show the N=O vibrations around 1650 cm^{-1}. These vibration values are close to the value observed for $[Tc(NO)(NH_3)_4(H_2O)]Cl_2$ (1680 cm^{-1}), but have lower frequencies than observed for the Tc(II) complex $[Tc(NO)(NH_3)_4(H_2O)]Cl_3$ (1830 cm^{-1}).[3] This reflects a considerable back donation from the metal ion to the NO ligand in the technetium(I) compounds. A detailed analysis of the vibrational frequencies is given in Table 4.10. The co-crystallized $(HF_2)^-$ anions in compounds **30** and **31** show resonances at around 1250 and 1230 cm^{-1} (ν_2(E)), the assignment of which has been done according to the spectrum of $NaHF_2$. [21]

The ^{99}Tc NMR signal of the diamagnetic $[Tc(NO)(NH_3)_4F]^+$ cation is at about 1930 ppm ($\Delta\nu_{1/2}$ = 2700 Hz). The large linewidth is due to distortions of the octahedral symmetry of the complex by three different ligands. The ^{19}F NMR spectra show signals at about -148 ppm for the fluorido ligands *trans* to the nitrosyl ligand. The chemical shift at -150 ppm was attributed to the bifluoride anion in compound **30** and **31** which is the same values as for KHF_2. Protons of the NH_3 ligands in these three compounds are rapidly exchanged with D_2O.

UV/visible spectra

UV/vis spectrum of an aqueous solution of compound **32** was measured. It shows three bands and was analyzed by comparison with the data of $[Ru(NO)(NH_3)_4L]^{q+}$, where L = NH_3, Cl^-, Br^-, OH^-, NCO^-, N_3^-, $CH_3CO_2^-$, pyrazine, pyridine and q= 2 or 3.[35,36] The experimental spectrum is shown in Figure 4.12.

The broad band at 458 nm (ε = 45.1 $M^{-1}cm^{-1}$) has a medium intensity and is characteristic for the inter-configurational spin forbidden d-d transitions in 4d and 5d compounds. The second band at 364 nm (ε = 36.1 $M^{-1}cm^{-1}$) is of low intensity and is characteristic of spin-allowed d-d transitions. The third band was observed at 269 nm (ε = 202.0 $M^{-1}cm^{-1}$). It is very intense and can be assigned to a charge-transfer band.

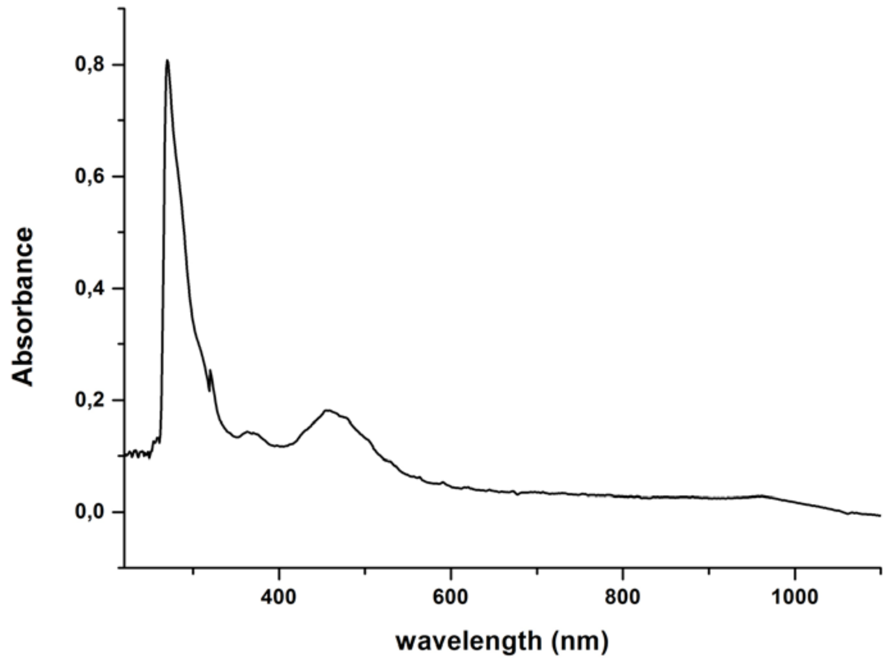

Figure 4.12: UV/visible spectrum of $[Tc(NO)(NH_3)_4F](PF_6)\cdot1/2\ KPF_6$ (**32**) in H_2O.

4.4.2. Single crystal analysis

Single crystals of the compounds **30** and **32** were studied by X-ray diffraction. They crystallize in the tetragonal crystal system. The structures consist of two distorted octahedral $[Tc(NO)(NH_3)_4F]^+$ cations and the corresponding counter ion. RbF or KPF_6 are co-crystallized in the two structures. The molecular structure of compound (**32**) is shown in Figure 4.13. Selected bond lengths and angles are summarized in Table 4.11.

The Tc–NO bond lengths of 1.719(4) Å (**30**) and 1.715(9) Å (**32**) are in the lower part of the range for Tc(I) nitrosyl complexes (1.716-1.793 Å).[37] The four ammine ligands are in the equatorial plane and fluorine is coordinated *trans* to the nitrosyl ligand. The Tc–N–O angles are 179.1(4)° (**30**) and 179.7(9)° (**32**), which confirms the linearity of the Tc–NO bond. The N1–Tc–NH_3 angles are larger than 90°. This is due to the steric bulk of the nitrosyl ligand. The technetium atoms of the $[Tc(NO)(NH_3)_4F]^+$ cations are displaced from the mean least-squares planes of the four NH_3 ligands by 0.17 Å (**30**) and 0.1831(4) Å (**32**), respectively.

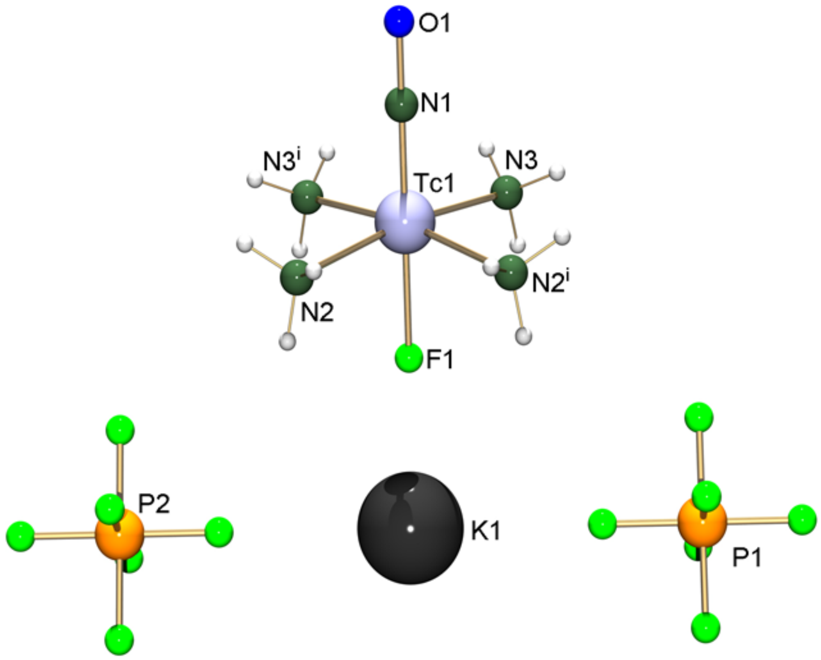

Figure 4.13: Molecular representation of [Tc(NO)(NH_3)$_4$F](PF_6)·1/2 KPF_6 (**32**).

Table 4.11: Selected bond lengths (Å) and angles (°) in [Tc(NO)(NH_3)$_4$F](HF_2)·1/2 RbF (**30**) and [Tc(NO)(NH_3)$_4$F](PF_6)·1/2 KPF_6 (**32**)

Bond lengths (Å)	**30**	**32**
Tc(1)–N(1)	1.719(4)	1.715(9)
Tc(1)–N(2)	2.169(3)	2.163(6)
Tc(1)–N(3)	2.156(3)	2.166(7)
N(1)–O(1)	1.208(5)	1.20(1)
Tc(1)–F(1)	2.036(3)	2.050(6)
Bond angles (°)		
Tc(1)–N(1)–O(1)	179.1(4)	179.7(9)
N(1)–Tc(1)–F(1)	179.9(2)	178.9(3)
N(1)–Tc(1)–N(2)	94.2(1)	93.9(3)
N(1)–Tc(1)–N(3)	95.3(1)	95.4(3)
N(2)–Tc(1)–N(3)	170.5(1)	87.2(3)

The *trans* Tc1–F1 bond lengths are 2.036(3) (**30**) and 2.050(6) (**32**) Å and are considerably longer than the Tc–F bonds in the $[TcF_6]^{2-}$ anions of a number of alkali and ammonium salts (see Chapter 3, Table 3.2). This shows that the structural *trans* influence of the NO^+ ligands plays a considerable role in the compounds **30** and **32**. Hydrogen bonds stabilize the solid state structure of the compound (**32**). Figure 4.14 illustrates the corresponding situation in the asymmetric unit of the structure. The complete summary is given in Table 4.12.

Table 4.12: Hydrogen bonds in $[Tc(NO)(NH_3)_4F](PF_6)\cdot 1/2\ KPF_6$ (**32**).

D-H...A	d(D-H)	d(H...A)	d(D...A)	<(DHA)
N(2)-H(2B)...O(1)^{viii}	0.89	2.40	3.207(5)	151.2
N(3)-H(3B)...F(5)^{vii}	0.89	2.34	3.224(4)	172.7
N(3)-H(3B)...F(2)^{vii}	0.89	2.39	3.033(4)	129.5
N(3)-H(3C)...F(7)^{vi}	0.89	2.54	3.235(5)	135.5
N(3)-H(3C)...F(7)	0.89	2.32	3.172(5)	160.7

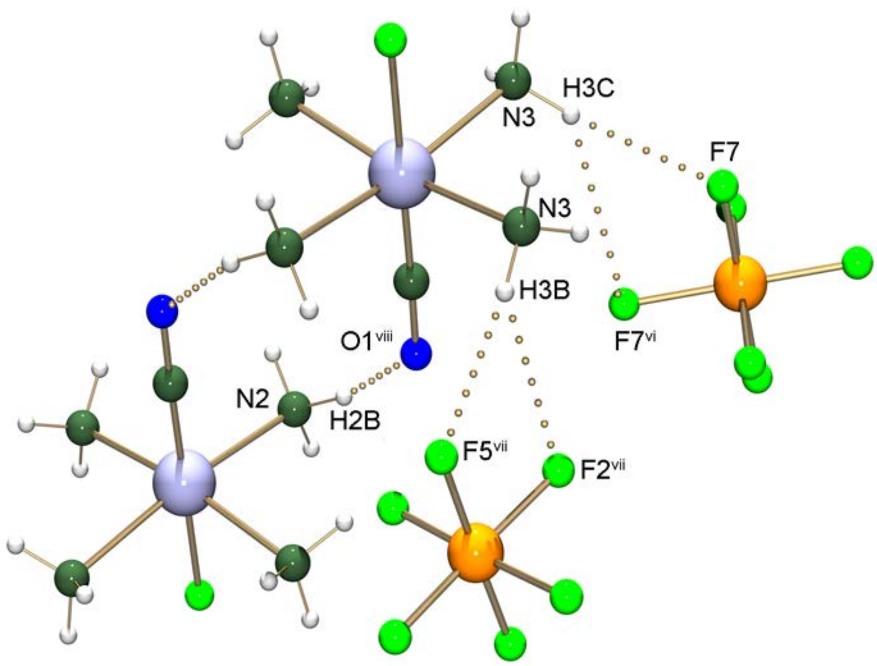

Figure 4.14: Hydrogen bonds within the asymmetric unit of **32**. Symmetry operators: ^{vi}: -y+1,x,z; ^{vii} -y+1,x,z-1; ^{viii} -x+1,-y,-z

4.5. Synthesis of $[Tc(NO)(py)_4F]PF_6$

The reactivity of pentafluoridonitrosyltechnetate(II) becomes more interesting after the isolation of this compound in pure form. Different reactions were attempted to study the reactivity of cesium pentafluoridonitrosyltechnetate(II). Attempted reactions of aqueous solutions of $[Tc(NO)F_5]^{2-}$ with phosphine ligands such as PR_3 (R = Ph, Me_2Ph) in CH_3CN failed. Similarly, an attempted reaction of aqueous $[Tc(NO)F_5]^{2-}$ with (hexafluorido)acetylacetone in CH_3CN failed even under reflux. A possible reason for the negative results might be the poor solubility of $Cs_2[Tc(NO)F_5]$ in organic solvents.

It was reported earlier that reactions of (n-Bu_4N)[$Tc(NO)X_4$] (X= Cl, Br) complexes with neat pyridine resulted in the formation of neutral $[Tc(NO)X_2(py)_3]$ (X= Cl, Br) compounds as stable Tc(I) complexes.[38] Thus, the synthesis of an analogous fluorido complex was attempted. The reaction between $Cs_2[Tc(NO)F_5]$ and pyridine did not occur at room temperature or at 50° C.

$$\underset{(\mathbf{29})}{Cs_2[Tc(NO)F_5]\cdot H_2O} + \text{pyridine} \xrightarrow[HF_{(aq)},\ KPF_6]{\text{reflux}} \underset{(\mathbf{33})}{[Tc(NO)(py)_4F]PF_6}$$

Scheme 4.3

However, a reaction of pentafluoridonitrosyltechnetate(II) with neat pyridine was achieved (Scheme 4.3), when the mixture was heated for 1h at reflux. Addition of KPF_6 to the resulting orange-red solution and slow evaporation at room temperature forms orange-red crystals of *trans*-fluoridonitrosyltetrakis(pyridine)technetium(I) hexafluoridophosphate (**33**).

4.5.1. Spectroscopic analysis

$[Tc(NO)(py)_4F]PF_6$ is soluble in common organic solvents and also in aqueous hydrofluoric acid. The infrared spectrum of the compound shows the N=O stretch at 1699 cm^{-1}. This value is somewhat higher than those of the otherTc(I) complexes, but significantly lower than those of the Tc(II) complexes $[Tc(NO)F_5]^{2-}$ (~1780 cm^{-1}) and $[Tc(NO)(NH_3)_4(H_2O)]Cl_3$(1830 cm^{-1}).[3] The band at

635 cm^{-1} is assigned for the δ(Tc–N–O) and the stretch at 505 cm^{-1} is assigned to the ν(Tc–F) vibration.

UV/visible spectra

The electronic spectrum of $[Tc(NO)(py)_4F]PF_6$ in acetonitrile exhibits three distinct absorption maxima between 210 and 700 nm (Figure 4.15). The 247 nm (ε = 18334 $M^{-1}cm^{-1}$) band is assigned to a pyridine π→π* transition based on the position and intensity of the absorption. The absorptions at 360 nm (ε = 16944 $M^{-1}cm^{-1}$) and the weak band at 442 nm (ε = 2616 $M^{-1}cm^{-1}$) are assigned to the $d \rightarrow \pi^*_{NO}$ transitions by comparison with $[Re(NO)X_2(py)_3]$ (X = Cl/Br) complexes.[39,40]

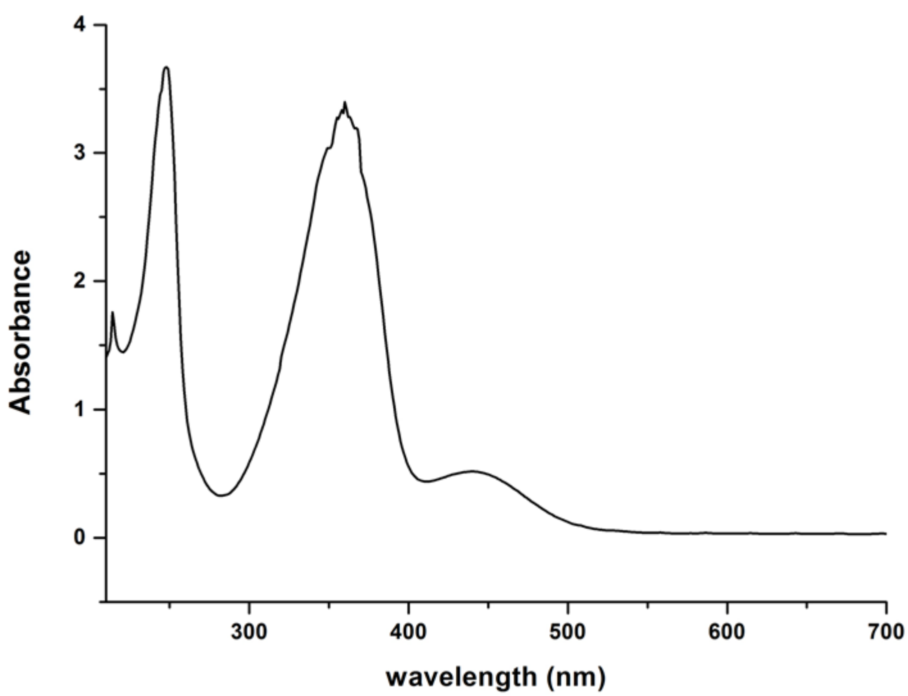

Figure 4.15: UV/visible spectrum of $[Tc(NO)(py)_4F]PF_6$.

The ^{99}Tc NMR signal of the diamagnetic $[Tc(NO)(py)_4F]^+$ cation can be found at 1721 ppm ($\Delta\nu_{1/2}$ = 650 Hz) and is shown in Figure 4.16. This value is outside the range of Tc(I) complexes, the signals of which appear between -400 to -3350 ppm. [22,23] However, the significant upfield shift of the pyridine complex compared to ammine complex $[Tc(NO)(NH_3)_4F]^+$ (~ 1930 ppm, see page 60 and 75 of Chapter 4) might be due to the considerable higher degree of back donation from the metal to the nitrosyl as well as to the pyridine ligands. The ^{19}F NMR spectrum shows a resonance at -171 ppm which can be assigned to the fluorido ligands in the axial position. The upfield shift of this signal with regard to the ^{19}F signals in the ammine complex $[Tc(NO)(NH_3)_4F]^+$ (~ -140 ppm, see page 60 and 76 of Chapter 4) is also explained by the back donation from the technetium metal center to the nitrosyl and pyridine ligands. The ^1H NMR spectrum of $[Tc(NO)(py)_4F]PF_6$ is unexceptional.

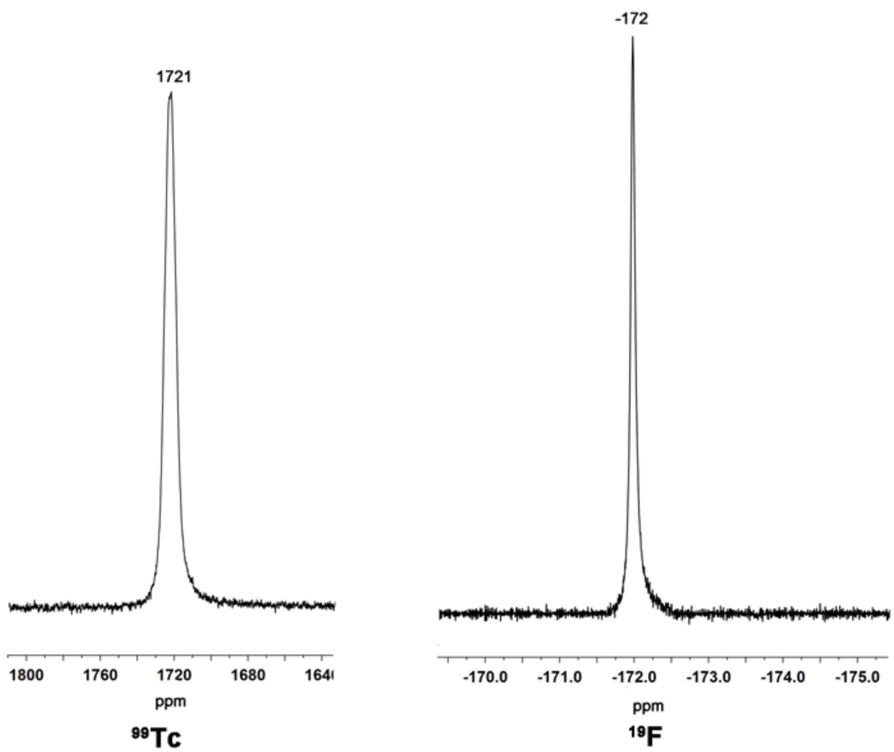

Figure 4.16: ^{99}Tc and ^{19}F NMR spectra of $[Tc(NO)(py)_4F]PF_6$.

4.5.2 Single crystal X-ray structural analysis

Orange blocks of $[Tc(NO)(py)_4F]PF_6$ crystals exhibit twinning by pseudomerohedry. The preliminary description of the structure of $[Tc(NO)(py)_4F]PF_6$ involves disorder within a lattice of C2/c symmetry. The structure was solved in the triclinic space group $P\bar{1}$ by applying the twin law 0 -

1 0, -1 0 0, 0 0 -1. The molecular structure of the $[Tc(NO)(py)_4F]^+$ cation is shown in Figure 4.17. The $[Tc(NO)(py)_4F]^+$ cations show a distorted octahedral coordination geometry with four pyridine ligands in the equatorial positions and the fluorido and nitrosyl ligands in axial positions. Selected bond lengths and angles are given in Table 4.13.

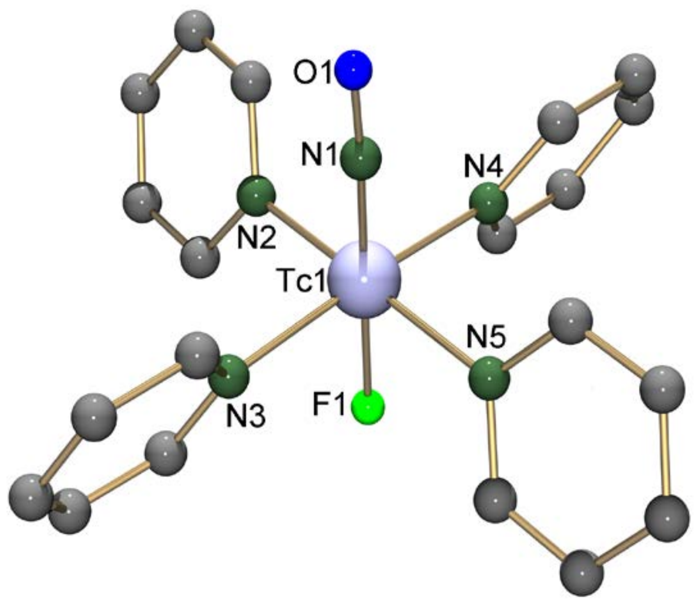

Figure 4.17: Molecular structure of $[Tc(NO)(py)_4F]^+$. Hydrogen atoms have been omitted for clarity.

Table 4.13: Selected bond lengths (Å) and angles (°) in $[Tc(NO)(py)_4F]PF_6$

Bond lengths (Å)			
Tc1–N1	1.730(7)	Tc1–N3	2.138(9)
N1–O1	1.209(8)	Tc1–N4	2.150(9)
Tc1–N2	2.141(8)	Tc1–N5	2.157(8)
Tc1–F1	1.954(4)		
Bond angles (°)			
Tc(1)–N(1)–O(1)	177.3(7)	N(1)–Tc(1)–N(2)	93.2(3)
N(1)–Tc(1)–F(1)	179.5(4)	N(1)–Tc(1)–N(4)	93.3(4)
N(1)–Tc(1)–N(3)	92.2(4)	N(1)–Tc(1)–N(5)	93.7(3)

The Tc(1)–N(1)–O(1) angle of 177.3° (7) is a strong evidence for the presence of a NO^+ moiety. A remarkable feature of the structure is the relatively short Tc–F bond *trans* to the nitrosyl ligand. The observed *trans* Tc–F lengths in a number of nitrosyl fluorido complexes of technetium are listed in Table 4.14. The *trans* Tc–F bond length in the pyridine complex is the shortest. This may be explained by back donation from the metal to the pyridine ligands, which may weaken the *trans* influence of the nitrosyl ligand.

Table 4.14: Tc–F bond length in *trans* position to a nitrosyl ligand

Compound	Bond lengths (Å)
$[Tc(NO)(NH_3)_4F]_4[TcF_6][HF_2]_2$	1.988(3), 2.036(3)
$K_2[Tc(NO)F_5]\cdot H_2O$	1.977(6)
$Rb_2[Tc(NO)F_5]\cdot H_2O$	2.003(10)
$Cs_2[Tc(NO)F_5]\cdot H_2O$	1.976(9)
$[Tc(NO)(NH_3)_4F](HF_2)\cdot 1/2\ RbF$	2.036(3)
$[Tc(NO)(NH_3)_4F](PF_6)\cdot 1/2\ KPF_6$	2.050(6)
$[Tc(NO)(py)_4F]PF_6$	1.954(4)

The average Tc–$N_{pyridine}$ bond length is 2.145 Å and is comparable to the values in $[Tc(NO)Cl_2(py)_3]\cdot CH_3CN$ (Tc–$N_{pyridine(av)}$: 2.129 Å).[38] The technetium atom of the $[Tc(NO)(py)_4F]^+$ cation is displaced from the mean least-square plane of the four pyridine nitrogen atoms by 0.117(1) Å toward the N1 atom of the nitrosyl ligand. The dihedral angles between the N_4 plane and the pyridine rings range from 63.9(3) to 66.5(3)° with an average value of 65.4°. The pyridine rings give a propeller-like structure around the F–Tc–NO rotation axis. A similar structure was also found for $[Ru(NO)(py)_4Cl](PF_6)_2\cdot {}^1/_2\ H_2O$. [41]

4.6. Synthesis of $[Tc(NO)(NH_3)_4(OOCCF_3)](OOCCF_3)\cdot(CF_3COOH)$

From all above results, it may be deduced that the bonds between the fluorido ligands and the metal atoms are quite stable. However, *trans* defluorination was achieved during the reaction of $[Tc(NO)(NH_3)_4F](HF_2)$ (**31**) with an excess of CF_3COOH. This resulted in the formation of the *trans*-trifluoroacetato compound $[Tc(NO)(NH_3)_4(OOCCF_3)](OOCCF_3)\cdot(CF_3COOH)$ **(34)** (Scheme 4.4).

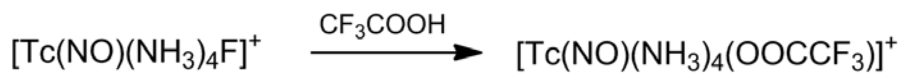

(31) (34)

Scheme 4.4

4.6.1. Spectroscopic analysis

The compound is soluble in common organic solvents such as acetone, ethanol, acetonitrile, tetrahydrofuran, dichloromethane. Its infrared spectrum shows the N=O stretch at 1670 cm^{-1}. This value is close to the N=O stretches observed for compound **26** (1677), **30** (1620), **31** (1622) and **32** (1677). Table 4.15 contains a more detailed analysis of the vibrational spectra of the compound. The IR bands of the coordinated NH_3 are found at 829, 1421 and 1656 cm^{-1} and the trifluoroacetate assignment has been done with respect to the IR of the trifluoridoacetic acid vapor. [42,43] The Tc–NO vibration gives a band at 614 cm^{-1}.

Table 4.15: Vibrational frequencies (IR: infrared, R: Raman)

Mode	$[Tc(NO)(NH_3)(OOCCF_3)](OOCCF_3)\cdot CF_3COOH$		
ν_{as}(N-O)	1670 IR	ν(Tc-O)	852 IR, 1088 R
ν_{as}(N-H)	3348, 3303, 3269	ν(C-C)	829, 799 IR, 834 R
ν_s(N-H)	3193	δ(Tc-N-H)	852 R
ν_s(O-H)	3147	$\delta(COO^-)$	752 IR, 726,264 R
δ_{as}(H-N-H)	1656 IR, 1684 R	$\nu_{as}(CF_3)$	717 IR, 598, 500 R
δ_s(H-N-H)	1421 IR, R	$\nu(C-CO_2)$	418, 404 R
δ(C-O)	1439 IR, 1439 R	δ(Tc-N-O)	614 IR, 625 R
ν(C-O)	1290 IR	$\delta(CF_3)$	599 IR, 436
ν(C-F)	1180 IR	$\rho_r(CF_3)$	264, 196 R
δ(O-H)	1139,1115 IR		

The ^{99}Tc NMR spectrum of the diamagnetic $[Tc(NO)(NH_3)_4(OOCCF_3)]^+$ cation shows a signal at 2017 ppm ($\Delta\nu_{1/2}$ = 3840 Hz). This value is downfield shifted by about 90 ppm with respect to the values found for the compounds **26** (1928 ppm), **30** (1926 ppm), **31** (1931 ppm) and **32** (1933 ppm). The reason for this shift may be explained by the electron withdrawing group of the trifluoroacetato ligand in the *trans* position to the nitrosyl group. The ^{19}F NMR spectrum shows two signals at -76.27 ppm and -76.30 ppm which can be assigned to the uncoordinated trifluoroacetate and coordinated trifluoroacetate anions present in the compound. The ^{1}H NMR spectrum in CD_3CN of the compound shows a peak at 2.54 ppm, which is assigned to NH_3 protons.

4.6.2 Single crystal structural analysis

Orange plates of $[Tc(NO)(NH_3)_4(OOCCF_3)](OOCCF_3)\cdot CF_3COOH$ crystallize in the triclinic space group $P\bar{1}$. The structure consists of a distorted octahedral $[Tc(NO)(NH_3)_4(OOCCF_3)]^+$ cation and a CF_3COO^- anion. One molecule of CF_3COOH is co-crystallized. The molecular structure of the complex cation is shown in Figure 4.18. Selected bond lengths and angles are summarized in Table 4.16.

The Tc–NO bond length is 1.720(3) Å, which is close to the value observed for the other nitrosyl complexes studied in this thesis. The equatorial coordination sphere is occupied by the four ammine ligands and the trifluoroacetato ligand is coordinated in *trans* position to the nitrosyl ligand. The bonding situation is very similar to that in the $[Tc(NO)(NH_3)_4F]^+$ cation. Again, a linear coordination of the nitrsoyl ligand is observed. The steric bulk of the nitrosyl ligand causes some roof effect which results in N1–Tc1–NH_3 angles which are all larger than 90°. The Tc–O bond length to the *trans*-trifluoroacetato ligand is 2.116(2) Å. This value is relatively long and similar to the value determined for $[Ru(NH_3)_4(SO_2)(OOCCF_3)]OOCCF_3\cdot CF_3COOH$ (Ru–O of TFA is 2.059 Å).[44] The carboxylate group is clearly monodentate with the non-bonded oxygen atom being 3.49 Å away from the metal.

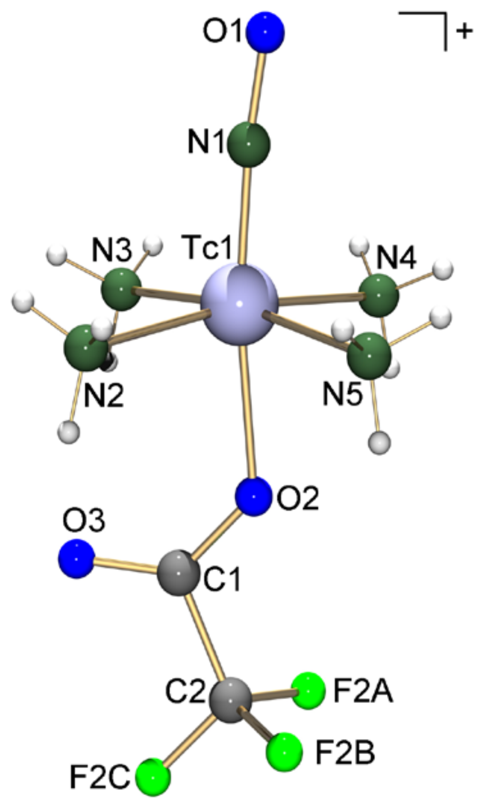

Figure 4.18: Molecular structure of the complex cation of $Tc(NO)(NH_3)_4(OOCCF_3)](OOCCF_3)$.

Table 4.16: Selected bond lengths (Å) and angles (°) in $[Tc(NO)(NH_3)_4(OOCCF_3)](OOCCF_3)\cdot CF_3COOH$

Bond lengths (Å)			
Tc1–N1	1.720(3)	Tc1–N5	2.165(2)
N1–O1	1.194(4)	Tc1–O2	2.116(2)
Tc1–N2	2.160(2)	C1–O2	1.260(3)
Tc1–N3	2.161(2)	C1–O3	1.219(4)
Tc1–N4	2.162(2)	C1–C2	1.541(4)
Bond angles (°)			
Tc1–N1–O1	174.6(3)	N1–Tc1–N3	96.5(1)
N1–Tc1–O2	172.1(1)	N1–Tc1–N4	97.5(1)
N1–Tc1–N2	92.26(1)	N1–Tc1–N5	93.2(1)

Several hydrogen bonds stabilize the solid state structure of **34**. Figure 4.19 illustrates the hydrogen bonding situation in the unit cell of the structure. A complete summary is given in Table 4.17. The ammine ligands of the cations form a complex N – H···F and N – H···O network with the counter ions and adjacent molecule respectively.

Table 4.17: Hydrogen bonds in $[Tc(NO(NH_3)_4(OOCCF_3)](OOCCF_3)\cdot CF_3COOH$

D-H...A	d(D-H)	d(H...A)	d(D...A)	<(DHA)
N(2)-H(2A)...F(2A)^{i}	0.89	2.34	3.142(4)	149.9
N(2)-H(2C)...O(3)^{ii}	0.89	2.15	2.987(3)	156.4
N(2)-H(2C)...F(2C)^{ii}	0.89	2.56	3.247(4)	134.2
N(3)-H(3A)...O(3)	0.89	2.41	3.091(3)	132.9
N(3)-H(3B)...O(1)^{iii}	0.89	2.20	3.042(4)	159.0
N(3)-H(3C)...O(7)^{iv}	0.89	2.22	2.993(4)	144.7
N(3)-H(3C)...O(8)^{iv}	0.89	2.60	3.180(3)	123.7
N(4)-H(4A)...O(9)^{v}	0.89	2.40	3.172(4)	145.2
N(4)-H(4A)...O(3)	0.89	2.59	3.216(3)	127.6
N(4)-H(4C)...O(1)^{ii}	0.89	2.34	3.167(4)	155.4
N(4)-H(4B)...O(6)^{v}	0.89	2.39	3.164(4)	145.2
N(5)-H(5C)...O(6)^{v}	0.89	2.38	3.115(4)	140.6
N(5)-H(5C)...F(3A)^{v}	0.89	2.42	3.208(4)	147.9
N(5)-H(5B)...O(3)^{ii}	0.89	2.50	3.308(4)	150.6
O(8)-H(1)...O(6)	0.91(6)	1.56(6)	2.469(4)	172(6)

Symmetry operators: (^{i}) -x+1,-y+1,-z; (^{ii}) 2 x-1,y,z; (^{iii}) -x+1,-y+1,-z+1; (^{iv}) -x+2,-y+1,-z; (^{v}) -x+2,-y,-z

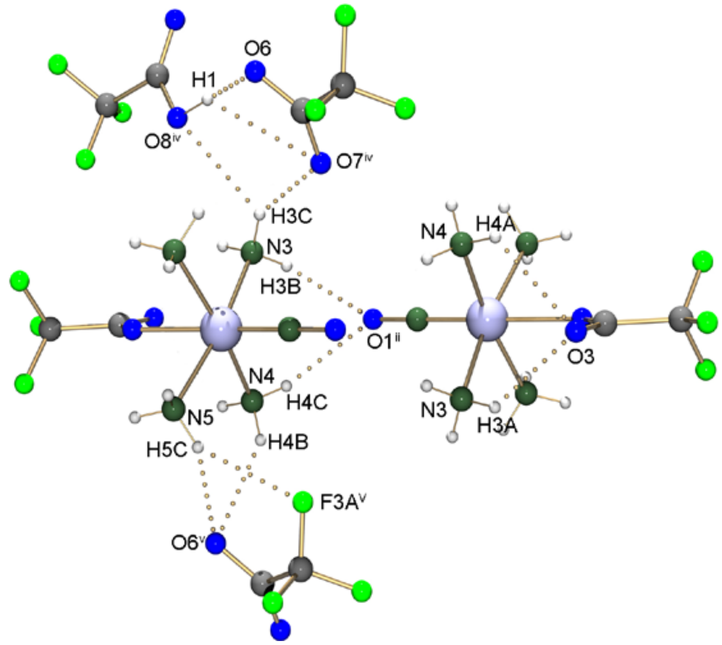

Figure 4.19: Unit cell plot of $[Tc(NO)(NH_3)_4(OOCCF_3)](OOCCF_3)\cdot CF_3COOH$.

4.7. Summary and conclusions

Acetohydroxamic acid was used as nitrosylating agent for the synthesis of nitrosyl complexes of technetium. Reductive nitrosylation starting from hexafluoridotechnetate(IV) gave a Tc(I) complex. Reactions starting from pertechnetate with acetohydroxamic acid gave a mixture of Tc(II) and Tc(I) complexes. For the first time, pentafluoridonitrosyltechnetate(II) was synthesized and isolated in crystalline form as alkali metal salts. It was analyzed spectroscopically and structurally. Different salts of *trans*-tetramminefluoridonitrosyltechnetium(I) were isolated and studied. The reactivities of the pentafluoridonitrosyltechnetate(II) and *trans*-tetramminefluoridonitrosyltechnetium(I) were studied and the resulting compounds were characterized completely. Fluorido complexes with the $[Tc(NO)]^{3+}$ and $[Tc(NO)]^{2+}$ cores may serve as a suitable precursors for further studies.

4.8. References

(1) Richter-Addo, G. B.; Legzdins, P. *Metal nitrosyls*; Oxford University Press: New York, **1992**,

(2) Eakins, J. D.; Humphreys, D. G.; Mellish, C. E. *J. Chem. Soc.* **1963**, 6012.

(3) Armstrong, R. A.; Taube, H. *Inorg. Chem.* **1976**, *15*, 1904.

(4) Radonovich, L. J.; Hoard, J. L. *J. Phys. Chem.* **1984**, *88*, 6711.

(5) Yang, G. C.; Heitzmann, M. W.; Ford, L. A.; Benson, W. R. *Inorg. Chem.* **1982**, *21*, 3242.

(6) Kirmse, R.; Lorenz, B.; Schmidt, K. *Polyhedron* **1983**, *2*, 935.

(7) Abram, U.; Kirmse, R.; Köhler, K.; Lorenz, B.; Kaden, L. *Inorg. Chim. Acta* **1987**, *129*, 15.

(8) Orvig, C.; Davison, A.; Jones, A. G. *J. Labelled Compd. Radiopharm.* **1981**, *18*, 148.

(9) Pearlstein, R. M.; Davis, W. M.; Jones, A. G.; Davison, A. *Inorg. Chem.* **1989**, *28*, 3332.

(10) Brown, D. S.; Newman, J. L.; Thornback, J. R.; Davison, A. *Acta Cryst.* **1987**, *C43*, 1692.

(11) Nicholson, T.; Müller, P.; Davison, A.; Jones, A. G. *Inorg. Chim. Acta* **2006**, *359*, 1296.

(12) Baldas, J.; Boas, J. F.; Bonnyman, J.; Williams, G. A. *J. Chem. Soc., Dalton Trans.* **1984**, 827.

(13) Linder, K. E.; Davison, A.; Dewan, J. C.; Costello, C. E.; Maleknia, S. *Inorg. Chem.* **1986**, *25*, 2085.

(14) Schibli, R.; Marti, N.; Maurer, P.; Spingler, B.; Lehaire, M. L.; Gramlich, V.; Barnes, C. L. *Inorg. Chem.* **2005**, *44*, 683.

(15) Rattat, D.; Verbruggen, A.; Schmalle, H.; Berke, H.; Alberto, R. *Tetrahedron Letters*. **2004**, *45*, 4089.

(16) de Vries, N.; Cook, J.; Davison, A.; Nicholson, T.; Jones, A. G. *Inorg. Chem.* **1990**, *29*, 1062.

(17) Chung, D. Y.; Lee, E. H. *J. Ind. Eng. Chem.* **2006**, *12*, 962.

(18) Gong, C.-M. S.; Lukens, W. W.; Poineau, F.; Czerwinski, K. R. *Inorg. Chem.* **2008**, *47*, 6674.

(19) Sinitsyn, M. N.; Svetlov, A. A.; Kanishcheva, A. S.; Mikhailov, Y. N.; Sadikov, G. G.; Kokunov, Y. V.; Buslaev, Y. A. *Zh. Neorg. Khim.* **1989**, *34*, 2795.

(20) Paulat, F.; Kuschel, T.; Nather, C.; Praneeth, V. K. K.; Sander, O.; Lehnert, N. *Inorg. Chem.* **2004**, *43*, 6979.

(21) Rush, J. J.; Schroeder, L. W.; Melveger, A. J. *J. Chem. Phys.* **1972**, *56*, 2793.

(22) O'Connell, L. A.; Pearlstein, R. M.; Davison, A.; Thornback, J. R.; Kronauge, J. F.; Jones, A. G. *Inorg. Chim. Acta* **1989**, *161*, 39.

(23) Alberto, R. *Technetium*, in *Comprehensive Coordination Chemistry* (Eds.: McCleverty, J. A., Meyer, T. J.); Elsevier: 2005; Vol. 5, 127.

(24) Mikhalev, V. A. *Radiochemistry.* **2005**, *47*, 319.

(25) Tarasov, V. P.; Kirakosyan, G. A.; Buslaev, Y. A.; Svetlov, A. A.; Sinitsyn, N. M. *Inorg. Chim. Acta* **1983**, *69*, 239.

(26) Rogalevich, N. L.; Bobkova, E. Y.; Novitskii, G. G.; Skutov, I. K.; Svetlov, A. A.; Sinitsyn, N. M. *Zh. Neorg. Khim.* **1986**, *31*, 1221.

(27) Reese, I.; Preetz, W. *Z. Anorg. Allg. Chem.* **2000**, *626*, 645.

(28) Casey, J. A.; Murmann, R. K. *J. Am. Chem. Soc.* **1970**, *92*, 78.

(29) Manoharan, P. T.; Rogers, M. T. *J. Chem. Phys.* **1968**, *49*, 5510.

(30) Shock, J. R.; Rogers, M. T. *J. Chem. Phys.* **1973**, *58*, 3356.

(31) Holloway, J. H.; Raynor, J. B. *J. Chem. Soc., Dalton Trans.* **1975**, 737.

(32) Kirmse, R.; Stach, J.; Lorenz, B.; Marov, I. N. *Z. Chem.* **1984**, *24*, 36.

(33) Kirmse, R.; Stach, J.; Abram, U. *Polyhedron* **1985**, *4*, 1275.

(34) Salomov, A. S.; Mikhailov, Y. N.; Kanishcheva, A. S.; Svetlov, A. A.; Sinitsyn, N. M.; Poraikoshits, M. A.; Parpiev, N. A. *Zh. Neorg. Khim.* **1989**, *34*, 386.

(35) Gorelsky, S. I.; da Silva, S. C.; Lever, A. B. P.; Franco, D. W. *Inorg. Chim. Acta* **2000**, *300*, 698.

(36) Schreiner, A. F.; Gunter, J. D.; Hamm, D. J.; Lin, S. W.; Hauser, P. J.; Hopcus, E. A. *Inorg. Chem.* **1972**, *11*, 880.

(37) *Cambridge Structural Database, Version 5.33*, Release November 2011.

(38) Blanchard, S. S.; Nicholson, T.; Davison, A.; Davis, W.; Jones, A. G. *Inorg. Chim. Acta* **1996**, *244*, 121.

(39) Machura, B.; Dziegielewski, J. O.; Bartczak, T. J.; Kusz, J. *J. Coord. Chem.* **2003**, *56*, 417.

(40) Machura, B.; Dziegielewski, J. O.; Kusz, J. *Pol. J. Chem.* **2003**, *77*, 519.

(41) Kimura, T.; Sakurai, T.; Shima, M.; Togano, T.; Mukaida, M.; Nomura, T. *Inorg. Chim. Acta* **1983**, *69*, 135.

(42) Kagarise, R. E. *J. Chem. Phys.* **1957**, *27*, 519.

(43) Fuson, N.; Josien, M. L.; Jones, E. A.; Lawson, J. R. *J. Chem. Phys.* **1952**, *20*, 1627.

(44) Kovalevsky, A. Y.; Bagley, K. A.; Cole, J. M.; Coppens, P. *Inorg. Chem.* **2003**, *42*, 140.

Chapter 5

5. Experimental section

5. Experimental Section

5.1. Starting materials

All chemicals and reagents were purchased from commercial sources (Acros Organics, Fluka, Sigma-Aldrich, Alfa Aesar).

All solvent were used as received (pure for synthesis) unless otherwise stated. Acetonitrile was dried intensively by heating over phosphorus pentoxide.

The technetium precursors were synthesized according to the cited references:

$Cs_2[TcNCl_5]$[1]

$[TcN(OH)_3]_n$[2]

$M_2[TcBr_6]$ ($M = NH_4$, Na, K)[3]

Radiation Precautions: ^{99}Tc is a weak β-emitter. Manipulations of ^{99}Tc compounds were performed in a laboratory approved for the handling of such radioactive materials. Special shieldings are commonly not required, since the low-energy β^- radiation is usually absorbed by glass or teflon. With large amounts of ^{99}Tc compounds, bremsstrahlung is produced from interactions with glass and precautions must be taken. Gloves and safety glasses are essential at all times. It is also preferable to work in plexiglass glove boxes fitted with a cover, using fixed gloves.

Caution! The handling of anhydrous HF or compounds that produce HF upon hydrolysis require eye and skin protection.

Materials and apparatus

Sample handling (anhydrous HF) is performed using Teflon-PFA tubes, which are sealed at one end and equipped at the other end with a metal valve. Thus, they are connectable to a stainless steel vacuum line.

Sample handling (hydrofluoric acid, 40 or 48%) is performed using Teflon-PFA tubes or flasks.

5.2. Analytical methods

IR spectra were measured from KBr pellets on a *Shimadzu*-FTIR 8300 spectrometer or Nicolet iS10 FT-IR spectrometer.

Raman spectra were recorded on a RFS 100 instrument (Bruker).

UV/vis spectra were taken on a SPECORD 40 instrument (Analytik Jena).

The ^{99}Tc, ^{19}F and ^{1}H NMR spectra were recorded on a *JEOL-400MHz* nuclear magnetic resonance spectrometer.

The EPR spectra were recorded on an ER 200D-SCR spectrometer with a Bruker B-E25 magnet and an ER 041MR microwave generator.

The technetium content was measured by a HIDEX 300 SL liquid scintillation counter.

5.3. Syntheses

5.3.1 Attempted synthesis of $(AsPh_4)_2[\{TcNF_2\}_2(\mu\text{-}O)_2]$ from $Cs_2[TcNCl_5]$ and $HF_{(aq)}$

Cesium pentachloridonitridotechnetate(VI) (0.2 mmol, 111 mg) was dissolved in 5 mL of water. 1 mL of methanesulfonic acid and 0.4 mmol of $AsPh_4Cl$ were added. Dropwise addition of $HF_{(aq)}$ to the rapidly stirred solution gave a yellow precipitate, which was recrystallized from CH_3CN. The compound was finally characterized as $AsPh_4[TcNCl_4]$. Yield: 110 mg, 86%.

5.3.2 Attempted synthesis of $Cs_2[TcNF_5]$ from $Cs_2[TcNCl_5]$ and aHF

Anhydrous hydrofluoric acid (2.5 mL) was filled in an 8 mm outer diameter PFA tube, kept under an inert gas atmosphere and cooled to -78 °C. Cesium pentachloridonitridotechnetate(VI) (0.3 mmol, 166 mg) was added and the mixture was allowed to warm up to room temperature. The red $Cs_2[TcNCl_5]$ was not completely soluble in HF when the mixture was kept under inert condition. The reaction mixture was allowed to evaporate at air. After the complete evaporation of the hydrofluoric acid, the color of the precipitate has changed to bluish-black and the product was identified as $[Tc_2N_2(\mu\text{-}O)_2(OH_2)_2(OH)_2]$. Yield: 39 mg.

IR (ν_{max}/cm^{-1}): 3425 w, 1631 m, 1523 m, 1053 s, 1083 s, 902 s, 740 m, 474 s cm^{-1}.

5.3.3 Attempted synthesis of $K_2[TcNF_5]$ from $[TcN(OH)_3]_n$ and $HF_{(aq)}$

Nitridotechnetic(VI) acid (0.25 mmol, 41 mg) was dissolved in 2 mL of 40% hydrofluoric acid and the reaction mixture was stirred for 1 h. This results in the formation of $[TcNF_4]^-$ in solution. 0.25 mmol (14.5 mg) of KF in a minimum of $HF_{(aq)}$ was added. Slow evaporation of the solvent at room temperature resulted in the formation of potassium pertechnetate, which was isolated as colorless crystals. Yield: 45 mg, 90%.

^{99}Tc NMR ($HF_{(aq)}$): δ - 4.35 ppm.

5.3.4 Synthesis of $M_4[Tc_2N_2F_8O]$ (M=Rb, Cs)

Nitridotechnetic(VI) acid (0.05 mmol, 9 mg) was dissolved in 3 mL of aqueous HF (48%) solution. 0.5 mmol of MF (M= Rb, Cs) dissolved in $HF_{(aq)}$ was added. Slow evaporation of this solution at room temperature resulted in the formation of $M_4[Tc_2N_2F_8O]$ (M = Rb, Cs) as orange-yellow crystals. Excess of MF was removed by washing with a mixture of cold H_2O and ethanol. $M_4[Tc_2N_2F_8O]$ was recrystallized from $HF_{(aq)}$.

$Rb_4[Tc_2N_2F_8O]$(**11**): Yield: 12 mg, 60%.

Anal. calcd for $Rb_4Tc_2N_2F_8O$: Tc, 26.9; Found: Tc, 26.0.

IR (ν_{max}/cm^{-1}): 3244 br, 1062 s, 974 m, 734 m, 615 s, 561 s,480 sh .

$Cs_4[Tc_2N_2F_8O]$(**12**): Yield: 16 mg, 64%.

Anal. calcd for $Cs_4Tc_2N_2F_8O$: Tc, 21.4; Found: Tc, 20.6.

IR (ν_{max}/cm^{-1}): 3561 b, 1053 s, 1024 sh, 907 m, 707 m, 642 m, 590 s .

5.3.5. Synthesis of $(NEt_4)_3(NH_4)[Tc_4N_4O_4F_8]$

Nitridotechnetic(VI) acid (0.055 mmol, 9 mg) was suspended in 3 mL of aqueous HF (48%) and the mixture was stirred until the precursor was dissolved. $NEt_4F{\cdot}2H_2O$ (0.5 mmol, 74.6 mg) dissolved in HF (48%) was added and slow evaporation of hydrofluoric acid resulted in the formation of $(NEt_4)_3(NH_4)[Tc_4N_4O_4F_8]$ as yellow-orange crystals. The excess of $NEt_4F{\cdot}2H_2O$ was washed out with a mixture of cold water and ethanol. $(NEt_4)_3(NH_4)[Tc_4N_4O_4F_8]$ (**13**) was recrystallized from $HF_{(aq)}$. Yield: 9 mg, 60%.

Anal. calcd for $C_{24}H_{64}N_8Tc_4O_4F_8$: Tc, 36.8; Found: Tc, 35.9.

IR (ν_{max}/cm^{-1}): 3422 b, 2987 m, 1684 s, 1643 m, 1480 s, 1391s, 1172 s, 1050 s, 999 s, 782 s, 707 s, 631m, 598 m, 556 s.

5.3.6. Synthesis of $Na_4[Tc_2N_2F_8O]$

Ammonium pertechnetate (0.32 mmol, 58 mg) was dissolved in 15 mL of $HF_{(aq)}$ (48%). NaN_3 (3.2 mmol, 200 mg) dissolved in 0.5 mL of water was added carefully to the mixture. The mixture was heated under reflux for 2 hr. Five portions of each 200 mg NaN_3 were added during this period. The volume was reduced to 3 mL under vacuum. Evaporation of the solution resulted in colorless NaF and pertechnetate crystals which were filtered off. Slow evaporation of the remaining hydrofluoric acid resulted in the formation of a few orange-red crystals of $Na_4[Tc_2N_2F_8O]$ (**14**).

IR (ν_{max}/cm^{-1}): 3450 b, 3217 m, 3056 b, 1639 m, 1431 m, 1329 m, 1183 s, 1042 s, 873 m, 854 m, 719 s, 584 m, 556 s.

5.3.7. Synthesis of $Cs_4[Tc_2N_2F_8O]$ from $NH_4[TcO_4]$ using $Na_2S_2O_4$ as reducing agent

$NH_4[TcO_4]$ (0.2 mmol, 38 mg) was dissolved in 10 mL $HF_{(aq)}$ (48%). NaN_3 (2 mmol, 131 mg) in 0.5 mL of H_2O was added followed by $Na_2S_2O_4$ (0.4 mmol, 64 mg) in 0.5 mL of H_2O. The reaction mixture was heated on reflux for 2 hr. The solution became orange-yellow. CsF (243 mg, 1.6 mmol) in $HF_{(aq)}$ was added. The volume was reduced by slow evaporation at room temperature. Colorless crystals of by-products were formed initially and were filtered off. $Cs_4[Tc_2N_2F_8O]$ was formed as orange-yellow crystals upon concentration of the reaction mixture. Yield: 69 mg ,75%.

Anal. calcd for $Cs_4Tc_2N_2F_8O$: Tc, 21.4; Found: Tc, 20.5.

IR (ν_{max}/cm^{-1}): 3493 b, 3300 m, 3218 b, 1419 m, 1236 m, 1191 m, 1072 s, 1038 sh, 968 m, 802 m, 742sh, 724 m, 609 s, 586 m, 562 s.

5.3.8. Reaction of $Rb_4[Tc_2N_2F_8O]$ with KCN

A solution of KCN (67 mg, 1.01 mmol) in 2 mL of water was added to solid $Rb_4[Tc_2N_2F_8O]$ (0.1 mmol, 77 mg) and the mixture was stirred until all the solid dissolved. $AsPh_4Cl$ (0.24 mmol, 100 mg) in 1 mL of water was added. The mixture was gently heated and allowed to evaporate at room temperature. Yellow crystals of $(AsPh_4)_2[TcN(CN)_4(OH_2)]\cdot 5H_2O$ were obtained. Yield: 190 mg, 87% based on $Rb_4[Tc_2N_2F_8O]$.

Anal. calcd for $C_{52}H_{52}As_2N_5O_6Tc$: Tc, 9.1; Found: Tc, 8.7.

IR (ν_{max}/cm^{-1}): 3460 m, 3.57 m, 2113 s, 1481 s, 1436 s, 1080 s, 1055 m, 997 vs, 896 s, 848 m, 742 s, 688 s, 476 s, 457 m.

5.3.9. Reaction of $Rb_4[Tc_2N_2F_8O]$ with diluted H_2O_2

$Rb_4[Tc_2N_2F_8O]$ (0.1 mmol, 77mg) were dissolved in 5 mL of 10% H_2O_2. The yellow solution was allowed to evaporate at room temperature. Rubidium pertechnetate was isolated as colorless crystals. Yield: 22 mg, 90% based on $Rb_4[Tc_2N_2F_8O]$.

^{99}Tc NMR ($HF_{(aq)}$): δ -4 ppm.

5.3.10. Attempted synthesis of $M_2[TcF_6]$ from $M_2[TcBr_6]$ (M= NH_4, K) and aHF

2.5 mL of anhydrous hydrofluoric acid was filled in an 8 mm outer diameter PFA tube, kept under an inert gas atmosphere and cooled to -78 °C. Addition of hexabromidotechnetate either as potassium or ammonium salt (0.25 mmol) did not result in any reaction even after 5 h. Evaporation of aHF at RT gave back the precursors.

5.3.11. Synthesis of $M_2[TcF_6]$ (M= Na, K)

$M_2[TcBr_6]$ (M= Na, K) (0.1 mmol) was suspended in 5 mL of $HF_{(aq)}$ (40%) solution. AgF (0.6 mmol, 76 mg) in $HF_{(aq)}$ was added dropwise. Colorless AgBr was filtered off after 10 hr and the solution became pale pink in color. After 14 hr, the reaction was complete. Evaporation of the hydrofluoric acid resulted in the formation of $M_2[TcF_6]$ as colorless crystals.

$Na_2[TcF_6]$(**19**): Yield 22 mg, 84%.

Anal. calcd for Na_2TcF_6: Tc, 38.2; Found: Tc, 37.9.

IR (ν_{max}/cm^{-1}): 561 s (Tc-F).

Raman (ν_{max}/cm^{-1}): 611 s, 530 m, 260 s, 240 m, 212 m.

$K_2[TcF_6]$(**20**): Yield 21 mg, 72%.

Anal. calcd for K_2TcF_6 : Tc, 34.0; Found: Tc, 33.1.

IR (ν_{max}/cm^{-1}): 561 s (Tc-F).

Raman (ν_{max}/cm^{-1}): 613 s, 525 m, 259 m, 243 s.

UV/vis: λ = 291 nm (ε = 22.5 $M^{-1}cm^{-1}$), λ = 352 nm (ε = 16.2 $M^{-1}cm^{-1}$).

5.3.12. Synthesis of $M_2[TcF_6]$ (M = Rb, Cs, NMe_4) by metathesis reaction

$K_2[TcF_6]$ (0.1 mmol) was dissolved in 1 mL of $HF_{(aq)}$ (40%). MF (M= Rb, Cs, NMe_4) (0.2 mmol) in 0.3 mL of $HF_{(aq)}$ was added. The solution was allowed to evaporate slowly at room temperature, which gave colorless crystals. The $M_2[TcF_6]$ complexes were separated from other fluorides by subsequent washing with cold water and recrystallized from aqueous HF.

$Rb_2[TcF_6]$(**21**): Yield: 32 mg, 83%.

Anal. calcd for Rb_2TcF_6 : Tc, 24.6; Found: Tc, 24.1.

IR (ν_{max}/cm^{-1}): 563 cm^{-1} (Tc-F).

Raman (ν_{max}/cm^{-1}): 605 s, 520 m, 249 m, 240 s.

$Cs_2[TcF_6]$(**22**): Yield: 39 mg, 83%.

Anal. calcd for Cs_2TcF_6 : Tc, 20.6; Found: Tc, 19.8.

IR (ν_{max}/cm^{-1}): 555 (Tc-F).

Raman (ν_{max}/cm^{-1}): 598 s, 514 m, 237 s.

$(NMe_4)_2[TcF_6]$(**23**): Yield: 30 mg, 83%.

Anal. calcd for $C_8H_{24}N_2TcF_6$: Tc, 27.4; Found: Tc, 26.9.

IR (ν_{max}/cm^{-1}): 3286 br, 3012m, 2351 m, 1525 s, 1487 s, 1463 s, 1255 sh, 1236 s, 948 s, 565 s (Tc-F).

5.3.13. Synthesis of $(NH_4)_2[TcF_6]$ from $NH_4[TcO_4]$

$NH_4[TcO_4]$ (0.1 mmol) was dissolved in 0.5 mL of water. HF (40%) (1 mL) and Zn dust (0.77 mmol, 50 mg) were added. The reaction mixture was heated at 50°C for 30 min. NH_4F (0.1 mmol, 4 mg) in 0.5 mL $HF_{(aq)}$ was added and the mixture was allowed to evaporate slowly at room temperature. $(NH_4)_2[TcF_6]$ was formed as colorless crystals and separated from $ZnF_2\cdot4H_2O$ by washing with water.

$(NH_4)_2[TcF_6]$ (**18**): Yield 12 mg, 50%.

Anal. calcd for $N_2H_8TcF_6$: Tc, 34.7; Found: Tc, 33.9.

IR (ν_{max}/cm^{-1}): 3282 br, 1616 m, 1523 m, 1415 s, 567 s (Tc-F).

5.3.14. Synthesis of $M_2[TcF_6]$ from $[TcO_4]^-$ by using $Na_2S_2O_4$ as reducing agent

$NH_4[TcO_4]$ (0.2 mmol, 36 mg) was dissolved in 10 mL of $HF_{(aq)}$ (48%). $Na_2S_2O_4$ (0.4 mmol, 69.6 mg) in 0.5 mL of water was added. Immediately, a small amount of a pale brown residue was formed. The solution was heated on reflux for 2h. The pale brown precipitate was filtered off and MF (M = Na, K, Rb, Cs or NMe_4) (0.45 mmol) in 0.3 mL of $HF_{(aq)}$ was added. The solution was kept for slow evaporation at room temperature. Colorless crystals of $M_2[TcF_6]$ together with by-products were obtained. The by-products were removed by washing with small amounts of cold water. $M_2[TcF_6]$ was recrystallized from aqueous HF. For the isolation of the sodium salt, washings must be repeated several times.

$Na_2[TcF_6]$(**19**): Yield: 25 mg, 50%.

Anal. calcd for Na_2TcF_6: Tc, 38.2; Found: Tc, 37.6.

Raman (ν_{max}/cm^{-1}): 611 s, 530 m, 260 s.

$K_2[TcF_6]$(**20**): Yield: 46 mg, 80%.

Anal. calcd for K_2TcF_6: Tc, 33.9; Found: Tc, 33.1.

Raman (ν_{max}/cm^{-1}): 613 s, 525 m, 259 m, 243 s.

$Rb_2[TcF_6]$(**21**): Yield: 61 mg, 80%.

Anal. calcd for Rb_2TcF_6: Tc, 25.8; Found: Tc, 25.0.

$Cs_2[TcF_6]$(**22**): Yield: 86 mg, 90%.

Anal. calcd for K_2TcF_6: Tc, 20.7; Found: Tc, 20.1.

$(NMe_4)_2[TcF_6]$(**23**): Yield: 65 mg, 90%.

Anal. calcd for $N_2C_8H_{24}TcF_6$: Tc, 27.4; Found: Tc, 26.9.

5.3.15. Synthesis of $Na(NH_4)_3[Tc_2OF_{10}]$

$(NH_4)_2[TcF_6]$ (0.1 mmol, 24 mg) was dissolved in 2 mL $NH_{3(aq)}$ (25 %). The color of the reaction mixture changed to pink. NaF (0.1 mmol, 4 mg) was added and the mixture was kept at room temperature for slow evaporation. Pink crystals of $Na(NH_4)_3[Tc_2OF_{10}]\cdot 2(NH_4F)$ (**24**) were isolated in a quantitative yield.

Anal. calcd for $N_5H_{20}NaOTc_2F_{12}$: Tc, 35.6; Found: Tc, 35.3.

IR (ν_{max}/cm^{-1}): 3242 br, 1414 m, 913 m (Tc – O), 731 m (Tc – O –Tc), 555 s (Tc-F).

Raman (ν_{max}/cm^{-1}): 3242 m, 1691 m, 1430 m, 1089 m, 606s, 583 sh, 518 m, 243 s.

UV/vis: λ = 291 nm (ε = 2096 $M^{-1}cm^{-1}$), λ = 547 nm (ε = 38.9 $M^{-1}cm^{-1}$)

5.3.16. Synthesis of $[Tc_2O(CH_3CN)_{10}][SbF_6]_4\cdot CH_3CN$

$K_2[TcF_6]$ (0.3 mmol, 87 mg) was poured into a solution of SbF_5 (14 mmol, 736 mg) in 2 mL of aHF at -173 °C. The reaction mixture was first brought to -72 °C in a dry-ice/ethanol bath. Then it was brought to room temperature. Solid $K_2[TcF_6]$ slowly dissolved and gave a pale blue solution, from which a precipitate was formed. After complete precipitation, the aHF was removed under vacuum. 4 mL of dry CH_3CN was added to the precipitate. The color turned to dark brown. The volume was reduced under vacumm. Green crystals of $[Tc_2O(CH_3CN)_5][SbF_6]_4\cdot CH_3CN$ (**25**) were obtained from the acetonitrile solution at 0 °C. Yield: 161 mg, 66%.

Anal. calcd for $C_{24}H_{36}Sb_4F_{24}N_{12}OTc_2$: Tc, 11.9; Found: Tc, 10.5.

IR (ν_{max}/cm^{-1}): 2324 m, 2299 m (C≡N), 1035 s, 974 s, 956 m, 935 m (Tc – N), 852, m (Tc – O – Tc), 657, s (Sb-F).

Raman (ν_{max}/cm^{-1}): 2943 m, 2327 sh, 2295 m, 955 m, 708 s, 644 m, 443 s, 346 s.

^1H NMR (CD_3CN): δ 2.84 ppm (coordinated CH_3CN), 1.94 ppm (free CH_3CN).

5.3.17. Attempted synthesis of TcF_4

$K_2[TcF_6]$ (0.3 mmol, 87 mg) was poured into SbF_5 (190 mg, 0.9 mmol) in aHF (5 mL) at -173 °C in an S shaped PFA tube. The reaction mixture was first brought to -73 °C in a dry-ice-ethanol bath. The solid dissolved completely upon warming to room temperature. A yellow-tan solid precipitated upon cooling to -20 °C. The excess of aHF and SbF_5 was decanted carefully. The solid was dried under vaccum at -20 °C.

Raman (ν_{max}/cm^{-1}): 673 sh, 658 s, 574 m, 277 sh.

IR (slightly decomposed) (ν_{max}/cm^{-1}): 854 m, 663 s, 617 sh, 563 s.

5.3.18. Synthesis of $[Tc(NO)(NH_3)_4F]_4[TcF_6][HF_2]_2$

Potassium hexafluoridotechnetate (0.1 mmol, 29 mg) was dissolved in 1 mL of aqueous HF (48%) and acetohydroxamic acid (1.3 mmol, 96 mg) in 2 mL of H_2O was added. The reaction mixture was stirred for 30 min and kept for evaporation. Orange-red crystals of $[Tc(NO)(NH_3)_4F]_4[TcF_6][HF_2]_2$ (**26**) appeared after a few days. Yield: almost quantitative.

Anal. calcd for $F_{14}H_{50}N_{20}O_4Tc_5$: Tc, 42.8; Found: Tc, 41.9.

IR (ν_{max}/cm^{-1}): 3341 w, 3262 w, 3187 w, 3096 m, 1677 s, 1444 m, 1377m, 1278 m, 1215 m, 1150 s, 1100 m, 1049 m, 1037 m, 1010 w, 959 m, 836 m, 766 m, 765 vs, 744 m, 655 m, 635 m, 559 s.

Raman (ν_{max}/cm^{-1}): 3351, 3312, 3273, 3203, 1669, 1626, 1608, 1312, 1290, 1257, 1087, 1000, 628, 619, 602,521, 504, 464, 450, 438, 426, 254, 233, 209.

^{99}Tc NMR (D_2O, ppm): δ 1928 ($\Delta\nu_{1/2}$ = 2600 Hz).

^{19}F NMR (D_2O, ppm): δ -143.5 (s) (*trans* Tc-F), -150.2 (s) (HF_2^-)

5.3.19. Synthesis of $K_2[Tc(NO)F_5]\cdot H_2O$ and $[Tc(NO)(NH_3)_4F]PF_6\cdot 1/2\ KPF_6$

$NH_4[TcO_4]$ (0.2 mmol, 36 mg) was dissolved in 7 mL of $HF_{(aq)}$ (48%). Acetohydroxamic acid (6 mmol, 0.450 g) dissolved in 1 mL of water was added. The color of the solution changed to dark orange-red immediately. The reaction mixture was refluxed for 2h. KPF_6 (0.5 mmol, 92 mg) in water was added and the solution was kept at room temperature for crystallization. Two products were obtained. Blue crystals of $K_2[Tc(NO)F_5]\cdot H_2O$ (**27**) crystallized first and were separated by filtration. From the remaining solution, orange-red crystals of $[Tc(NO)(NH_3)_4F]PF_6\cdot 1/2\ KPF_6$ (**32**) were isolated.

$K_2[Tc(NO)F_5]\cdot H_2O$ (**27**): Yield: 32 mg, 50%.

Anal. calcd for $F_5H_2K_2NO_2Tc$: Tc, 30.9; Found: Tc, 30.1.

IR(ν_{max}/cm^{-1}): 3585 br, 1780 s, 1768 sh, 1643 m, 1525 m, 1431 m, 1234 m, 627sh, 610 s, 567 sh, 529 s, 482 s, 287 sh, 265 s, 212 vw.

Raman (ν_{max}/cm^{-1}): 1778 s, 1766 sh, 627 sh, 610 s, 574 s, 527 vw, 534 vww, 501 m, 482 vw, 291 sh, 274 s, 227 s, 218 sh, 137 s, 97 m.

$[Tc(NO)(NH_3)_4F]PF_6\cdot 1/2\ KPF_6$, (**32**) Yield 16 mg, 36%.

Anal. calcd for $F_{10}H_{12}K_{0.5}N_5OP_{1.5}Tc$: Tc, 21.8; Found: Tc, 20.9.

IR (ν_{max}/cm^{-1}): .3367 w, 3303 w, 3202 w, 2958 w, 2640 w, 1677 s, 1626 m, 1532 m, 1291 s, 1268 sh, 997 m, 868 sh, 824 sh, 740 m, 629 m, 553 s.

UV/vis: in H_2O: λ = 269 nm (ε = 202.0 M^{-1}cm^{-1}), 364 nm (ε = 36.1 M^{-1}cm^{-1}) and 458 nm (ε = 45.1 M^{-1}cm^{-1}).

^{99}Tc NMR (D_2O, ppm): δ 1933 ppm ($\Delta\nu_{1/2}$ = 2700 Hz).

^{19}F NMR (D_2O, ppm): δ -73 (d, PF_6^-), -142 (*trans* Tc-F).

5.3.20. Synthesis of $Rb_2[Tc(NO)F_5]\cdot H_2O$ and $[Tc(NO)(NH_3)_4F]HF_2\cdot 1/2\ RbF$

NH_4TcO_4 (0.2 mmol, 36 mg) was dissolved in 7 mL of $HF_{(aq)}$ (48%). Acetohydroxamic acid (6 mmol, 0.450 g) in 1 mL of water was added. The color of the solution changed to dark orange-red. The reaction mixture was refluxed for 2h. RbF (0.5 mmol, 52 mg) in $HF_{(aq)}$ (48%) was added and the resulting solution was kept at room temperature for crystallization. Two products were obtained. Blue crystals of $Rb_2[Tc(NO)F_5]\cdot H_2O$ (**28**) crystallized first and were separated by filtration. From the remaining mother solution, orange-red crystals of $[Tc(NO)(NH_3)_4F](HF_2)\cdot 1/2\ RbF$ (**30**) crystallized.

$Rb_2[Tc(NO)F_5]\cdot H_2O$ (**28**): Yield: 41 mg, 50%.

Anal. calcd for $F_5H_2Rb_2NO_2Tc$: Tc, 23.9; Found: Tc, 23.1.

IR(ν_{max}/cm^{-1}): 3582 br, 1780 s, 1768 sh, 1648 m, 1432 m, 1194 m, 626 sh, 610 s, 561 sh, 525 s, 505 sh, 480 s, 279 m, 260 s, 208 vw.

Raman (ν_{max}/cm^{-1}): 1775 s, 1766 sh, , 622 s, 568 s, 499 w, 288 s, 267 s, 224 s, 130 s, 112 s, 97 m.

$[Tc(NO)(NH_3)_4F](HF_2)\cdot 1/2\ RbF$ (**30**): Yield: 12.3 mg, 40%.

Anal. calcd for $F_{3.5}H_{13}N_5ORb_{0.5}Tc$: Tc, 32.2; Found: Tc, 31.5.

IR (ν_{max}/cm^{-1}): 3578 w, 3322 w, 3194 w, 3089 w, 2878 w, 1782 m, 1620s, 1485 m, 1417 s, 1298 m, 1270 m, 1211 s, 1066 m, 999 m, 757 s, 734 s, 635 m, 525 s.

^{99}Tc NMR (D_2O, ppm): δ 1926 ($\Delta\nu_{1/2}$ = 2700 Hz).

^{19}F NMR (D_2O, ppm): δ -147.9 (s), (*trans* Tc-F), -151.1 (s), (HF_2^-).

5.3.21. Synthesis of $Cs_2[Tc(NO)F_5]\cdot H_2O$ and $[Tc(NO)(NH_3)_4F]HF_2\cdot 1/2\ CsF$

$NH_4[TcO_4]$ (0.2 mmol, 36 mg) was dissolved in 7 mL of $HF_{(aq)}$ (48%). Acetohydroxamic acid (6 mmol, 0.450 g) in 1 mL of water was added. The color of the solution changed to dark orange-red. The reaction mixture was heated on reflux for 2h. CsF (0.5 mmol, 76 mg) in $HF_{(aq)}$ (48%)was added and the solution was kept at room temperature for crystallization. Two products were obtained. Blue crystals of $Cs_2[Tc(NO)F_5]\cdot H_2O$ (**29**) crystallized first and were separated by filtration. From the remaining mother solution, orange-red crystals of $[Tc(NO)(NH_3)_4F](HF_2)_2\cdot 1/2\ CsF$ (**31**) crystallized.

$Cs_2[Tc(NO)F_5]\cdot H_2O$ (**29**): Yield: 50 mg, 50%.

Anal. calcd for $F_5H_2Cs_2NO_2Tc$: Tc, 19.5; Found: Tc, 19.1.

IR(ν_{max}/cm^{-1}): 3575 br, 1752 s, 1748 sh, 1646 m, 1440 m, 623 sh, 607 s, 559 sh, 519 s, 505 sh, 493 sh, 476 s, 278 m, 255 s, 205 vw.

Raman (ν_{max}/cm^{-1}): 1772 s, 1764 sh, , 644 s, 619 s, 560 s, 513 vw, 495 w, 285 s, 260 s, 232 s, 221 s, 123 s, 111 s, 82 m.

UV/vis: in HF (13.8 M): λ = 216 nm (ε = 541.3 M^{-1}cm^{-1}), 237(sh) nm (ε = 334.2 M^{-1}cm^{-1}), 315 nm (ε = 28.8 M^{-1}cm^{-1}), 397 nm (ε = 23.1 M^{-1}cm^{-1}), 586 nm (ε = 13.9 M^{-1}cm^{-1}).

UV/vis: in H_2O: λ = 269 nm, 319 nm, 396 nm, 585 nm.

$[Tc(NO)(NH_3)_4F](HF_2)\cdot 1/2\ CsF$ (**31**): Yield: 13.6 mg, 40%.

Anal. calcd for $F_{3.5}H_{13}N_5OCs_{0.5}Tc$: Tc, 29.9; Found: Tc, 28.1.

IR (ν_{max}/cm^{-1}): 3532 w, 3328 w, 3194 w, 3046 w, 2701 w, 1772 m, 1622 s, 1428 s, 1301 sh, 1267 m, 1197 m, 998 m, 742 sh, 723 s, 635 m, 604 m, 528 s.

Raman(ν_{max}/cm^{-1}): 3360 w, 3344 w, 3262 w, 3206w, 1686 m, 1631 m, 1251, 1000 m, 792 m, 635 s, 559 m, 469 s, 441 s, 422 sh, 399 sh, 229 s, 187 m.

UV/vis: in H_2O: λ = 269 nm (ε = 133.9 M^{-1}cm^{-1}), 284(sh) nm (ε = 114.5 M^{-1}cm^{-1}), 364 nm (ε = 32.2 M^{-1}cm^{-1}), 458 nm (ε = 39.5 M^{-1}cm^{-1}).

^{99}Tc NMR (D_2O, ppm): δ 1931 ($\Delta\nu_{1/2}$ = 2700 Hz).

^{19}F NMR(D_2O, ppm): δ -143.6 (s), (*trans* Tc-F), -150.2 (s) (HF_2^-)

5.3.22. Synthesis of $[Tc(NO)(py)_4F]PF_6$

$Cs_2[Tc(NO)F_5]\cdot H_2O$ (0.1 mmol, 50 mg) was dissolved in 1 mL of HF_{aq} (48%). Pyridine (2 mL) was added and heated on reflux for 1h. The volume was reduced to 0.5 mL. KPF_6 (0.1 mmol, 18.4 mg) was added in 0.3 mL of water. Orange-red crystals of $[Tc(NO)(py)_4F]PF_6$ (**33**) were formed by slow evaporation of the solution.

Yield : 36 mg, 60%. Anal. calcd for $C_{20}H_{20}F_7N_5OPTc$: Tc, 16.2; Found: Tc, 15.7.

IR (ν_{max}/cm^{-1}): 3115 w, 1699, 1604 m, 1566 m, 1487 s, 1448 s, 1363 m, 1219 m, 1155 m, 1066 m, 1049 m, 877 sh, 840 s, 763 sh, 761 s, 698 s, 635 m, 557 s, 505 m, 464 m.

UV/vis: in CH_3CN: λ = 247 nm (ε = 18334 $M^{-1}cm^{-1}$), 360 nm (ε = 16944 $M^{-1}cm^{-1}$) and 442 nm (ε = 39.5 $M^{-1}cm^{-1}$).

^{99}Tc NMR (CD_3CN, ppm): δ 1721 ($\Delta\nu_{1/2}$ = 650 Hz).

^{19}F NMR (CD_3CN, ppm): δ -73.7(d, PF_6^-), -171(*trans* Tc-F).

^{1}H NMR (CD_3CN, ppm): δ 8.63(d), 7.37 (t), 7.80 (t).

^{13}C NMR (CD_3CN, ppm): δ 150.82(d), 138.89 (s), 125.89 (d).

5.3.23. Synthesis of $[Tc(NO)(NH_3)_4(OOCCF_3)](OOCCF_3)\cdot CF_3COOH$

$[Tc(NO)(NH_3)_4F]HF_2\cdot$1/2 CsF (0.01 mmol, 7 mg) was dissolved in trifluoroacetic acid (0.5 mL) and the solution was left to evaporate slowly at room temperature. Orange crystals of $[Tc(NO)(NH_3)_4(OOCCF_3)](OOCCF_3)\cdot CF_3COOH$ (**34**) were obtained.

Yield: 10 mg, 90%.

Anal. calcd for $[Tc(NO)(NH_3)_4(OOCCF_3)](OOCCF_3)\cdot CF_3COOH$: Tc, 18.4; Found: 17.7 Tc.

IR (ν_{max}/cm^{-1}): 3348 br, 3303 br, 3269 br, 3147 br, 1670 s, 1656 sh, 1439 s, 1421 m, 1290 s, 1180s, 1139 s, 1115 m, 852 m, 829 s, 799 s, 752 m, 717 s, 614 m, 599 m.

Raman(ν_{max}/cm^{-1}): 1684 m, 1439 s, 1421 m, 1088 br, 852 m, 834 m, 726 m, 625 s, 598 sh, 500 m, 463 m, 418 m, 404 m, 264 m, 196 s.

^{99}Tc NMR (CD_3CN, ppm): δ 2017 ($\Delta\nu_{1/2}$ = 3840 Hz).

^{19}F NMR (CD_3CN, ppm): δ -76.27 and -76.3 (CF_3).

^{1}H NMR (CD_3CN, ppm): δ 2.54 (s) (NH_3).

5.4. Crystal structure determinations

The intensities for the X-ray structure determinations were collected on a *STOE* IPDS 2T or Enraf Nonius CAD 4 instruments with Mo Kα radiation. The space groups were determined using CHECK-HKL.[4] Absorption corrections were carried out by Psi-Scans[5] or X-RED32.[6] Structure solution and refinement were performed with the *SHELXS* 97,[7] *SHELXS* 86[7] and *SHELXL* 97[8] programs. Hydrogen atoms were calculated based on the electron density of the Fourier map difference and refined isotropically whenever is possible. Otherwise, they were calculated for idealized positions and treated with the 'riding model' option of *SHELXL* 97.

5.5. References

(1) Baldas, J.; Bonnyman, J.; Williams, G. A. *Inorg. Chem.* **1986**, *25*, 150.

(2) Baldas, J.; Boas, J. F.; Bonnyman, J. *Aust. J. Chem.* **1989**, *42*, 639.

(3) Dalziel, J.; Gill, N. S.; Nyholm, R. S.; Peacock, R. D. *J. Chem. Soc.* **1958**, 4012.

(4) *CHECK HKL* Kretschmar, M., Universität Tübingen, **1998**.

(5) North, A. C. T.; Phillips, D. C.; Mathews, F. S. *Acta Crystallographica Section A-Crystal Physics Diffraction Theoretical and General Crystallography* **1968**, *A 24*, 351.

(6) *X-RED32.* STOE&Cie GmbH, Darmstadt, Germany.

(7) *SHELXS 86*, *97* Sheldrick, G. M., Universität Göttingen, **1986, 1997**.

(8) *SHELXL 97* Sheldrick, G. M., Universität Göttingen, **1997**.

Summary

This thesis describes the synthesis and characterization of novel fluorido complexes of technetium with the metal in the oxidation states of "+1", "+2", "+4" and "+6".

The first chapter reports about the isolation of fluoridonitridotechnetate(VI) salts either from nitridotechnetic(VI) acid or directly from pertechnetate by the use of additional reducing agents. The cesium salt of the compound forms a dimeric oxido-bridged complex, whereas the tetraethylammonium salt forms a tetrameric oxido-bridged complex. Both the dimeric and the tetrameric oxido-bridged complexes re-form the monomeric $[TcNF_4]^-$ in solution. This could be identified by EPR spectroscopy.

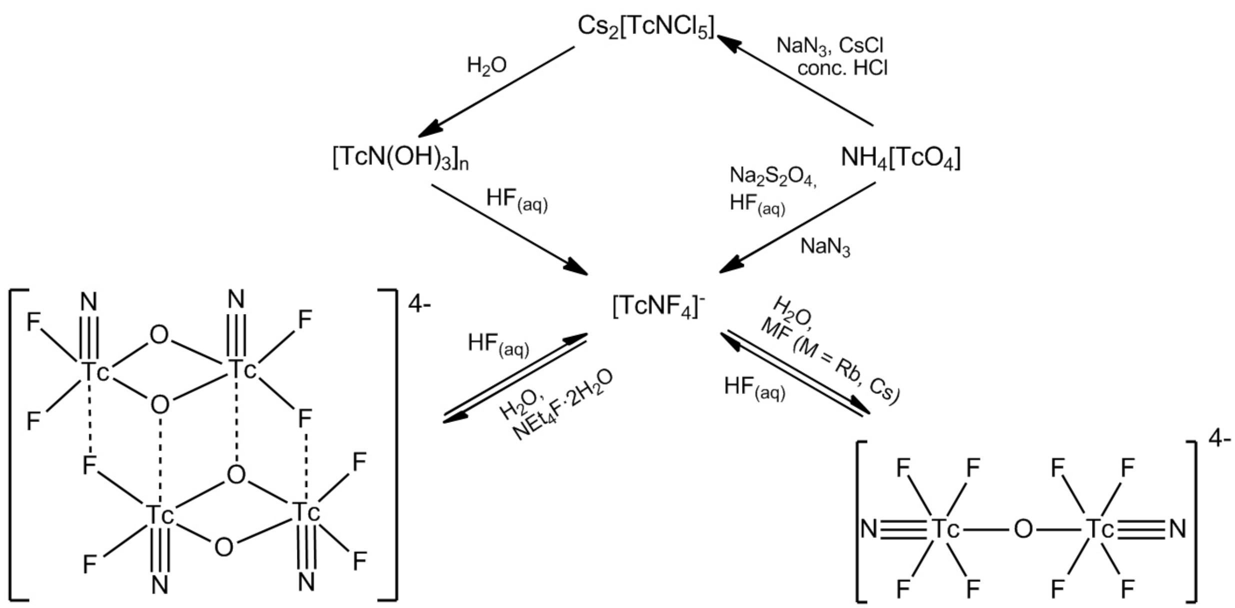

In the second chapter, syntheses, structural chemistry and reactivity of hexafluoridotechnetate(IV) salts are reported. Hitherto, the known synthetic routes for the preparation of hexafluoridotechnetate(IV) were either tedious or time-consuming. This thesis contains novel and improved syntheses for $[TcF_6]^{2-}$ salts. The products are colorless and have been identified for the first time by single-crystal X-ray analysis of the ammonium, sodium, potassium, rubidium, cesium and tetramethylammonium salts.

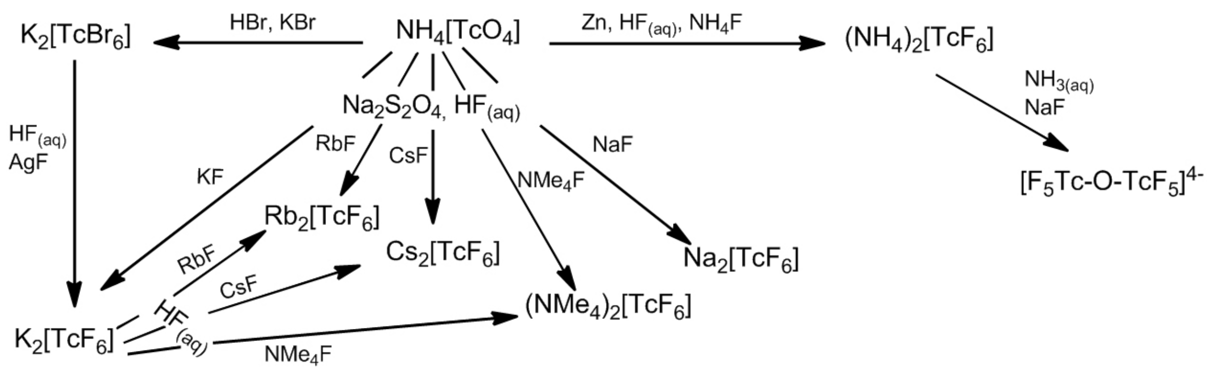

The work in this thesis explains the origin of the pink color of $[TcF_6]^{2-}$, which has been reported in the literature before. This color is exclusively due to the initial hydrolysis product of the compound. In alkaline media, a slow hydrolysis of $[TcF_6]^{2-}$ is observed and the first step hydrolysis product, the dimeric oxido-bridged complex $[F_5Tc–O–TcF_5]^{4-}$, could be isolated and studied structurally. The attempted synthesis of the binary fluoride TcF_4 from hexafluoridotechnetate(IV), SbF_5 and aHF resulted in the formation of a yellow tan solid.

The third chapter of this thesis reports the synthesis and characterization of fluoridonitrosyltechnetium compounds with the metal in the oxidation states “+2” and “+1” by using acetohydroxamic acid as reducing agent. The reduction of hexafluoridotechnetate(IV) by acetohydroxamic acid under aqueous acidic conditions at room temperature gives the technetium(I) cation $[Tc(NO)(NH_3)_4F]^+$ as $[TcF_6]^{2-}/(HF_2)^-$ salt directly from the reaction mixture. This compound represents the first nitrosyltechnetium complex with a fluorido ligand. The source for the nitrosyl/ammine ligands is the hydroxamic acid. The oxidation state of the metal in $[Tc(NO)(NH_3)_4F]^+$ was confirmed by ^{99}Tc and ^{19}F NMR spectroscopy.

Reactions of pertechnetate with acetohydroxamic acid in the presence of conc. $HF_{(aq)}$ result in the formation of mixtures of two products: pentafluoridonitrosyltechnetate(II) and the Tc(I) nitrosyl complex, $[Tc(NO)(NH_3)_4F]^+$. The compounds were characterized by IR, Raman, EPR, NMR spectroscopy and their structures were confirmed by single crystal X-ray analysis. $[Tc(NO)F_5]^{2-}$ reacts with pyridine under formation of the Tc(I) pyridine complex, $[Tc(NO)(py)_4F]^+$. The compound was characterized by IR, ^{99}Tc, ^{19}F NMR spectroscopy and single crystal structure analysis.

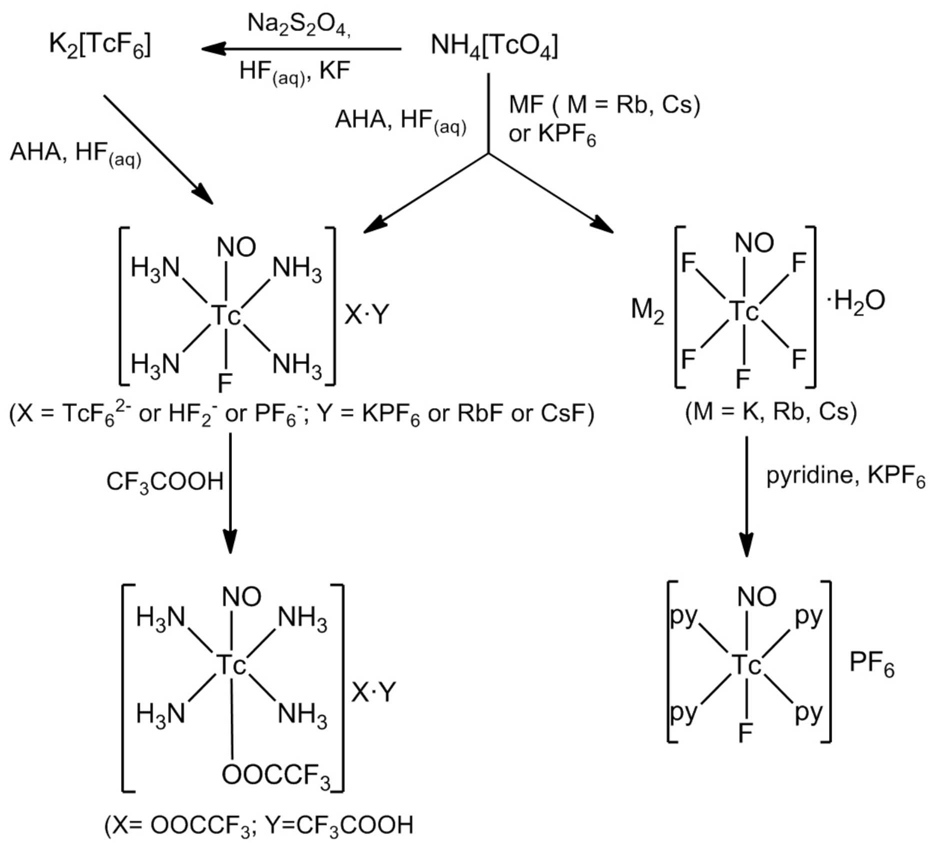

The second product, the Tc(I) nitrosyl complex $[Tc(NO)(NH_3)_4F]^+$ was isolated as $(HF_2)^-$ or PF_6^- salts. It was characterized by IR, Raman, ^{99}Tc and ^{19}F NMR spectroscopy. The crystal structure confirms the moiety of the complex to be similar to that of "Eakin's pink complex", $[Tc(NO)(NH_3)(OH_2)]Cl_2$. During the reaction with trifluoroacetic acid, the fluorido ligand of $[Tc(NO)(NH_3)_4F]$ is replaced by the trifluoroacetato ligand. The resulting compound is crystallized as trifluoridoacetate. It was characterized by IR, ^{99}Tc, ^{19}F NMR spectroscopy and single crystal X-ray diffraction.

Zusammenfassung

Diese Dissertationsscrift befasst sich mit der Synthese und Charakterisierung neuer Technetiumfluoride mit dem Metall in den Oxidationsstufen “+1”, “+2”, “+4” und “+6”.

Im ersten Kapitel wird über die Isolierung von unterschiedlichen Salzen von Fluoridonitridotechnetaten(VI) entweder aus Nitridotechnetium(VI)-säure oder aus Pertechnetat durch den Einsatz geeigneter Reduktionsmittel berichtet. Das Cäsiumsalz dieser Verbindung bildet einen oxido-verbrückten, dimeren Komplex, während das Tetraethylammoniumsalz einen tetrameren Komplex bildet. Beide Salze dissoziieren in HF-Lösung und bilden $[TcNF_4]^-$. Dies konnte durch EPR Spektroskopie nachgewiesen werden.

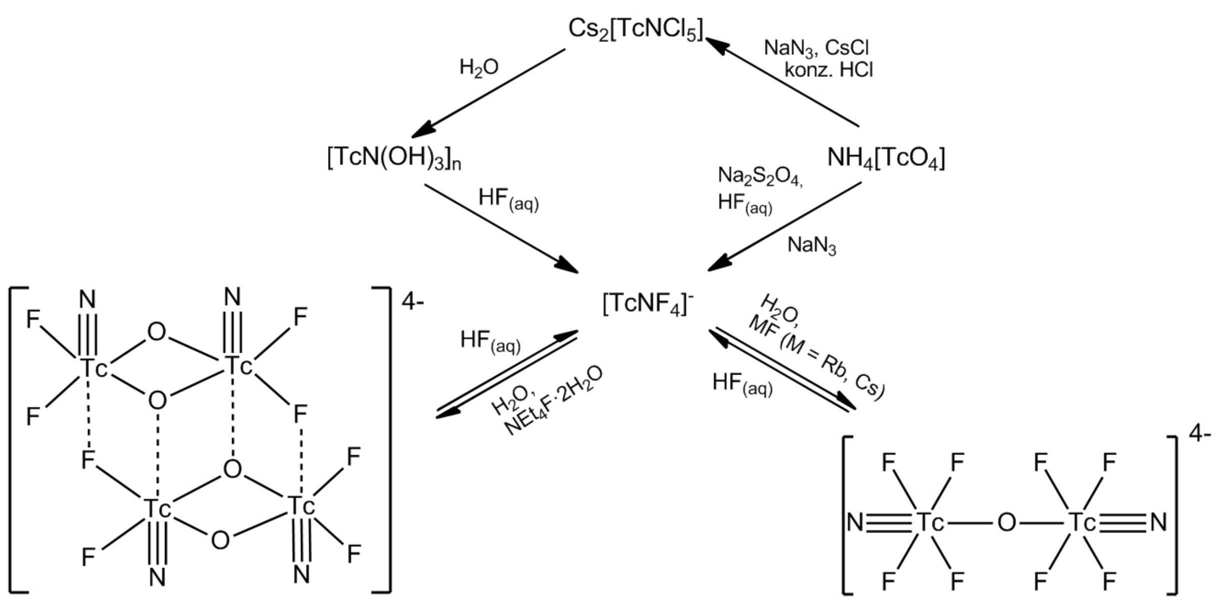

Im zweiten Kapitel wird über Synthese, Struktur und Reaktivität von Hexafluoridotechnetat(IV) berichtet. Die wenigen, bisher bekannten Syntheserouten für Hexafluoridotechnetat(IV)- Salze sind entweder präparativ aufwändig oder zeitaufwändig. Diese Arbeit beschreibt ein Reihe neuer und verbesserter Synthesen für $[TcF_6]^{2-}$ und dessen Salze. Die Natrium-, Kalium-, Rubidium-, Cäsium- und Tetramethylammoniumsalze dieser Verbindung wurden als farblose Kristalle isoliert und durch Röntgenkristallstrukturanalyse charakterisiert.

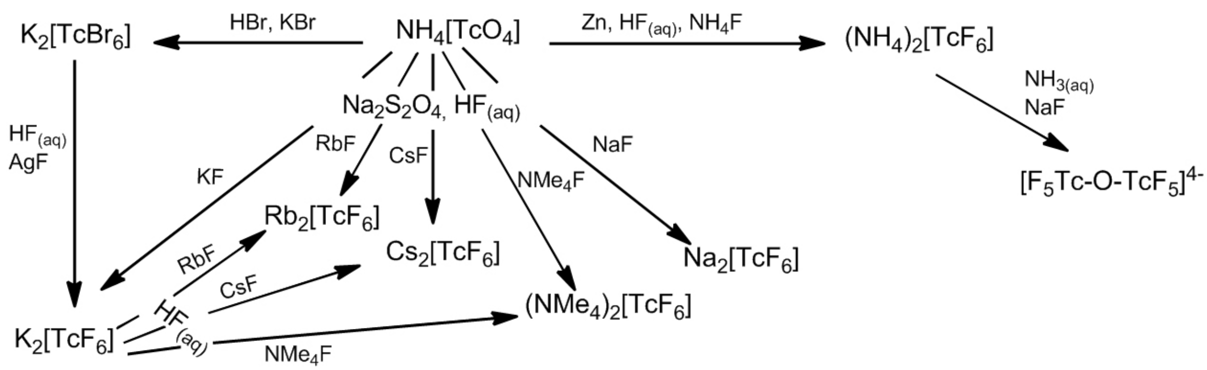

Der Ursprung für die in der Literatur beschriebene rosa Farbe von $[TcF_6]^{2-}$ wurde untersucht. Diese Farbe kommt durch ein Hydrolyseprodukt von $[TcF_6]^{2-}$ zustande. Im alkalischen Medium wird eine langsame Hydrolyse von $[TcF_6]^{2-}$ beobachtet und das erste Hydrolyseprodukt, $[F_5Tc\text{-}O\text{-}TcF_5]^{4-}$, konnte kristallin isoliert und strukturell charakterisiert werden. Die Synthese des binären Fluorids TcF_4 aus Hexafluoridotechnetetat(IV) mit SbF_5 in aHF führte zur Bildung eines hellgelben Niederschlags.

Im dritten Kapitel dieser Arbeit wird die Synthese von Fluoridonitrosylverbindungen mit dem Metal in den Oxidationstufen “+2” und “+1” mit Acetohydroxamsäure als NO-Lieferant und Reduktionsmittel beschrieben. Die Reduktion von Hexafluoridotechnetat(IV) durch Acetohydroxamsäure in wässriger HF führt bei Raumtemperatur zur Bildung des Technetium(I)-Kations $[Tc(NO)(NH_3)_4F]^+$, das als $[TcF_6]^{2-}/(HF_2)^-$ Salz direkt aus der Reaktionsmischung kristallisiert wurden. Diese Verbindung ist der erste Nitrosyltechnetiumkomplex mit einem Fluoridoliganden. Die Quelle für die Nitrosyl- und Amminliganden ist die Acetohydroxamsäure. Die Oxidationsstufe des Metals in $[Tc(NO)(NH_3)_4F]^+$ wurde durch ^{99}Tc- und ^{19}F NMR-Spektroskopie bestätigt.

Die Reaktion von Pertechnetat mit Acetohydroxamsäure in konz. $HF_{(aq)}$ (48%) ergab eine Mischung aus zwei Produkten: Pentafluoridonitrosyltechnetat(II) und $[Tc(NO)(NH_3)_4F]^+$. Die Verbindungen wurden durch IR-, Raman-, EPR- und NMR-Spektroskopie charakterisiert und ihre Strukturen wurden durch Röntgenstrukturanalyse bestätigt.

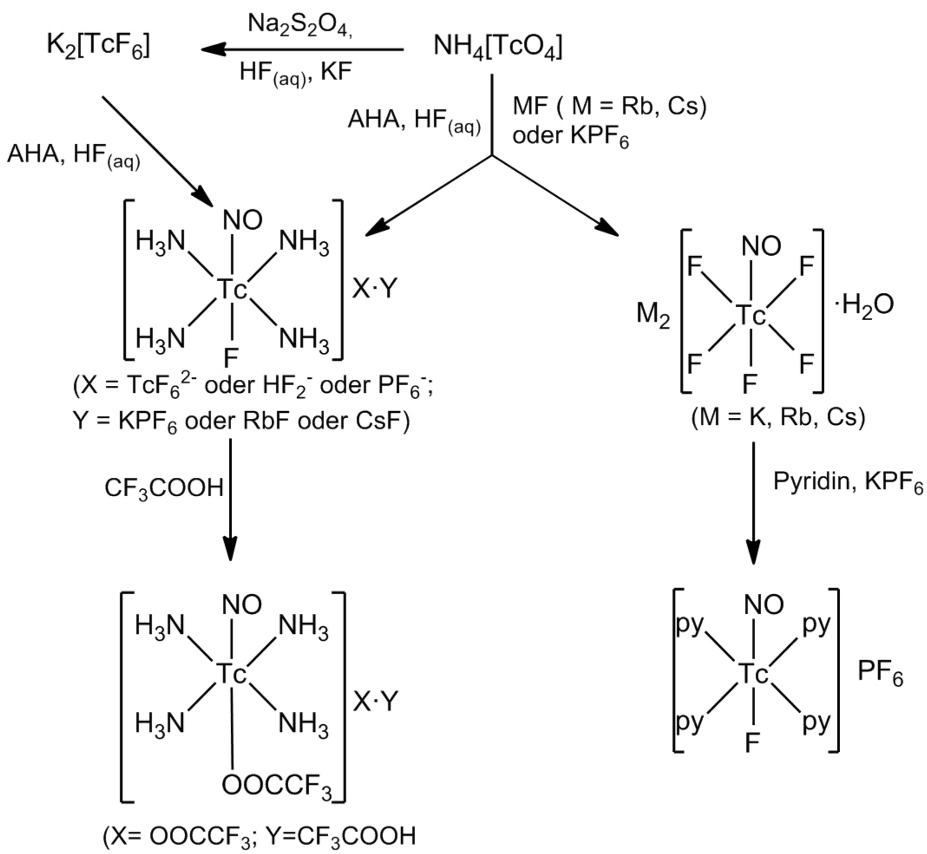

Das zweite Produkt, $[Tc(NO)(NH_3)_4F]^+$, wurde als Salz von $(HF_2)^-$ oder PF_6^- isoliert und durch IR-, Raman-, ^{99}Tc-NMR und ^{19}F-NMR-Spektroskopie charakterisiert. Beider Reaktion von $[Tc(NO)(NH_3)_4F]^+$ mit Trifluoressigsäure wird der Fluoridoligand durch einen Trifluoracetatoliganden ersetzt. Das Produkt kristallisiert als Trifluoracetat und wurde durch IR, ^{99}Tc-NMR- und ^{19}F-NMR-Spektroskopie und Röntgenstrukturanalyse charakterisiert.

Appendix

Crystallographic data

$(NEt_4)_3(NH_4)[Tc_4N_4F_8O_4]$, (13)

Table 1: Crystal data and structure refinement for $(NEt_4)_3(NH_4)[Tc_4N_4F_8O_4]$.

Empirical formula	$C_{24}H_{60}F_8N_8O_4Tc_4$	
Formula weight	1068.80	
Temperature	200(2) K	
Wavelength	0.71073 Å	
Crystal system	Monoclinic	
Space group	$P2_1/c$	
Unit cell dimensions	a = 11.063(1) Å	α = 90°
	b = 17.847(1) Å	β= 115.48(1)°
	c = 22.412(2) Å	γ= 90°
Volume	3994.6(6) $Å^3$	
Z	4	
Density (calculated)	1.777 g/cm^3	
Absorption coefficient	1.431 mm^{-1}	
F(000)	2144	
Crystal description	Plate	
Crystal color	Yellow	
Crystal size	0.15 x 0.1 x 0.06 mm^3	
Theta range for data collection	2.01 to 29.27	
Index ranges	-15<=h<=11, -21<=k<=24, -30<=l<=30	
Reflections collected	21539	
Independent reflections	10462 [R(int) = 0.0789]	
Completeness to theta = 29.27°	96.1 %	
Absorption correction	None	
Hydrogen treatment	Riding model	
Data / restraints / parameters	10462 / 0 / 429	
Goodness-of-fit on F^2	0.999	
Final R indices [I>2sigma(I)]	R_1 = 0.0796, wR_2 = 0.2172	
R indices (all data)	R_1 = 0.1162, wR_2 = 0.2730	
Extinction coefficient	0.016(1)	
Largest diff. peak and hole	3.751 and -2.307 e·$Å^{-3}$	

Table 2: Atomic coordinates (x 10^4) and equivalent isotropic displacement parameters ($Å^2$ x 10^3) for $(NEt_4)_3(NH_4)[Tc_4N_4F_8O_4]$.

	x	y	z	U(eq)
C(5)	3067(13)	6860(7)	10241(6)	70(3)
C(6)	2466(15)	7602(8)	9883(8)	95(5)
C(7)	2553(14)	6038(7)	9277(5)	76(3)
C(8)	3964(16)	6010(7)	9341(7)	77(4)
C(9)	950(11)	6148(8)	9751(5)	75(3)
C(10)	663(15)	6247(10)	10352(8)	102(5)
C(11)	3140(14)	5512(7)	10408(6)	75(3)
C(12)	2742(18)	4735(10)	10168(9)	111(6)
C(13)	-572(13)	6328(6)	6153(6)	69(3)
C(14)	164(19)	6490(9)	5730(8)	107(6)
C(15)	-749(10)	5699(5)	7078(5)	52(2)
C(16)	-257(9)	5145(5)	7646(4)	48(2)
C(17)	-40(11)	4943(5)	6349(4)	53(2)
C(18)	-1411(14)	4650(7)	5927(7)	82(3)
C(19)	1511(10)	5858(5)	7099(5)	55(2)
C(20)	1819(15)	6578(6)	7488(6)	74(3)
C(21)	-4507(10)	5852(5)	2666(5)	52(2)
C(22)	-4743(10)	5156(5)	2258(5)	50(2)
C(23)	-4963(12)	6685(5)	3412(6)	60(3)
C(24)	-5752(13)	6900(6)	3793(6)	66(3)
C(25)	-6783(10)	5827(5)	2662(5)	51(2)
C(26)	-7335(12)	6384(6)	2116(5)	66(3)
C(27)	-4861(11)	5301(5)	3589(5)	56(2)
C(28)	-3366(16)	5221(11)	4027(7)	111(6)
F(4)	9072(5)	8338(2)	8631(2)	45(1)
F(3)	9198(4)	6950(2)	8216(2)	39(1)
F(6)	8253(7)	7174(3)	9110(3)	60(1)
F(5)	8209(5)	5708(2)	8672(2)	50(1)
F(7)	5670(6)	6587(3)	6131(2)	51(1)
F(8)	5620(5)	7982(2)	6546(2)	39(1)

F(1)	6534(6)	7816(3)	5649(3)	60(1)
F(2)	6504(6)	9245(3)	6120(3)	53(1)
N(2)	10437(8)	8087(4)	7855(4)	48(2)
N(3)	5848(8)	6451(4)	8371(4)	45(2)
N(4)	4343(8)	6886(4)	6920(4)	49(2)
N(1)	8948(8)	8566(4)	6407(3)	48(2)
N(5)	2454(8)	6142(5)	9928(3)	53(2)
N(6)	43(8)	5706(4)	6668(4)	45(2)
N(7)	-5254(8)	5919(4)	3095(4)	45(2)
N(8)	7311(8)	7398(5)	4852(4)	55(2)
O(1)	8020(5)	8896(3)	7383(3)	37(1)
O(2)	8036(5)	7385(3)	6955(2)	37(1)
O(3)	6816(5)	7569(3)	7803(2)	34(1)
O(4)	6745(6)	6043(3)	7393(3)	45(1)
Tc(2)	8914(1)	7969(1)	7760(1)	35(1)
Tc(3)	7139(1)	6576(1)	8213(1)	36(1)
Tc(4)	5883(1)	6975(1)	7007(1)	36(1)
Tc(1)	7655(1)	8394(1)	6559(1)	37(1)

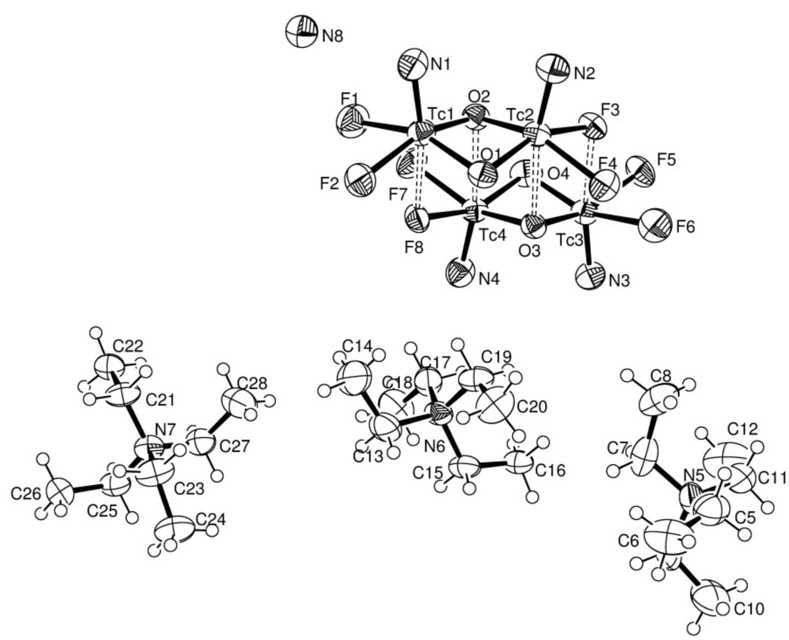

Figure 1: Ellipsoid plot (50% probability) of $(NEt_4)_3(NH_4)[Tc_4N_4F_8O_4]$.

$(NH_4)_2[TcF_6]$, (18)

Table 3: Crystal data and structure refinement for $(NH_4)_2[TcF_6]$.

Empirical formula	F_6N_2Tc	
Formula weight	240.00	
Temperature	200(2) K	
Wavelength	0.71073 Å	
Crystal system	Trigonal	
Space group	$P\bar{3}m$	
Unit cell dimensions	a = 5.943(1) Å	α= 90°
	b = 5.943(1) Å	β= 90°
	c = 4.738(1) Å	γ= 120°
Volume	144.92(5) $Å^3$	
Z	1	
Density (calculated)	2.750 g/cm^3	
Absorption coefficient	2.531 mm^{-1}	
F(000)	111	
Crystal description	Plate	
Crystal color	Colorless	
Crystal size	0.300 x 0.177 x 0.030 mm^3	
Theta range for data collection	3.96 to 27.32	
Index ranges	-7<=h<=7, -7<=k<=7, -6<=l<=6	
Reflections collected	1366	
Independent reflections	147 [R(int) = 0.1620]	
Completeness to theta = 27.32°	100.0 %	
Absorption correction	Integration	
Max. and min. transmission	0.7873 and 0.4538	
Data / restraints / parameters	147 / 0 / 12	
Goodness-of-fit on F^2	1.389	
Final R indices [I>2sigma(I)]	R_1 = 0.0544, wR_2 = 0.1670	
R indices (all data)	R_1 = 0.0544, wR_2 = 0.1670	
Largest diff. peak and hole	2.161 and -1.199 $e\cdot Å^{-3}$	

Table 4: Atomic coordinates (x 10^4) and equivalent isotropic displacement parameters (Å^2 x 10^3) for $(NH_4)_2[TcF_6]$.

	x	y	z	U(eq)
Tc(1)	0	0	0	31(1)
F(1)	3109(12)	1554(6)	2247(11)	40(1)
N(1)	3333	6667	3020(20)	17(2)

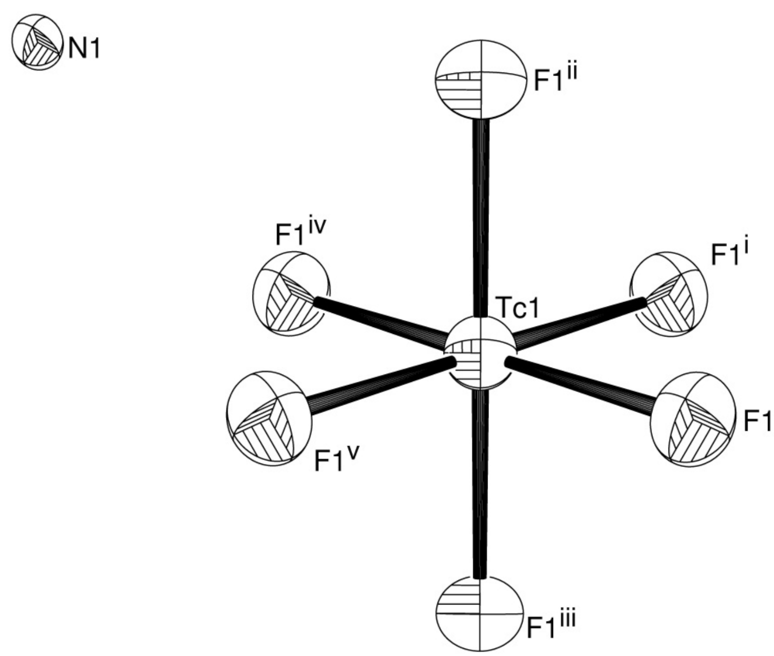

Figure 2: Ellipsoid plot (50% probability) of $(NH_4)_2[TcF_6]$.

$Na_2[TcF_6]$, (19)

Table 5: Crystal data and structure refinement for $Na_2[TcF_6]$.

Empirical formula	F_6Na_2Tc	
Formula weight	257.97	
Temperature	200(2) K	
Wavelength	0.71073 Å	
Crystal system	Trigonal	
Space group	$P\bar{3}m$	
Unit cell dimensions	a = 5.958(1) Å	α= 90°
	b = 5.958(1) Å	β= 90°
	c = 4.757(1) Å	γ= 120°
Volume	146.24(5) $Å^3$	
Z	1	
Density (calculated)	2.929 g/cm^3	
Absorption coefficient	2.640 mm^{-1}	
F(000)	119	
Crystal description	Block	
Crystal color	Colorless	
Crystal size	0.150 x 0.140 x 0.130 mm^3	
Theta range for data collection	3.95 to 29.09	
Index ranges	-6<=h<=8, -8<=k<=8, -6<=l<=6	
Reflections collected	1669	
Independent reflections	173 [R(int) = 0.1111]	
Completeness to theta = 29.09°	100.0 %	
Absorption correction	Integration	
Max. and min. transmission	0.7405 and 0.5874	
Data / restraints / parameters	173 / 0 / 12	
Goodness-of-fit on F^2	1.257	
Final R indices [I>2sigma(I)]	R_1 = 0.0819, wR_2 = 0.2035	
R indices (all data)	R_1 = 0.0819, wR_2 = 0.2035	
Largest diff. peak and hole	1.287 and -2.337 $e \cdot Å^{-3}$	

Table 6:.Atomic coordinates (x 10^4) and equivalent isotropic displacement parameters ($Å^2$ x 10^3) for $Na_2[TcF_6]$.

	x	y	z	U(eq)
Tc(1)	0	0	0	40(1)
F(1)	3061(13)	1530(7)	2203(12)	49(1)
Na(1)	3333	6667	3050(30)	80(3)

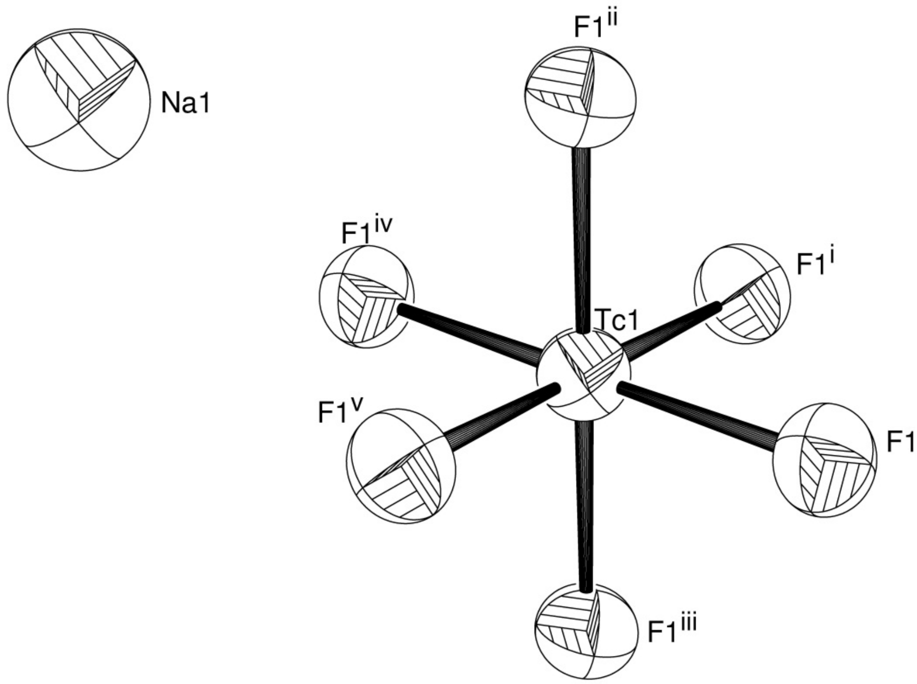

Figure 3: Ellipsoid plot (50% probability) of $Na_2[TcF_6]$.

$K_2[TcF_6]$, (20)

Table 7: Crystal data and structure refinement for $K_2[TcF_6]$.

Empirical formula	F_6K_2Tc	
Formula weight	290.18	
Temperature	213(2) K	
Wavelength	0.71073 Å	
Crystal system	Trigonal	
Space group	$P\bar{3}m$	
Unit cell dimensions	a = 5.796(1) Å	α= 90°
	b = 5.796(1) Å	β= 90°
	c = 4.614(1) Å	γ= 120°
Volume	134.22(4) $Å^3$	
Z	1	
Density (calculated)	3.590 g/cm^3	
Absorption coefficient	4.268 mm^{-1}	
F(000)	135	
Crystal description	Plate	
Crystal color	Colourless	
Crystal size	0.25 x 0.10 x 0.05 mm^3	
Theta range for data collection	4.06 to 26.86	
Index ranges	-7<=h<=7, -7<=k<=7, -5<=l<=5	
Reflections collected	1168	
Independent reflections	130 [R(int) = 0.0389]	
Completeness to theta = 26.86°	100.0 %	
Absorption correction	Psi-Scan	
Max. and min. transmission	0.4734 and 0.3025	
Data / restraints / parameters	130 / 0 / 13	
Goodness-of-fit on F^2	1.145	
Final R indices [I>2sigma(I)]	R_1 = 0.0136, wR_2 = 0.0285	
R indices (all data)	R_1 = 0.0141, wR_2 = 0.0285	
Extinction coefficient	0.09(1)	
Largest diff. peak and hole	0.501 and -0.492 $e \cdot Å^{-3}$	

Table 8: Atomic coordinates (x 10^4) and equivalent isotropic displacement parameters (Å^2 x 10^3) for $K_2[TcF_6]$.

	x	y	z	U(eq)
Tc(1)	0	0	0	8(1)
K(1)	3333	6667	2993(2)	15(1)
F(1)	3220(2)	1610(1)	2280(2)	17(1)

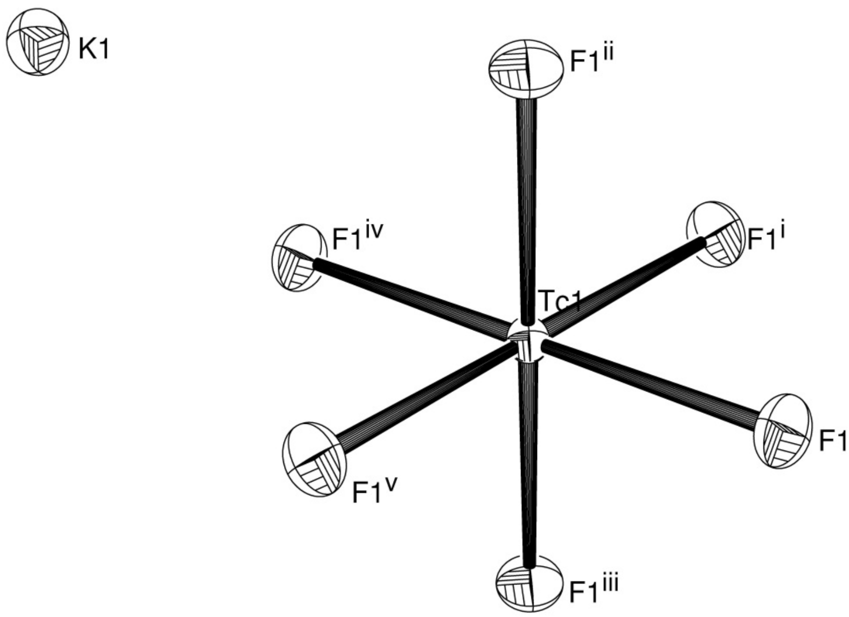

Figure 4: Ellipsoid plot (50% probability) of $K_2[TcF_6]$.

$Rb_2[TcF_6]$, (21)

Table 9: Crystal data and structure refinement for $Rb_2[TcF_6]$.

Empirical formula	F_6Rb_2Tc	
Formula weight	382.92	
Temperature	200(2) K	
Wavelength	0.71073 Å	
Crystal system	Trigonal	
Space group	$P\bar{3}m$	
Unit cell dimensions	a = 5.949(1) Å	α= 90°
	b = 5.949(1) Å	β= 90°
	c = 4.759(1) Å	γ= 120°
Volume	145.86(5) $Å^3$	
Z	1	
Density (calculated)	4.359 g/cm^3	
Absorption coefficient	19.079 mm^{-1}	
F(000)	171	
Crystal description	Plate	
Crystal color	Colorless	
Crystal size	0.12 x 0.12 x 0.06 mm^3	
Theta range for data collection	3.96 to 29.11	
Index ranges	-6<=h<=8, -8<=k<=8, -6<=l<=6	
Reflections collected	1577	
Independent reflections	173 [R(int) = 0.0846]	
Completeness to theta = 29.11°	100.0 %	
Absorption correction	Integration	
Max. and min. transmission	0.1917 and 0.0398	
Data / restraints / parameters	173 / 0 / 13	
Goodness-of-fit on F^2	1.140	
Final R indices [I>2sigma(I)]	R_1 = 0.0429, wR_2 = 0.1089	
R indices (all data)	R_1 = 0.0432, wR_2 = 0.1097	
Extinction coefficient	0.16(3)	
Largest diff. peak and hole	1.431 and -0.764 $e\cdot Å^{-3}$	

Table 10: Atomic coordinates (x 10^4) and equivalent isotropic displacement parameters ($Å^2$ x 10^3) for $Rb_2[TcF_6]$.

	x	y	z	U(eq)
Tc(1)	0	0	0	27(1)
F(1)	3137(6)	1569(3)	2229(8)	35(1)
Rb(2)	3333	6667	3003(3)	35(1)

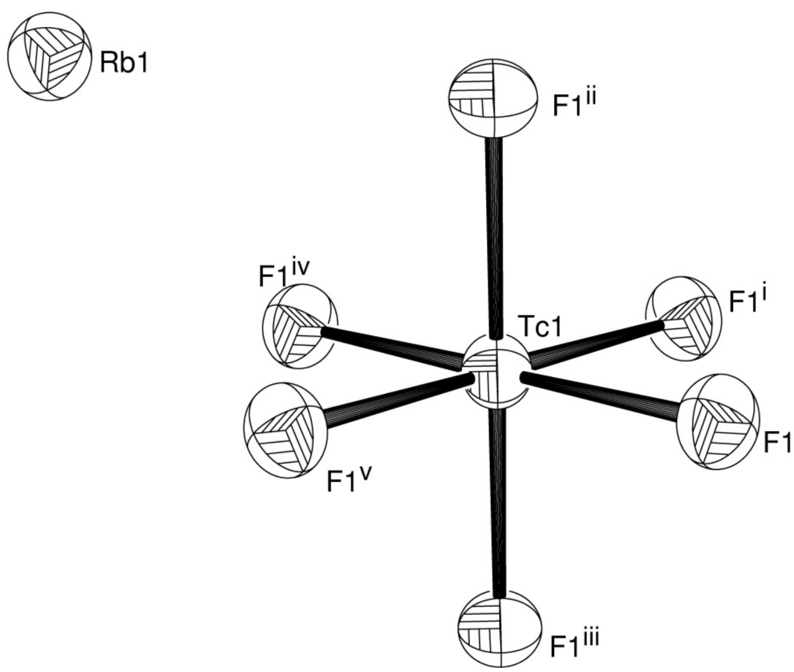

Figure 5: Ellipsoid plot (50% probability) of $Rb_2[TcF_6]$.

$Cs_2[TcF_6]$, (22).

Table 11: Crystal data and structure refinement for $Cs_2[TcF_6]$.

Empirical formula	Cs_2F_6Tc	
Formula weight	477.82	
Temperature	200(2) K	
Wavelength	0.71073 Å	
Crystal system	Trigonal	
Space group	$P\bar{3}m$	
Unit cell dimensions	a = 6.240(1) Å	α= 90°
	b = 6.240(1) Å	β= 90°
	c = 4.980(1) Å	γ= 120°
Volume	167.93(5) $Å^3$	
Z	1	
Density (calculated)	4.725 g/cm^3	
Absorption coefficient	12.856 mm^{-1}	
F(000)	207	
Crystal description	Block	
Crystal color	Colorless	
Crystal size	0.100 x 0.077 x 0.040 mm^3	
Theta range for data collection	3.77 to 29.02	
Index ranges	-8<=h<=8, -6<=k<=8, -6<=l<=6	
Reflections collected	1871	
Independent reflections	193 [R(int) = 0.0773]	
Completeness to theta = 29.02°	99.5 %	
Absorption correction	Integration	
Max. and min. transmission	0.3900 and 0.0995	
Data / restraints / parameters	193 / 0 / 13	
Goodness-of-fit on F^2	1.501	
Final R indices [I>2sigma(I)]	R_1 = 0.0522, wR_2 = 0.1267	
R indices (all data)	R_1 = 0.0535, wR_2 = 0.1267	
Extinction coefficient	0.26(4)	
Largest diff. peak and hole	3.808 and -2.779 $e \cdot Å^{-3}$	

Table 12: Atomic coordinates (x 10^4) and equivalent isotropic displacement parameters ($Å^2$ x 10^3) for $Cs_2[TcF_6]$.

	x	y	z	U(eq)
Tc(1)	0	0	0	14(1)
Cs(2)	3333	6667	3025(3)	20(1)
F(1)	2980(7)	1490(4)	2155(12)	23(1)

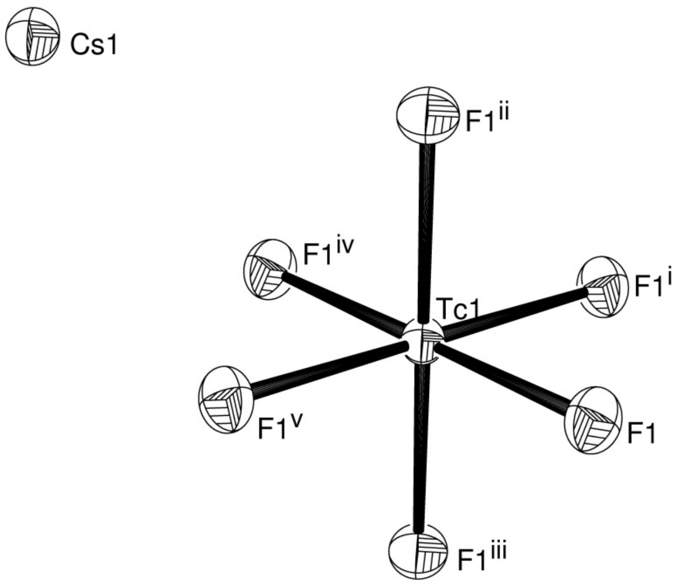

Figure 6: Ellipsoid plot (50% probability) of $Cs_2[TcF_6]$.

$(NMe_4)_2[TcF_6]$, (23)

Table 13: Crystal data and structure refinement for $(NMe_4)_2[TcF_6]$.

Empirical formula	$C_8H_{24}F_6N_2Tc$	
Formula weight	360.29	
Temperature	200(2) K	
Wavelength	0.71073 Å	
Crystal system	Rhombohedral	
Space group	$R\bar{3}$	
Unit cell dimensions	a = 7.992(1) Å	α= 90°
	b = 7.992(1) Å	β= 90°
	c = 20.039(1) Å	γ= 120°
Volume	1108.5(2) $Å^3$	
Z	3	
Density (calculated)	1.619 g/cm^3	
Absorption coefficient	1.022 mm^{-1}	
F(000)	549	
Crystal description	Block	
Crystal color	Colorless	
Crystal size	0.140 x 0.130 x 0.120 mm^3	
Theta range for data collection	3.05 to 29.22	
Index ranges	-10<=h<=10, -9<=k<=10, -27<=l<=27	
Reflections collected	4139	
Independent reflections	666 [R(int) = 0.0708]	
Completeness to theta = 29.22°	99.9 %	
Absorption correction	None	
Hydrogen treatment	Riding model	
Data / restraints / parameters	666 / 0 / 28	
Goodness-of-fit on F^2	1.138	
Final R indices [I>2sigma(I)]	R_1 = 0.0481, wR_2 = 0.1189	
R indices (all data)	R_1 = 0.0486, wR_2 = 0.1193	
Extinction coefficient	0.056(6)	
Largest diff. peak and hole	0.845 and -0.303 e·$Å^{-3}$	

Table 14: Atomic coordinates (x 10^4) and equivalent isotropic displacement parameters (Å^2 x 10^3) for $(NMe_4)_2[TcF_6]$.

	x	y	z	U(eq)
Tc(1)	6667	3333	3333	37(1)
N(1)	6667	3333	5814(3)	39(1)
F(1)	8233(4)	2682(4)	3887(1)	56(1)
C(1)	7311(6)	5327(6)	5562(2)	50(1)
C(2)	6667	3333	6555(3)	54(2)

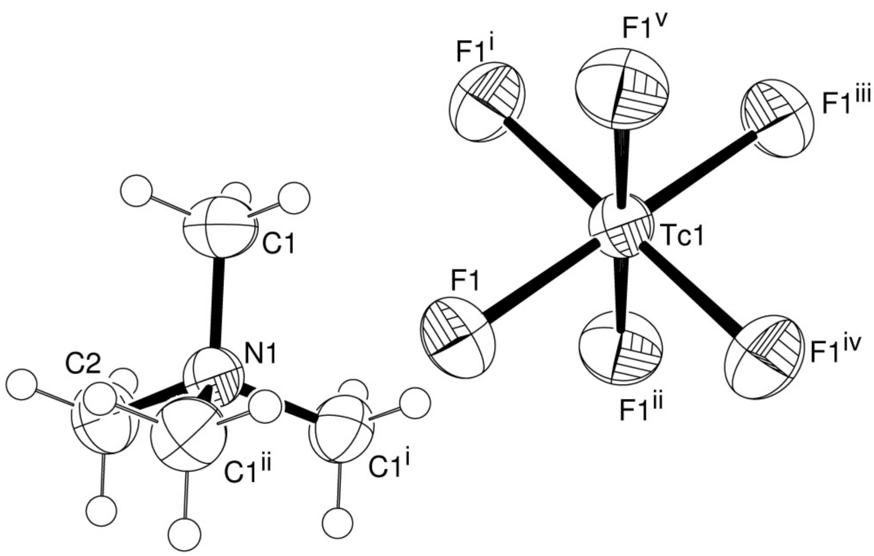

Figure 7: Ellipsoid plot (50% probability) of $(NMe_4)_2[TcF_6]$.

$(NH_4)_3Na[Tc_2OF_{10}]\cdot 2\ (NH_4F)$, (24)

Table 15: Crystal data and structure refinement for $(NH_4)_3Na[Tc_2OF_{10}]\cdot 2\ (NH_4F)$.

Empirical formula	$F_{12}N_5NaOTc_2$	
Formula weight	533.04	
Temperature	200(2) K	
Wavelength	0.71073 Å	
Crystal system	Orthorhombic	
Space group	Pbam	
Unit cell dimensions	a = 7.583(1) Å	α= 90°
	b = 15.350(2) Å	β= 90°
	c = 6.135(1) Å	γ= 90°
Volume	714.1(2) $Å^3$	
Z	2	
Density (calculated)	2.479 g/cm^3	
Absorption coefficient	2.102 mm^{-1}	
F(000)	496	
Crystal description	Needle	
Crystal color	Pink	
Crystal size	0.08 x 0.03 x 0.02 mm^3	
Theta range for data collection	2.65 to 26.00	
Index ranges	-9<=h<=9, -17<=k<=18, -6<=l<=7	
Reflections collected	3738	
Independent reflections	770 [R(int) = 0.0776]	
Completeness to theta = 26.00°	99.9 %	
Absorption correction	Integration	
Max. and min. transmission	0.9472 and 0.8870	
Data / restraints / parameters	770 / 0 / 62	
Goodness-of-fit on F^2	1.070	
Final R indices [I>2sigma(I)]	R_1 = 0.0379, wR_2 = 0.0819	
R indices (all data)	R_1 = 0.0516, wR_2 = 0.0865	
Extinction coefficient	0.009(2)	
Largest diff. peak and hole	0.747 and -0.530 $e\cdot Å^{-3}$	

Table 16: Atomic coordinates (x 10^4) and equivalent isotropic displacement parameters ($Å^2$ x 10^3) for $(NH_4)_3Na[Tc_2OF_{10}]\cdot 2(NH_4F)$.

	x	y	z	U(eq)
Tc(1)	1539(1)	9063(1)	5000	17(1)
F(1)	252(5)	8465(2)	2740(6)	35(1)
F(2)	3165(6)	8056(3)	5000	29(1)
F(3)	3019(5)	9577(2)	7251(6)	34(1)
F(4)	6396(8)	8723(4)	0	53(2)
O(1)	0	10000	5000	25(2)
N(1)	6611(10)	8633(5)	5000	47(2)
N(2)	8352(10)	7222(5)	0	34(2)
N(3)	10000	10000	0	38(3)
Na(1)	5000	10000	0	25(1)

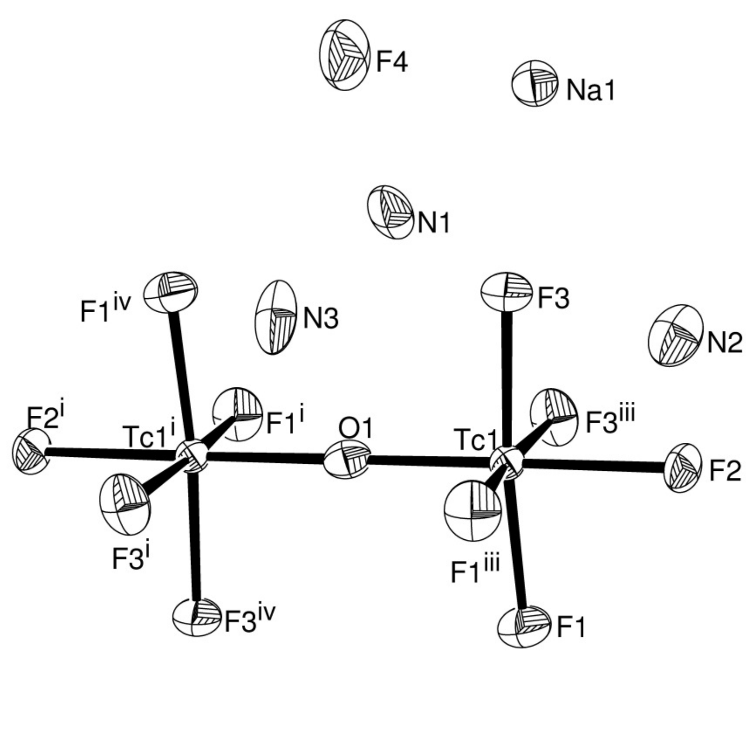

Figure 8: Ellipsoid plot (50% probability) of $(NH_4)_3Na[Tc_2OF_{10}]\cdot 2(NH_4F)$.

$[Tc_2O(CH_3CN)_{10}](SbF_6)_4 \cdot CH_3CN$, (25)

Table 17: Crystal data and structure refinement for $[Tc_2O(CH_3CN)_{10}](SbF_6)_4 \cdot CH_3CN$.

Empirical formula	$C_{22}H_{33}F_{24}N_{11}OSb_4Tc_2$	
Formula weight	1606.59	
Temperature	200(2) K	
Wavelength	0.71073 Å	
Crystal system	Monoclinic	
Space group	C2/c	
Unit cell dimensions	a = 11.517(1) Å	α= 90°
	b = 21.201(1) Å	β= 93.94(1)°
	c = 20.937(1) Å	γ= 90°
Volume	5100.1(6) $Å^3$	
Z	4	
Density (calculated)	2.092 g/cm^3	
Absorption coefficient	2.735 mm^{-1}	
F(000)	3024	
Crystal description	Plate	
Crystal color	Green	
Crystal size	0.190 x 0.140 x 0.080 mm^3	
Theta range for data collection	4.83 to 29.27	
Index ranges	-15<=h<=15, -29<=k<=25, -28<=l<=28	
Reflections collected	27983	
Independent reflections	6877 [R(int) = 0.0704]	
Completeness to theta = 29.27°	98.7 %	
Absorption correction	Integration	
Max. and min. transmission	0.7540 and 0.5938	
Hydrogen treatment	Riding model	
Data / restraints / parameters	6877 / 90 / 279	
Goodness-of-fit on F^2	1.047	
Final R indices [I>2sigma(I)]	R_1 = 0.0587, wR_2 = 0.1621	
R indices (all data)	R_1 = 0.0807, wR_2 = 0.1756	
Extinction coefficient	0.0023(2)	
Largest diff. peak and hole	1.302 and -1.014 $e \cdot Å^{-3}$	

Table 18: Atomic coordinates (x 10^4) and equivalent isotropic displacement parameters ($Å^2$ x 10^3) for $[Tc_2O(CH_3CN)_{10}](SbF_6)_4 \cdot CH_3CN$.

	x	y	z	U(eq)
C(1)	4002(6)	4068(3)	6427(3)	59(2)
C(2)	7584(5)	4945(3)	6173(3)	56(1)
C(3)	3794(6)	3458(3)	4372(3)	53(1)
C(4)	6863(6)	2947(3)	5768(3)	56(1)
C(5)	7418(6)	4348(4)	4158(3)	60(2)
C(6)	3324(8)	3961(5)	6976(5)	84(3)
C(7)	8492(7)	5254(5)	6569(4)	81(2)
C(8)	2963(7)	3097(4)	3979(4)	70(2)
C(9)	7395(9)	2363(4)	5997(4)	82(2)
C(10)	8230(8)	4402(6)	3672(5)	94(3)
C(31)	0	3021(13)	7500	230(20)
C(32)	0	3627(10)	7500	123(7)
Sb(1)	444(1)	3654(1)	5389(1)	71(1)
F(1)	-902(17)	3375(10)	4918(9)	186(3)
F(2)	130(20)	3146(9)	6058(8)	186(3)
F(3)	-370(20)	4313(8)	5686(9)	186(3)
F(4)	80(20)	2905(8)	4955(9)	186(3)
F(5)	1991(14)	3398(10)	5459(10)	186(3)
F(6)	700(20)	4026(10)	4604(8)	186(3)
F(1A)	-506(17)	4150(10)	4859(9)	186(3)
F(2A)	-745(16)	3542(10)	5914(9)	186(3)
F(3A)	927(19)	4350(9)	5853(8)	186(3)
F(4A)	1070(20)	2947(8)	4999(9)	186(3)
F(5A)	1579(18)	3597(9)	6025(9)	186(3)
F(6A)	1360(20)	4147(9)	4901(9)	186(3)
Sb(2)	0	2834(1)	2500	61(1)
F(7A)	216(13)	3526(6)	1998(7)	123(2)
F(8A)	-227(13)	2312(7)	1799(6)	123(2)
F(9A)	-1586(10)	3009(7)	2503(7)	123(2)
F(7)	-179(13)	3279(7)	1707(6)	123(2)

F(8)	373(13)	2112(6)	2024(7)	123(2)
F(9)	-1588(9)	2623(7)	2394(7)	123(2)
F(10)	4455(9)	3448(4)	1917(4)	146(3)
F(11)	4413(11)	4675(4)	1950(5)	178(4)
F(12)	6394(10)	4063(7)	2138(7)	225(7)
N(1)	4560(4)	4156(2)	6015(2)	49(1)
N(2)	6873(4)	4711(3)	5858(2)	50(1)
N(3)	4449(4)	3745(3)	4676(2)	50(1)
N(4)	6412(4)	3394(3)	5571(3)	51(1)
N(5)	6776(4)	4302(3)	4540(3)	52(1)
N(6)	0	4130(10)	7500	179(11)
Sb(3)	5000	4066(1)	2500	57(1)
Tc(1)	5631(1)	4262(1)	5259(1)	43(1)
O(1)	5000	5000	5000	44(1)

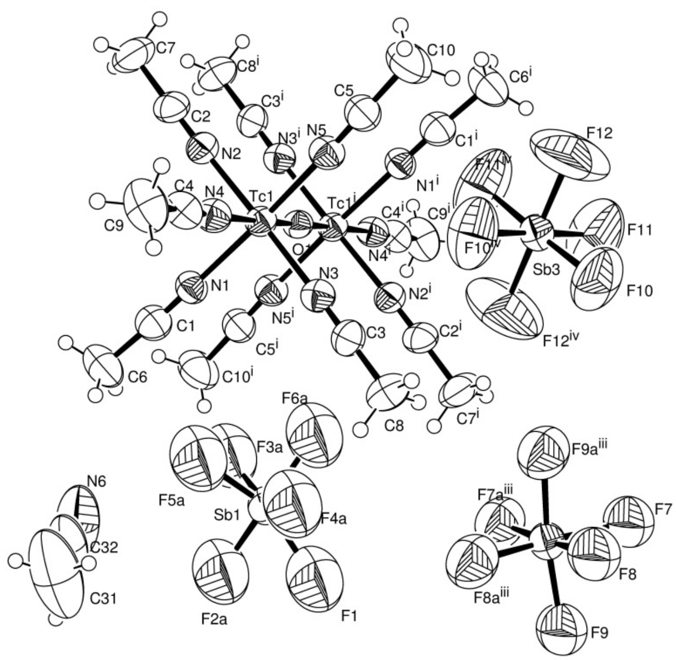

Figure 9: Ellipsoid plot (50% probability) of $[Tc_2O(CH_3CN)_{10}](SbF_6)_4 \cdot CH_3CN$.

$[Tc(NO)(NH_3)_4F]_4[TcF_6](HF_2)_2$, (26)

Table 19: Crystal data and structure refinement for $[Tc(NO)(NH_3)_4F]_4[TcF_6](HF_2)_2$.

Empirical formula	$F_{14}H_{50}N_{20}O_4Tc_5$	
Formula weight	1150.60	
Temperature	200(2) K	
Wavelength	0.71073 Å	
Crystal system	Monoclinic	
Space group	C2/m	
Unit cell dimensions	a = 17.483(2) Å	α= 90°
	b = 7.639(1) Å	β= 112.19(1)°
	c = 13.766(2) Å	γ= 90°
Volume	1702.3(4) $Å^3$	
Z	2	
Density (calculated)	2.245 g/cm^3	
Absorption coefficient	2.100 mm^{-1}	
F(000)	1126	
Crystal description	Plate	
Crystal color	Orange-yellow	
Crystal size	0.20 x 0.20 x 0.08 mm^3	
Theta range for data collection	3.45 to 25.00	
Index ranges	-20<=h<=20, -8<=k<=9, -16<=l<=16	
Reflections collected	6398	
Independent reflections	1604 [R(int) = 0.0679]	
Completeness to theta = 25.00°	98.8 %	
Absorption correction	Integration	
Max. and min. transmission	0.7303 and 0.6239	
Hydrogen treatment	Riding model	
Data / restraints / parameters	1604 / 0 / 120	
Goodness-of-fit on F^2	1.145	
Final R indices [I>2sigma(I)]	R_1 = 0.0283, wR_2 = 0.0764	
R indices (all data)	R_1 = 0.0288, wR_2 = 0.0769	
Extinction coefficient	0.0069(4)	
Largest diff. peak and hole	0.849 and -0.699 e·$Å^{-3}$	

Table 20: Atomic coordinates (x 10^4) and equivalent isotropic displacement parameters ($Å^2$ x 10^3) for $[Tc(NO)(NH_3)_4F]_4[TcF_6](HF_2)_2$.

	x	y	z	U(eq)
Tc(1)	3528(1)	5000	1612(1)	21(1)
F(1)	2657(2)	5000	176(2)	37(1)
O(1)	4858(3)	5000	3710(3)	35(1)
N(4)	4334(3)	5000	738(4)	38(1)
N(5)	3432(2)	2178(4)	1506(2)	31(1)
N(6)	2498(3)	5000	2095(3)	30(1)
N(1)	4293(3)	5000	2844(3)	24(1)
Tc(2)	1121(1)	5000	4219(1)	21(1)
F(2)	-137(2)	5000	3659(2)	29(1)
O(2)	2924(3)	5000	4971(4)	44(1)
N(8)	1045(2)	3044(4)	5314(2)	29(1)
N(7)	949(2)	2942(4)	3069(2)	29(1)
N(2)	2180(3)	5000	4665(3)	28(1)
F(5)	2438(2)	1479(3)	2880(2)	42(1)
Tc(3)	0	5000	0	22(1)
F(3)	223(2)	5000	-1265(2)	49(1)
F(4)	817(2)	3228(4)	603(2)	55(1)

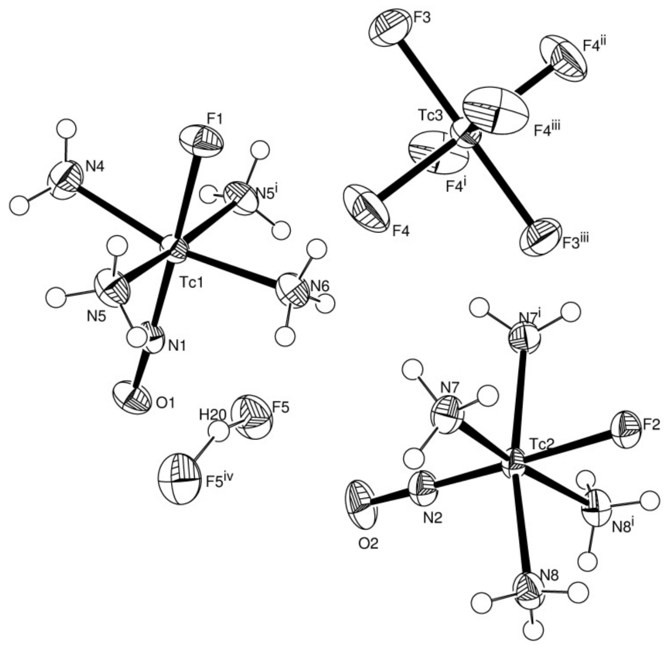

Figure 10: Ellipsoid plot (50% probability) of $[Tc(NO)(NH_3)_4F]_4[TcF_6](HF_2)_2$.

$K_2[Tc(NO)F_5]\cdot H_2O$, (27)

Table 21: Crystal data and structure refinement for $K_2[Tc(NO)F_5]\cdot H_2O$.

Empirical formula	$F_5K_2NO_2Tc$	
Formula weight	317.21	
Temperature	200(2) K	
Wavelength	0.71073 Å	
Radiation	MoK	
Crystal system	Orthorhombic	
Space group	Cmcm	
Unit cell dimensions	a = 6.203(1) Å	α= 90°
	b = 18.654(4) Å	β= 90°
	c = 6.301(2) Å	γ= 90°
Volume	729.1(3) $Å^3$	
Z	4	
Density (calculated)	2.890 g/cm^3	
Absorption coefficient	3.161 mm^{-1}	
F(000)	596	
Crystal description	Plate	
Crystal color	Blue-violet	
Crystal size	0.3 x 0.3 x 0.02 mm^3	
Theta range for data collection	3.90 to 25.00	
Index ranges	-7<=h<=6, -22<=k<=20, -5<=l<=7	
Reflections collected	886	
Independent reflections	384 [R(int) = 0.0595]	
Completeness to theta = 25.00°	98.2 %	
Absorption correction	Integration	
Max. and min. transmission	0.8771 and 0.5579	
Data / restraints / parameters	384 / 0 / 39	
Goodness-of-fit on F^2	1.111	
Final R indices [I>2sigma(I)]	R_1 = 0.0636, wR_2 = 0.1784	
R indices (all data)	R_1 = 0.0677, wR_2 = 0.1855	
Extinction coefficient	0.010(3)	
Largest diff. peak and hole	1.642 and -2.070 $e\cdot Å^{-3}$	

Table 22: Atomic coordinates (x 10^4) and equivalent isotropic displacement parameters ($Å^2$ x 10^3) for $K_2[Tc(NO)F_5]\cdot H_2O$.

	x	y	z	U(eq)
Tc(1)	5000	6405(1)	7500	35(1)
K(2)	0	6111(2)	2500	44(1)
K(1)	0	7518(2)	7500	45(1)
F(4)	7207(12)	6503(4)	9656(13)	68(2)
F(5)	5000	7458(7)	7500	58(4)
N(1)	5000	5474(10)	7500	63(6)
O(2)	0	4682(16)	2500	190(20)
O(1)	5000	4858(9)	7500	141(13)

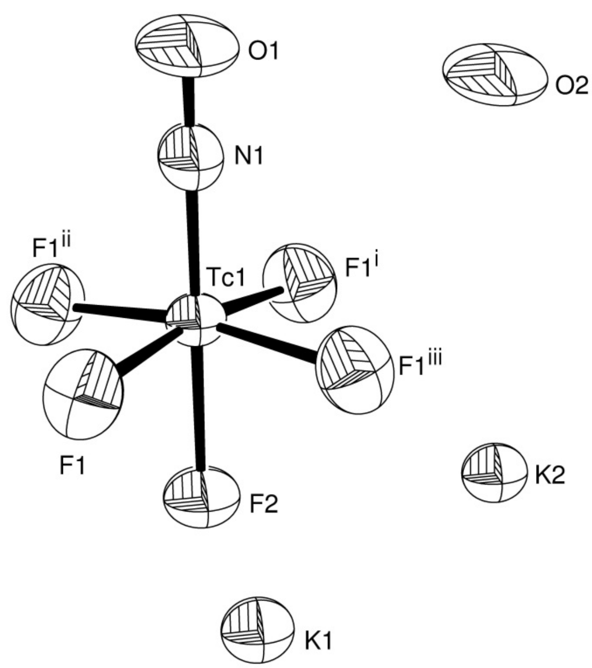

Figure 11: Ellipsoid plot (50% probability) of $K_2[Tc(NO)F_5]\cdot H_2O$.

$Rb_2[Tc(NO)F_5]\cdot H_2O$, (28)

Table 23: Crystal data and structure refinement for $Rb_2[Tc(NO)F_5]\cdot H_2O$.

Empirical formula	$F_5NO_2Rb_2Tc$	
Formula weight	409.95	
Temperature	200(2) K	
Wavelength	0.71073 Å	
Crystal system	Orthorhombic	
Space group	Cmcm	
Unit cell dimensions	a = 6.469(1) Å	α= 90°
	b = 18.960(3) Å	β= 90°
	c = 6.492(1) Å	γ= 90°
Volume	796.3(2) $Å^3$	
Z	4	
Density (calculated)	3.420 g/cm^3	
Absorption coefficient	13.997 mm^{-1}	
F(000)	740	
Crystal description	Plate	
Crystal color	Blue-violet	
Crystal size	0.400 x 0.227 x 0.090 mm^3	
Theta range for data collection	5.33 to 29.16	
Index ranges	-8<=h<=7, -26<=k<=25, -7<=l<=8	
Reflections collected	2951	
Independent reflections	620 [R(int) = 0.1095]	
Completeness to theta = 29.16°	98.1 %	
Absorption correction	Integration	
Max. and min. transmission	0.5039 and 0.0782	
Data / restraints / parameters	620 / 0 / 38	
Goodness-of-fit on F^2	1.113	
Final R indices [I>2sigma(I)]	R_1 = 0.0546, wR_2 = 0.1430	
R indices (all data)	R_1 = 0.0592, wR_2 = 0.1563	
Largest diff. peak and hole	2.314 and -1.977 $e\cdot Å^{-3}$	

Table 24: Atomic coordinates (x 10^4) and equivalent isotropic displacement parameters ($Å^2$ x 10^3) for $Rb_2[Tc(NO)F_5]\cdot H_2O$.

	x	y	z	U(eq)
Tc(1)	5000	1407(1)	2500	29(1)
F(1)	2841(6)	1493(2)	395(7)	47(1)
F(2)	5000	2462(5)	2500	42(2)
O(1)	5000	-111(7)	2500	87(5)
N(1)	5000	471(7)	2500	49(3)
Rb(1)	0	2532(1)	2500	37(1)
Rb(2)	0	1045(1)	7500	39(1)
O(2)	0	-441(9)	7500	95(6)

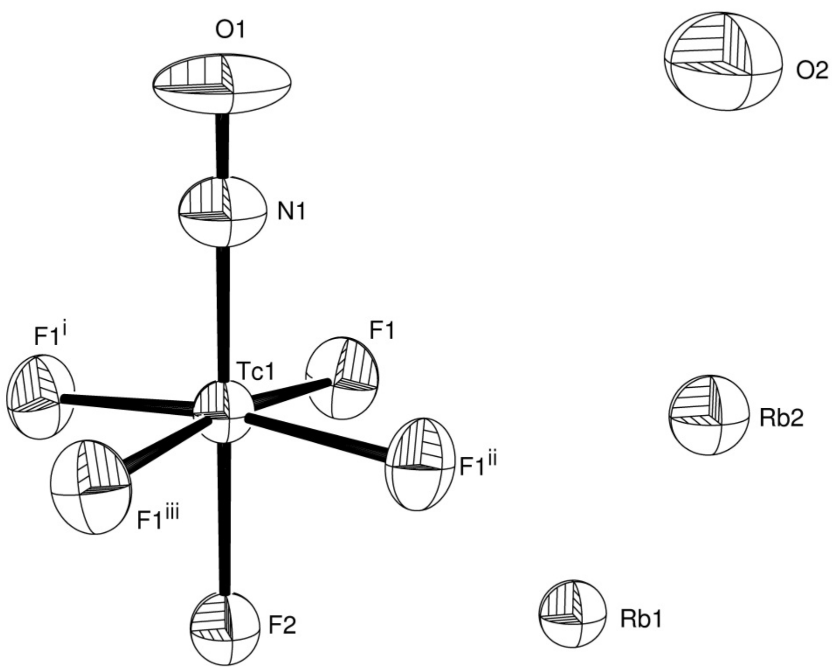

Figure 12: Ellipsoid plot (50% probability) of $Rb_2[Tc(NO)F_5]\cdot H_2O$.

$Cs_2[Tc(NO)F_5]\cdot H_2O$, (29)

Table 25: Crystal data and structure refinement for $Cs_2[Tc(NO)F_5]\cdot H_2O$.

Empirical formula	$Cs_2F_5NO_2Tc$	
Formula weight	504.83	
Temperature	200(2) K	
Wavelength	0.71073 Å	
Crystal system	Orthorhombic	
Space group	Cmcm	
Unit cell dimensions	a = 6.688(1) Å	α= 90°
	b = 19.479(2) Å	β= 90°
	c = 6.765(1) Å	γ= 90°
Volume	881.3(2) $Å^3$	
Z	4	
Density (calculated)	3.805 g/cm^3	
Absorption coefficient	9.814 mm^{-1}	
F(000)	884	
Crystal description	Plate	
Crystal color	Blue-violet	
Crystal size	0.29 x 0.14 x 0.03 mm^3	
Theta range for data collection	3.67 to 29.21	
Index ranges	-8<=h<=9, -26<=k<=26, -9<=l<=8	
Reflections collected	4819	
Independent reflections	696 [R(int) = 0.0439]	
Completeness to theta = 29.21°	99.1 %	
Absorption correction	Integration	
Max. and min. transmission	0.6312 and 0.2308	
Data / restraints / parameters	696 / 0 / 39	
Goodness-of-fit on F^2	1.144	
Final R indices [I>2sigma(I)]	R_1 = 0.0375, wR_2 = 0.1005	
R indices (all data)	R_1 = 0.0412, wR_2 = 0.1019	
Extinction coefficient	0.0012(2)	
Largest diff. peak and hole	2.069 and -2.308 e·$Å^{-3}$	

Table 26: Atomic coordinates (x 10^4) and equivalent isotropic displacement parameters (Å^2 x 10^3) for $Cs_2[Tc(NO)F_5]\cdot H_2O$.

	x	y	z	U(eq)
Cs(1)	5000	7459(1)	2500	29(1)
Tc(1)	5000	6386(1)	-2500	23(1)
Cs(2)	0	6003(1)	2500	36(1)
F(1)	7095(8)	6465(3)	-4513(7)	38(1)
F(2)	5000	7401(4)	-2500	32(2)
N(1)	5000	5499(8)	-2500	37(3)
O(2)	0	4479(8)	2500	64(5)
O(1)	5000	4901(7)	-2500	79(6)

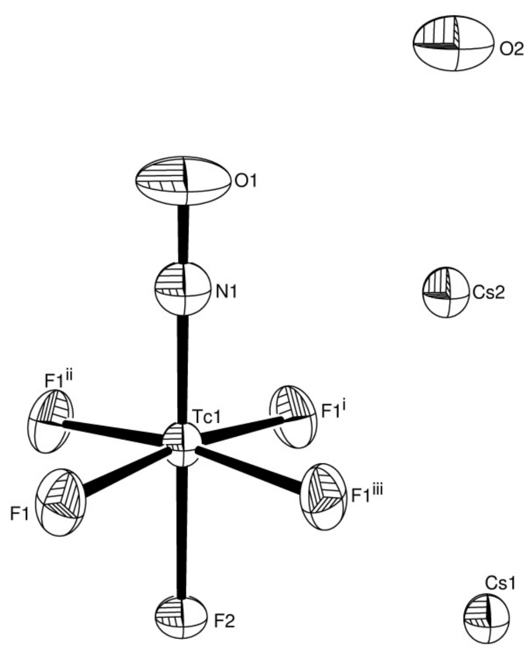

Figure 13: Ellipsoid plot (50% probability) of $Cs_2[Tc(NO)F_5]\cdot H_2O$.

$[Tc(NO)(NH_3)_4F](HF_2)\cdot 1/2\ RbF$, (30)

Table 27: Crystal data and structure refinement for $[Tc(NO)(NH_3)_4F](HF_2)\cdot 1/2\ RbF$.

Empirical formula	$H_{26}F_7N_{10}O_2RbTc_2$	
Formula weight	612.78	
Temperature	200(2) K	
Wavelength	0.71073 Å	
Crystal system	Tetragonal	
Space group	I4/m	
Unit cell dimensions	a = 16.454(2) Å	α= 90°
	b = 16.454(2) Å	β= 90°
	c = 6.938(1) Å	γ= 90°
Volume	1878.4(4) $Å^3$	
Z	4	
Density (calculated)	2.167 g/cm^3	
Absorption coefficient	4.127 mm^{-1}	
F(000)	1192	
Crystal description	Needle	
Crystal color	Orange	
Crystal size	0.210 x 0.103 x 0.050 mm^3	
Theta range for data collection	3.50 to 24.99	
Index ranges	-19<=h<=19, -19<=k<=19, -8<=l<=8	
Reflections collected	7205	
Independent reflections	909 [R(int) = 0.0806]	
Completeness to theta = 24.99°	99.7 %	
Absorption correction	Integration	
Max. and min. transmission	0.6413 and 0.4338	
Hydrogen treatment	Mixed	
Data / restraints / parameters	909 / 0 / 67	
Goodness-of-fit on F^2	1.356	
Final R indices [I>2sigma(I)]	R_1 = 0.0612, wR_2 = 0.1791	
R indices (all data)	R_1 = 0.0670, wR_2 = 0.1841	
Extinction coefficient	0.0025(8)	
Largest diff. peak and hole	1.668 and -3.480 $e\cdot Å^{-3}$	

Table 28: Atomic coordinates (x 10^4) and equivalent isotropic displacement parameters (Å^2 x 10^3) for $[Tc(NO)(NH_3)_4F](HF_2)\cdot 1/2\ RbF$.

	x	y	z	U(eq)
F(1)	7488(4)	7492(4)	5000	26(1)
F(2)	8252(6)	10031(5)	0	50(2)
F(3)	6866(7)	10053(5)	0	55(2)
N(1)	7475(6)	9770(6)	5000	23(2)
N(2)	8380(4)	8642(5)	2762(11)	33(2)
N(3)	6565(5)	8607(4)	2745(10)	31(2)
O(1)	7472(6)	10499(5)	5000	36(2)
Rb(1)	10000	10000	5000	51(1)
Rb(2)	10000	10000	0	64(1)
Tc(1)	7472(1)	8730(1)	5000	20(1)
F(4)	5000	10000	0	330(40)

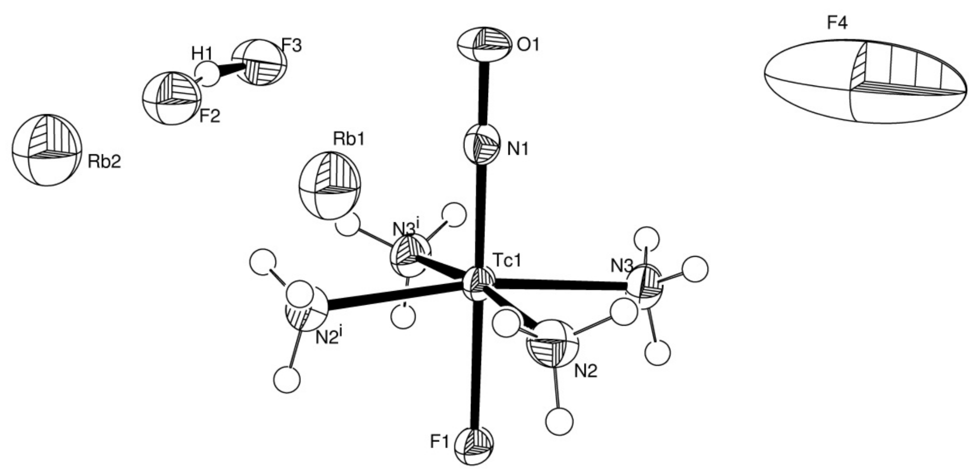

Figure 14: Ellipsoid plot (50% probability) of $[Tc(NO)(NH_3)_4F](HF_2)\cdot 1/2\ RbF$.

$[Tc(NO)(NH_3)_4F](PF_6)\cdot 1/2\ KPF_6$, (32)

Table 29: Crystal data and structure refinement for $[Tc(NO)(NH_3)_4F](PF_6)\cdot 1/2\ KPF_6$.

Empirical formula	$F_{20}H_{24}KN_{10}O_2P_3Tc_2$	
Formula weight	904.30	
Temperature	200(2) K	
Wavelength	0.71073 Å	
Radiation	MoK	
Crystal system	Tetragonal	
Space group	P4/m	
Unit cell dimensions	a = 12.304(1) Å	α= 90°
	b = 12.304(1) Å	β= 90°
	c = 8.488(1) Å	γ= 90°
Volume	1285.0(2) $Å^3$	
Z	2	
Density (calculated)	2.337 g/cm^3	
Absorption coefficient	1.592 mm^{-1}	
F(000)	880	
Crystal description	Block	
Crystal color	Orange	
Crystal size	0.270 x 0.260 x 0.250 mm^3	
Theta range for data collection	3.31 to 29.16	
Index ranges	-14<=h<=16, -9<=k<=16, -11<=l<=11	
Reflections collected	6114	
Independent reflections	1848 [R(int) = 0.0489]	
Completeness to theta = 29.16°	99.1 %	
Absorption correction	None	
Hydrogen treatment	Mixed	
Data / restraints / parameters	1848 / 0 / 105	
Goodness-of-fit on F^2	1.079	
Final R indices [I>2sigma(I)]	R_1 = 0.0400, wR_2 = 0.1043	
R indices (all data)	R_1 = 0.0449, wR_2 = 0.1067	
Largest diff. peak and hole	0.890 and -1.836 $e\cdot Å^{-3}$	

Table 30: Atomic coordinates (x 10^4) and equivalent isotropic displacement parameters (Å^2 x 10^3) for $[Tc(NO)(NH_3)_4F](PF_6)\cdot 1/2\ KPF_6$.

	x	y	z	U(eq)
F(1)	1439(2)	1564(2)	0	27(1)
F(2)	2873(2)	4933(2)	6328(3)	47(1)
F(3)	2183(5)	3513(3)	5000	63(1)
F(4)	1080(3)	4652(3)	3650(4)	64(1)
F(5)	1742(4)	6070(3)	5000	51(1)
F(6)	5000	5000	1857(7)	70(2)
F(7)	3710(3)	4894(3)	0	51(1)
F(8)	0	0	3290(20)	336(17)
F(9)	969(9)	710(9)	5000	240(8)
K(1)	5000	5000	5000	28(1)
K(2)	0	0	0	60(1)
N(1)	4490(3)	1419(3)	0	23(1)
N(2)	2901(3)	249(3)	1807(4)	31(1)
N(3)	2986(2)	2741(2)	-1765(4)	28(1)
O(1)	5467(3)	1355(3)	0	32(1)
P(1)	1952(1)	4786(1)	5000	26(1)
P(2)	5000	5000	0	21(1)
P(3)	0	0	5000	54(1)
Tc(1)	3092(1)	1483(1)	0	18(1)

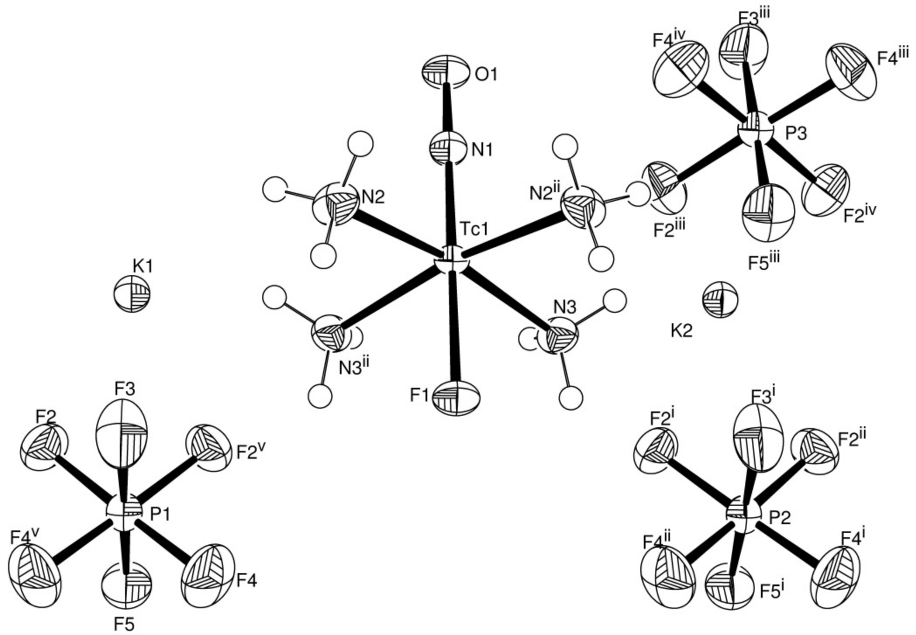

Figure 15: Ellipsoid plot (50% probability) of $[Tc(NO)(NH_3)_4F](PF_6)\cdot 1/2\ KPF_6$.

$[Tc(NO)(py)_4F]PF_6$, (33)

Table 31: Crystal data and structure refinement for $[Tc(NO)(py)_4F]PF_6$.

Empirical formula	$C_{20}H_{20}F_7N_5OPTc$	
Formula weight	608.38	
Temperature	200(2) K	
Wavelength	0.71073 Å	
Crystal system	Triclinic	
Space group	$P\bar{1}$	
Unit cell dimensions	a = 9.374(1) Å	α= 104.47(1)°
	b = 9.379(1) Å	β= 104.42(1)°
	c = 14.443(2) Å	γ= 98.24(1)°
Volume	1161.8(2) $Å^3$	
Z	2	
Density (calculated)	1.739 g/cm^3	
Absorption coefficient	0.768 mm^{-1}	
F(000)	608	
Crystal description	Block	
Crystal color	Orange	
Crystal size	0.19 x 0.10 x 0.10 mm^3	
Theta range for data collection	3.32 to 29.22	
Index ranges	-12<=h<=12, -12<=k<=12, -19<=l<=19	
Reflections collected	12961	
Independent reflections	6238 [R(int) = 0.1327]	
Completeness to theta = 29.22°	98.9 %	
Absorption correction	None	
Hydrogen treatment	Riding model	
Data / restraints / parameters	6238 / 0 / 318	
Goodness-of-fit on F^2	0.865	
Final R indices [I>2sigma(I)]	R_1 = 0.0647, wR_2 = 0.1290	
R indices (all data)	R_1 = 0.1185, wR_2 = 0.1523	
Extinction coefficient	0.0022(7)	
Largest diff. peak and hole	1.258 and -1.700 $e \cdot Å^{-3}$	

Table 32: Atomic coordinates (x 10^4) and equivalent isotropic displacement parameters (Å^2 x 10^3) for $[Tc(NO)(py)_4F]PF_6$.

	x	y	z	U(eq)
C(1)	8448(13)	7857(13)	8850(8)	47(3)
C(2)	9856(13)	7811(15)	9366(8)	61(3)
C(3)	11132(18)	8627(18)	9232(9)	65(4)
C(4)	10837(12)	9546(14)	8633(9)	54(3)
C(5)	9346(12)	9499(12)	8109(8)	39(2)
C(6)	6685(11)	5888(12)	6129(7)	40(2)
C(7)	6774(14)	4421(14)	5745(8)	45(3)
C(8)	5923(15)	3291(14)	5931(7)	52(2)
C(9)	5026(13)	3642(11)	6502(8)	50(3)
C(10)	4966(12)	5156(11)	6913(7)	42(2)
C(11)	7020(13)	12047(13)	8218(8)	41(3)
C(12)	7166(12)	13510(11)	8817(8)	50(3)
C(13)	6344(16)	13732(15)	9487(8)	56(3)
C(14)	5369(15)	12556(15)	9536(7)	57(3)
C(15)	5240(12)	11144(13)	8913(7)	44(2)
C(16)	3072(11)	9115(12)	6034(7)	38(2)
C(17)	1507(13)	8911(16)	5509(8)	50(3)
C(18)	463(12)	7944(14)	5704(7)	50(3)
C(19)	955(11)	7197(12)	6389(8)	48(3)
C(20)	2463(11)	7473(11)	6884(7)	39(2)
F(1)	5300(7)	7966(7)	8471(3)	40(1)
F(2)	-276(15)	12185(13)	6992(5)	139(5)
F(3)	885(11)	13234(11)	8592(5)	91(3)
F(4)	1372(9)	13732(10)	6602(5)	80(3)
F(5)	160(20)	14646(18)	7675(14)	174(7)
F(6)	2096(17)	12245(16)	7489(13)	152(5)
F(7)	2510(15)	14723(18)	8181(5)	171(8)
N(1)	6437(9)	9153(9)	6466(5)	32(2)
N(2)	8165(9)	8666(10)	8219(5)	32(2)
N(3)	5820(9)	6282(10)	6714(6)	34(2)

N(4)	6053(9)	10880(10)	8266(6)	35(2)
N(5)	3527(10)	8393(10)	6710(6)	32(2)
O(1)	6758(8)	9507(8)	5781(4)	53(2)
P(1)	1120(3)	13476(3)	7606(2)	46(1)
Tc(1)	5897(1)	8602(1)	7408(1)	27(1)

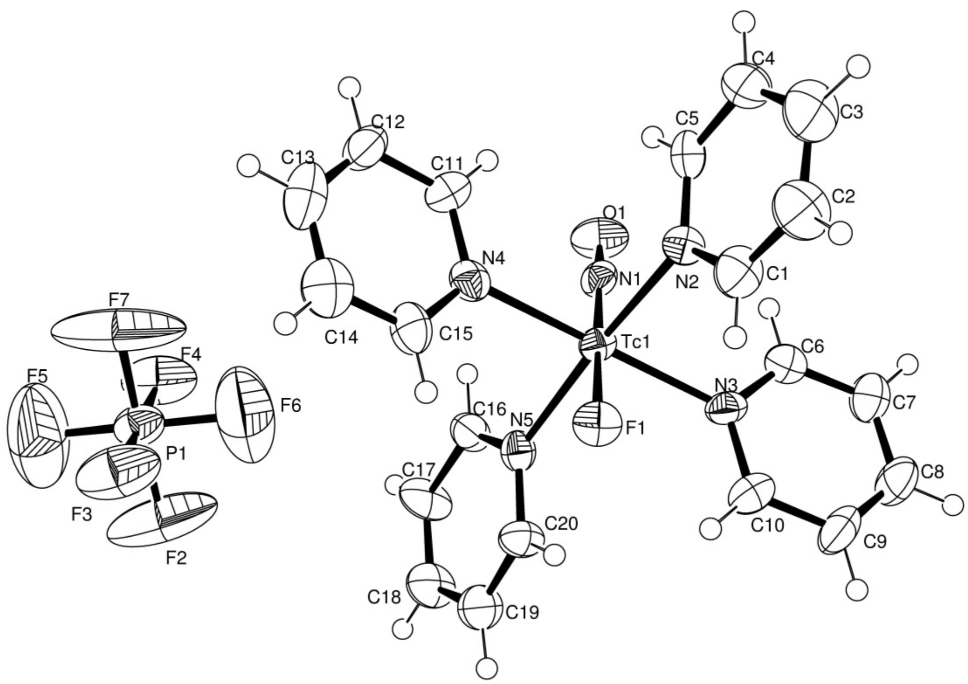

Figure 16: Ellipsoid plot (50% probability) of $[Tc(NO)(py)_4F]PF_6$.

$[Tc(NO)(NH_3)_4(OOCCF_3)](OOCCF_3)\cdot CF_3COOH$, (34)

Table 33: Crystal data and structure refinement for $[Tc(NO)(NH_3)_4(OOCCF_3)](OOCCF_3)\cdot CF_3COOH$.

Empirical formula	$C_6H_{13}F_9N_5O_7Tc$	
Formula weight	536.21	
Temperature	200(2) K	
Wavelength	0.71073 Å	
Crystal system	Triclinic	
Space group	$P\bar{1}$	
Unit cell dimensions	a = 7.133(1) Å	α= 99.64(1)°
	b = 9.323(1) Å	β= 100.09(1)°
	c = 14.198(1) Å	γ= 98.18(1)°
Volume	902.01(17) $Å^3$	
Z	2	
Density (calculated)	1.974 g/cm^3	
Absorption coefficient	0.928 mm^{-1}	
F(000)	528	
Crystal description	Block	
Crystal color	Orange	
Crystal size	0.60 x 0.22 x 0.09 mm^3	
Theta range for data collection	3.36 to 29.20	
Index ranges	-9<=h<=8, -12<=k<=12, -19<=l<=19	
Reflections collected	10086	
Independent reflections	4834 [R(int) = 0.0273]	
Completeness to theta = 29.20°	99.0 %	
Absorption correction	None	
Hydrogen treatment	Mixed	
Data / restraints / parameters	4834 / 0 / 268	
Goodness-of-fit on F^2	1.040	
Final R indices [I>2sigma(I)]	R_1 = 0.0387, wR_2 = 0.1010	
R indices (all data)	R_1 = 0.0444, wR_2 = 0.1041	
Extinction coefficient	0.025(2)	
Largest diff. peak and hole	0.944 and -0.818 e·$Å^{-3}$	

Table 34: Atomic coordinates (x 10^4) and equivalent isotropic displacement parameters (Å^2 x 10^3) for $[Tc(NO)(NH_3)_4(OOCCF_3)](OOCCF_3)\cdot CF_3COOH$.

	x	y	z	U(eq)
C(1)	7422(4)	3646(3)	1624(2)	34(1)
C(2)	7588(5)	3134(5)	557(2)	52(1)
C(3)	18143(5)	433(4)	-4215(2)	43(1)
C(4)	16448(5)	1000(3)	-3826(2)	40(1)
C(5)	11562(5)	1633(4)	-1208(3)	49(1)
C(6)	12658(5)	784(3)	-1888(2)	41(1)
F(1A)	12558(6)	2074(7)	-339(3)	105(2)
F(1B)	9894(6)	856(5)	-1194(4)	111(2)
F(1C)	11109(10)	2850(5)	-1515(4)	109(2)
F(1)	11690(20)	1070(30)	-395(10)	105(2)
F(2)	9980(30)	1570(20)	-1545(17)	111(2)
F(3)	12330(40)	2980(20)	-903(17)	109(2)
F(2A)	6784(6)	3964(4)	-5(2)	94(1)
F(2B)	6661(5)	1775(3)	179(2)	82(1)
F(2C)	9393(4)	3171(6)	466(2)	134(2)
F(3A)	18236(4)	-953(3)	-4153(2)	69(1)
F(3B)	19802(4)	1235(4)	-3702(2)	81(1)
F(3C)	18083(4)	533(3)	-5136(2)	68(1)
N(1)	3205(4)	4438(3)	3874(2)	37(1)
N(2)	2896(4)	5344(3)	2068(2)	40(1)
N(3)	6772(4)	5987(3)	3516(2)	37(1)
N(4)	6379(4)	2798(3)	3678(2)	37(1)
N(5)	2449(4)	2110(3)	2215(2)	39(1)
Tc(1)	4487(1)	4087(1)	2967(1)	28(1)
O(1)	2179(4)	4656(3)	4444(2)	56(1)
O(2)	5689(3)	3578(2)	1717(1)	37(1)
O(3)	8917(3)	4054(3)	2237(2)	45(1)
O(6)	16053(4)	447(3)	-3110(2)	49(1)
O(7)	15714(5)	1904(3)	-4219(3)	69(1)
O(8)	13932(4)	1670(3)	-2161(2)	48(1)
O(9)	12265(5)	-541(3)	-2114(2)	62(1)

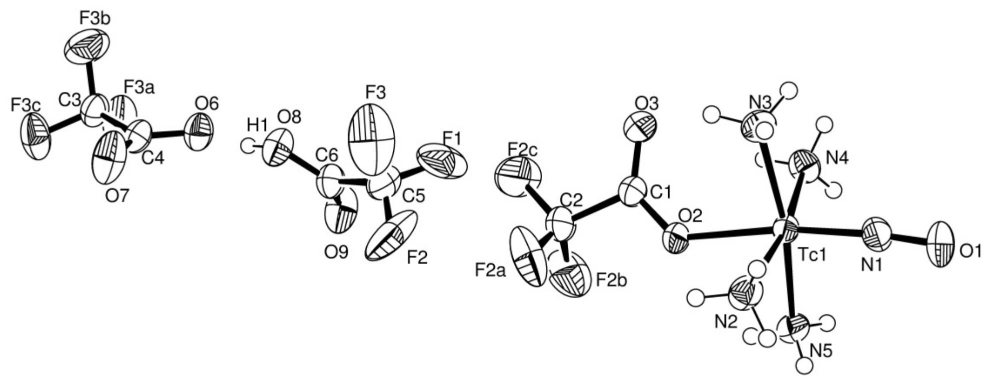

Figure 17: Ellipsoid plot (50% probability) of $[Tc(NO)(NH_3)_4(OOCCF_3)](OOCCF_3)\cdot CF_3COOH$.